Meprin β: A prominent player in the sequence specific generation of N-terminally truncated Aβ in the human brain

Dissertation

zur Erlangung des Grades
„Doktor der Naturwissenschaften“

am Fachbereich Biologie

der Johannes Gutenberg-Universität

in Mainz

von

Caroline Schönherr

geboren am 16. Juni 1986 in Troisdorf

Mainz, im Juni 2016

Dekan:

1. Berichterstatter:

2. Berichterstatter:

Tag der mündlichen Prüfung: 13.07.2016

I hereby declare that I wrote this dissertation submitted without any unauthorized external assistance and used only sources acknowledged in the work. All textual passages which are appropriated verbatim or paraphrased from published and unpublished texts as well as all information obtained from oral sources are duly indicated and listed in accordance with bibliographical rules. In carrying out this research, I complied with the rules of standard scientific practice as formulated in the statutes of the Johannes Gutenberg-University Mainz to insure standard scientific practice.

Caroline Schönherr

Meinen Eltern gewidmet

CONTENT

ABBREVIATIONS

Ac	acetic domain
AD	Alzheimer´s Disease
ADAM	a disintegrin and metalloproteinase
AICD	APP intracellular domain
APA	aminopeptidase A
APH	anterior pharynx defective
apl-1	β-amyloid-like protein
APLP1	amyloid-like protein 1
APLP2	amyloid-like protein 2
Apo E	apolipoprotein E
APP	amyloid precursor protein
appa	amyloid beta (A4) precursor protein a
appb	amyloid beta (A4) precursor protein b
astacin like protease domain	CAT
Aβ	amyloid β
BACE-1	β-site amyloid precursor protein cleaving enzyme 1
BCA	bicinchoninic acid
BMP-1	bone morphogenetic protein-1
bp	base pairs
CD	Crohn´s Disease
CSF	cerebrospinal fluid
CTF	C-terminal fragment
CuBD	copper binding domain
DMEM	Dulbecco´s modified eagle medium
ECL	electrochemiluminescence
EGF	epidermal growth factor
ELISA	enzyme linked immunosorbent assay
EOAD	early-onset AD
ER	endoplasmic reticulum
EtBr	ethidium bromide
FAD	familial AD
FCS	fetal calf serum
GFP	green fluorescent protein
GFP	green fluorescent protein
GSK-3β	glycogen synthase kinase-3 beta
GSM	γ-secretase modulator
h	hours
HBD	heparin-binding-domain/growth factor-like-domain
HEK	human embryonic kidney cell
HEPES	4-(2-hydroxyethyl)-1-piperazineethanesulfonic acid
HRP	horseradish peroxidase
IBD	inflammatory bowel disease
i-CLiPs	intramembrane cleaving proteases
IDE	insulin-degrading enzyme

interleukin	IL
IP	immunoprecipitation
IPEGAL	octylphenoxy polyethoxyethanol
iPSC	induced pluripotent stem cells
KLK	kallikrein-related peptidase
ko	knockout
KPI	Kunitz-type protease inhibitor domain
LOAD	late-onset AD
m/z	mass to charge
MALDI-MS	matrix assisted laser desorption ionization mass-spectrometry analysis
MAM	meprin A5 protein tyrosine phosphatase µ
MAPT	microtubule-associated protein tau
MEF	murine embryonic fibroblast
min	minutes
MMP	matrix metalloprotease
MT2	matriptase-2
MUC2	mucin 2
N-APP	N-terminal APP fragment
NCT	nicastrin
NFT	neurofibrillary tangles
NP-40	nonidet P-40
NSAID	non-steroidal anti-inflammatory agent
NTF	N-terminal fragment
OD	optical density
PAGE	polyacrylamide gel electrophoresis
PBS	phosphate buffered saline
PCR	polymerase chain reaction
pE(3)-Aβ	pyroglutamated Aβ
PEI	polyethlenimine
PS1	presenilin 1
PS2	presenilin 2
PSEN1 (gene)	presenilin 1
PVDF	polyvinylidene difluoride
qPCR	quantitative PCR
RIP	regulated intramembrane proteolysis
RIPA	radio-immunoprecipitation
RT	room temperature
SAD	sporadic AD
SAM	synaptic adhesion molecule
sAPP	soluble APP
SDS	sodium dodecyl sulfate
SNP	single nucleotide polymorphism
TACE	tumor necrosis factor-α-converting enzyme
TAE	tris-acetate-EDTA
TGN	trans-Golgi network
TOF	time of flight
TRAF	tumor-necrosis-factor-receptor-associated-factor

TRAM2	Translocating chain-associated membrane protein 2
VSV	vesicular stomatitis virus
wt	wild type

1 SUMMARY

The generation of amyloid β (Aβ) variants by sequential cleavage of the amyloid precursor protein (APP) is a normal process and occurs in the healthy brain. However, it is one of the most studied peptides in Alzheimer´s Disease (AD), since shifts in the composition of Aβ variants varying in length, and the increased occurrence of toxic variants that are prone to aggregate, are one of the major pathological hallmarks of AD pathogenesis. The primary secretases that are responsible for producing these peptides are the β-secretase BACE-1 (beta-site amyloid precursor protein cleaving enzyme 1), cleaving N-terminally at position 1 or 11 of the Aβ sequence, and the γ-secretase, cleaving at various positions of the C-terminus of Aβ. Though, N-terminally truncated Aβ variants that have been detected in cerebrospinal fluid (CSF) and brain of AD patients that cannot be attributed to BACE-1 cleavage. These became the focus of recent studies, since they appear to be more prone to aggregate. One candidate enzyme for this cleavage event is the metalloprotease meprin β. Recently, a proteomics study identified APP as a potential substrate (Jefferson et al., 2011) which could be further verified by demonstrating the role of meprin β in the generation of N-terminally truncated Aβ2-40 (Bien et al., 2012). Moreover, increased levels of meprin β mRNA were observed in brains of AD patients.

In line with this study, in this dissertation human brain samples of AD patients were analyzed and compared to non-demented age matched controls as well as to non-AD but neurodegeneration patients. An increased number of meprin β positive neurons and increased meprin β expression levels in lysates could be detected in AD samples compared to both control groups. Moreover, increased levels of sAPPα were observed in brains of *Mep1b*$^{-/-}$ mice compared to wild type (wt) mice, indicating that in the absence of meprin β more substrate is available for ADAM10. This difference could be detected even though endogenous meprin β levels are very low under physiological conditions. Additionally, a decrease of Aβ2-40 and an increase of mature APP in primary cortical neurons of *Mep1b*$^{-/-}$ mice infected with a recombinant adenovirus expressing human APP695 were detected. Moreover, the same Aβ variant could be detected in human brain homogenates and even more interesting, the Aβ2-40/1-40 ratio was increased in frontal lobe of AD patients. As seen for other N-terminally truncated Aβ peptides, Aβ2-40 has been shown to have an increased aggregation behavior compared to non-truncated variants and only little amounts of this variant had a drastic seeding effect on Aβ1-40 (Schonherr et al., 2016).

To study the interaction of APP and meprin β in more detail, the localization of this processing event was analyzed *in vitro*. Via confocal microscopy of a surface staining and a compartment staining in a split GFP based complementation assay, the interaction could be spatialized to the late secretory pathway and the cell surface, which locally separates it to the cleavage of BACE-1 that rather occurs in endosomal compartments.

Most interestingly, the results of this work show that meprin β is incapable of generating N-terminally truncated Aβ2-40 of the Swedish mutated APPswe (K670N/M671L). Moreover, the results demonstrate that the recently described protective APP A673T mutation does not only decrease BACE-1 cleavage, but also diminishes meprin β cleavage.

Furthermore, preliminary results suggest that Aβ1-42 has an effect on meprin β gene regulation since increased meprin β mRNA levels could be detected upon treatment of N2a cells with Aβ1-42.

Concluding, this work underlines that the protease meprin β appears as an important candidate for further studies on APP processing and Aβ generation and may have a contributing role in the pathogenesis of AD.

Data included in this work is partly published in:

C Schönherr et al. “Generation of aggregation prone N-terminally truncated amyloid β peptides by meprin β depends on the sequence specificity at the cleavage site” Mol Neurodegener. 2016 Feb 19;11(1):19

2 ZUSAMMENFASSUNG

Die Generierung von amyloid β (Aβ) Peptiden durch sequentielle Prozessierung des Amyloiden Vorläufer Proteins (APP) durch Sekretasen ist ein normaler Prozess der im gesunden Gehirn auftritt. Trotzdem ist dieses Peptid eines der meist untersuchtesten *Targets* in der Alzheimer (AD) Forschung, da das erhöhte Auftreten von aggregationsanfälligen Varianten dieses Peptids und die daraus resultierenden Ablagerungen, bzw. senilen Plaques ein pathologisches Merkmal der Erkrankung darstellen. Die verantwortlichen Sekretasen zur Aβ Generierung sind zum einen die β-Sekretase BACE-1 (beta-site amyloid precursor protein cleaving enzyme 1), welche den N-Terminus in Position p1 oder p11 des Peptids schneidet, und zum anderen die γ-Sekretase, welche den C-Terminus an variablen Positionen scheiden kann, und somit Peptide variierender Länge sezerniert. Allerdings wurden sowohl in der Zerebrospinalflüssigkeit (CSF) als auch im Gehirn von AD Patienten N-terminal trunkierte Aβ Varianten entdeckt, die nicht der BACE-1 Prozessierung zugeordnet werden können. Diese Varianten wurden als besonders aggregationsanfällig charakterisiert und rückten dadurch in aktuellen AD Studien mehr in den Fokus. Einen Kandidaten für diesen C-terminal verschobenen Schnitt des N-Terminus stellt die Metalloprotease Meprin β dar. 2011 zeigten Jefferson und Kollegen in einer *Proteomics* Analyse, dass APP ein potentielles Substrat für Meprin β repräsentiert. Die Ergebnisse zeigten des Weiteren, dass Meprin β N-terminale APP Fragmente generieren kann (Jefferson et al., 2011). Die Prozessierung von APP durch Meprin β wurde in einer weiteren Studie bestätigt, die zeigt, dass die Protease N-terminal trunkierte Aβ Peptide erzeugt (Bien et al., 2012). Zudem konnten erhöhte Meprin β mRNA Level in Gehirnen von AD Patienten gemessen werde.

In Einklang mit diesen Ergebnissen konnten in der vorliegenden Arbeit erhöhte Meprin β Proteinlevel in Gehirnen von AD Patienten im Vergleich zu gesunden Kontrollen und einer nicht-AD, aber neurodegenerativ erkrankten Kontrollgruppe detektiert werden. Zudem legen die Ergebnisse dieser Arbeit dar, dass sAPPα Level in Hirnhomogenaten von *Mep1b*$^{-/-}$ Mäusen höher ausfallen als in jenen wildtypischer Kontrollen, obgleich die endogenen Meprin β Proteinlevel unter physiologischen Bedingungen sehr niedrig sind, was darauf hindeutet, dass die Protease einen hohen Substratumsatz aufweist. Bei einem Fehlen der Protease scheint folglich mehr Substrat für die α-Sekretase ADAM10 (A disintegrin and metalloprotease) zur Verfügung zu stehen. In Präzipitaten aus Zellkulturüberständen primärer Neuronen derselben Mäuse, welche mit einem

rekombinanten Virus, der humanes APP überexprimiert, infiziert wurden, konnte für *Mep1b*$^{-/-}$ eine geringere Konzentration an Aβ2-40 gemessen werden.

Dieselbe N-terminal trunkierte Aβ Variante konnten in dieser Arbeit in humanen Gehirnen detektiert werden. Es zeigte sich, dass das Aβ2-40/1-40 Verhältnis in Frontallappen von AD Patienten erhöht ist. Wie bereits zuvor für andere N-terminal trunkierte Aβ Varianten beschrieben, wurde kürzlich gezeigt, das Aβ2-40 sehr aggregationsanfällig ist (Schonherr et al., 2016).

Um die Interaktion von APP und Meprin β genauer zu untersuchen, wurde die subzelluläre Lokalisation dieser analysiert. Dies erfolgte durch konfokale Mikroskopie einer Zelloberflächenfärbung und eines „split-GFP“ basierten Komplementationsversuchs. Somit konnte die Interaktion dem späten Sektretionsweg und der Zelloberfläche zugeordnet werden. Dadurch scheint diese räumlich von der Interaktion von APP mit BACE-1 getrennt zu sein, welche in endosomalen Vesikeln stattfindet.

Ein weiterer Hauptbestandteil dieser Arbeit war die Untersuchung von Mutationen in der APP Sequenz, welche mit der familiären Form von AD (FAD) assoziiert werden, und deren Effekt auf die Spaltung durch Meprin β. Interessanterweise stellte sich heraus, dass die Schwedische Doppelmutation APPswe (K670N/M671L) die Protease derartig beeinflusst, dass kein Aβ2-40 generiert werden kann. Neben den bekannten APP Mutationen, welche mit FAD in Verbindung gebracht werden, wurde kürzlich eine APP Mutation unmittelbar an der β-Schnittstelle entdeckt. Die APP A673T Mutation wurde als protektiv beschrieben, welche vor BACE-vermittelter Aβ Produktion schützt. Ein weiteres Ziel dieser Arbeit war deshalb, den Effekt der Mutation auf Meprin β zu untersuchen. Es stellte sich heraus, dass die Mutation auch einen protektiven Effekt gegen den Meprin β Schnitt aufweist.

Vorläufige Ergebnisse dieser Arbeit weisen auf einen Effekt von Aβ1-42 auf die Meprin β Genregulation hin, da nach Inkubation mit Aβ1-42 erhöhte Meprin β mRNA Level in N2a gemessen werden konnten.

Zusammenfassend zeigen die Ergebnisse, dass Meprin β ein wichtiger Kandidat für zukünftige Studien bezüglich der APP Prozessierung darstellt. Aufgrund des Potenzials N-terminal trunkiertes Aβ2-40 zu generieren, scheint Meprin β eine wichtige Rolle in der AD Pathogenese einzunehmen.

3 INTRODUCTION

3.1 ALZHEIMER´S DISEASE

1901, the German psychiatrist and neuropathologist Alois Alzheimer first met his patient Auguste Deter. She suffered from loss of memory, cognitive decline and spatial and mental disorientation at an age of only 51 years. Deter´ s atrophic brain that Alzheimer studied after her death showed proteinogenic deposits, the so called plaques. Her disease that was first described by Alzheimer in 1907 (Alzheimer et al., 1995) was later on named after the neuropathologist.

Due to a growing population that continuously gets older the numbers of affected people is increasing tremendously. In 2015 about 46.8 million people suffered from AD worldwide with estimated numbers of 9.9 million new cases each year (Prince, 2015). These numbers are estimated to double every 20 years (Prince et al., 2013). The highest risk factor for AD still remains growing age; however, the disease has a very heterogeneous appearance that renders to determine a distinct causation for developing AD impossible. Though, it is subdivided into sporadic AD (SAD) and familial AD (FAD). SAD is with about 95 % of all cases the most common form of AD and is characterized by a late-onset at age 60 or older with increasing risk to fall ill at higher age. Besides several risk factors that could contribute to developing the disease, such as the occurrence of the ε4 allele of the apolipoprotein E (Apo E), high cholesterol levels or environmental factors like head injury (Gentleman et al., 1993) or the more controversial hypotheses of high exposure to aluminum or malnutrition, the basic cause still remains elusive. Contrary, FAD is characterized by a comparatively early-onset already starting from the age of 30 or 40 years. Several studies could show that these cases are associated with mutations in one of three genes, encoding for proteins involved in the processing of the amyloid precursor protein (APP). Albeit these differences the appearance of both, clinical symptoms and disease progression as well as pathological phenotype, are kindred. First symptoms for both are for instance declined memory and loss of orientation that are attended by depressions or aggressive behavior; 3 to 9 years after diagnosis the disease leads to death.

Brains of AD patients all show a common histopathology; they are marked by an atrophy and degeneration of the temporal lobe, parietal lobe, frontal cortex, cingulate gyrus and also locus ceruleus that is caused by a severe loss of neurons and synapses (Braak and Del Tredici, 2012; Wenk, 2003). Moreover, so called extracellular senile

plaques that consist of predominantly insoluble amyloid β (Aβ) peptides can be detected in the grey matter where they surround neurons. These peptides are cleavage products of the amyloid precursor protein (APP). Besides these plaques that also may appear as a by-product of senescence, intracellular neurofibrillary tangles (NFT), aggregates of hyperphosphorylated tau, are one other primary marker for AD. The physiological function of tau is to stabilize microtubules; however, hyperphosphorylated tau loses the affinity to bind to the cytoskeletal component (Kosik, 1990). Both of these microscopic visible changes start decades before the onset of the disease. Since mutations causing FAD all lead to an increased generation of Aβ peptides, it is obvious to consider this peptide as an important factor that might be involved as a trigger for the disease. This idea is called the amyloid hypothesis.

3.1.1 APP AND THE APP FAMILY

The amyloid precursor protein (APP) is a type I transmembrane protein and belongs to a gene family including APP, amyloid-like protein 1 (APLP1) and amyloid-like protein 2 (APLP2) in mammals, amyloid beta (A4) precursor protein a (appa) and amyloid beta (A4) precursor protein b (appb) in zebrafish, β-amyloid-like protein (APPL) in Drosophila and β-amyloid-like protein (apl-1) in C. elegans (reviewed in Shariati and De Strooper, 2013). This evolutionarily conserved family shares a large sequence homology. They all have an E1 domain that contains a heparin-binding-domain/growth-factor-like-domain (HBD) and a copper binding domain (CuBD), an acetic domain (Ac), an E2 domain and a C-terminal cytosolic tail bearing a YENPTY motif. However, only APP contains the AD critical Aβ region (reviewed in Kaden et al., 2012).

The processing of APLP1 and APLP2 is very similar to APP, despite the lack of secreted Aβ. Moreover, the shedding of APLP1 has been shown to be BACE-1 (beta-site amyloid precursor protein cleaving enzyme 1) independent (Eggert et al., 2004; Minogue et al., 2009). APP and APLP2 are ubiquitously expressed in overlapping patterns during development, but also in adult tissue and show a high expression in neurons of the central and peripheral nervous system, while APLP1 is primarily expressed in the nervous system (Lorent et al., 1995). It was shown that there is a redundancy between APLP2 and both, APLP1 and APP. APLP1/APP deficient mice are viable and fertile (Heber et al., 2000), whereas APLP2/APLP1 and APLP2/APP deficiency in mice is lethal, since animals die shortly after birth (Heber et al., 2000; von Koch et al., 1997).

The APP gene is located on the long (q) arm of chromosome 21. There are three different major isoforms of APP which are a result of alternative splicing at exons 7 and

8: APP695, APP751, which contains an additional Kunitz-type protease inhibitor (KPI) domain, and APP770, which contains the KPI domain and the OX2 domain (Sandbrink et al., 1997) (Fig. 1). The most prominent splicing variant in the human brain appears to be APP695, which is almost exclusively expressed in neurons, since the ratio of APP770/APP751/APP695 mRNA is approximately 1:10:20 (Tanaka et al., 1990). It has been shown that the E1 domain is critical for the formation of APP cis-dimers in APP695 via disulfide bridges. However, the additional KPI domain in the longer isoforms seems to block the dimer formation (Isbert et al., 2012). Moreover, it was shown that the E2 domain mediates the formation of anti-parallel dimers (Soba et al., 2005; Wang and Ha, 2004) that could be relevant for cell-cell adhesion. Therefore, APP was described as a novel synaptic adhesion molecule (SAM) with overlapping biological properties to the presynaptic protein neurexin or the postsynaptic cell-adhesion proteins neuroligins (Biederer and Sudhof, 2000; Graf et al., 2004; Scheiffele et al., 2000). However, the primary biological functions are still elusive.

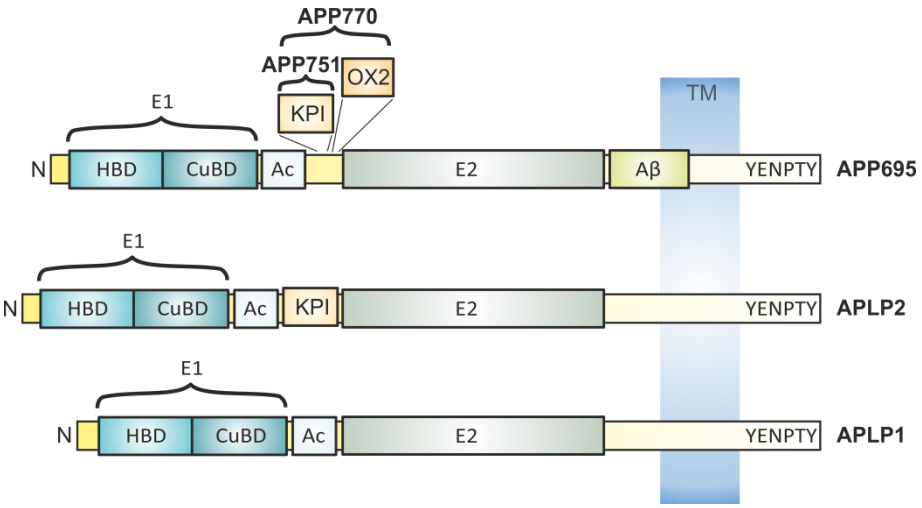

FIGURE 1 The APP family

The amyloid precursor protein (APP) is a type I transmembrane protein and belongs to a gene family including APP, amyloid-like protein 1 (APLP1) and amyloid-like protein 2 (APLP2) in mammals. The evolutionarily conserved family shares a large sequence homology, since they all have an E1 domain that contains a heparin-binding-domain/growth-factor-like-domain (HBD) and a copper binding domain (CuBD), an acetic domain (Ac), an E2 domain and a C-terminal cytosolic tail bearing a YENPTY motif. Though, only APP contains the AD critical Aβ region. The three major isoforms of APP differ in the absence or presence of the Kunitz-type protease inhibitor (KPI) and/or the OX2 domain.

The YENPTY motif has been identified to be important for clathrin-mediated endocytosis from the cell surface (Koo and Squazzo, 1994; Perez et al., 1999).

However, only a small portion of APP reaches the cell surface (approximately 10 %), while the bulk remains at steady-state in the Golgi and trans-Golgi network (TGN). First, the protein undergoes post-translational modifications in the secretory pathway, including N- and O-glycosylation, phosphorylation and sulfation (Buxbaum et al., 1990; Oltersdorf et al., 1990; Weidemann et al., 1989). Once at the cell surface, the mature APP that is not shed is rapidly internalized within minutes (Lai et al., 1995; Marquez-Sterling et al., 1997) and transported to endosomes. It is then either trafficked by sorting endosomes to the TGN, in recycling endosomes recycled to the cell surface or degraded in lysosomes (Haass et al., 1992).

3.1.2 APP PROCESSING

There are two independent pathways regulating the processing of APP, both proceeded by sequential cleavage of different secretases (Fig. 2). The favored one under healthy conditions is the anti-amyloidogenic pathway. In this pathway the α-secretase and the γ-secretase are involved (Esch et al., 1990; Sisodia et al., 1990; Wang et al., 1991). The α-secretase that is designated as A Disintegrin And Metalloproteinase, or short ADAM, is a type I transmembrane protein that is ubiquitously expressed. The proteolytic activity of the evolutionarily conserved protease is dependent on the presence of a relevant domain (HEXGHXXGXXHD) (Stocker et al., 1990). ADAM9 (Koike et al., 1999), ADAM10 (Lammich et al., 1999), ADAM17/TACE (Slack et al., 2001) and ADAM19 (Tanabe et al., 2007) have been shown to be capable in cleaving APP however, in neurons ADAM10 appears to be the relevant secretase to do this job. The γ-secretase is a complex of four subunits: presinilin-1 (PS1) or presenilin-2 (PS2), that are both part of the proteolytic domain, nicastrin (NCT), anterior pharynx defective (APH-)1a or APH1b and PS enhancer (PEN)-2. This high molecular weight complex has several substrates including E-cadherin (Marambaud et al., 2002), tyrosine-protein kinase ErbB4 (Ni et al., 2001), CD44 (Lammich et al., 2002), tyrosinase (Wang et al., 2006b), translocating chain-associated membrane protein 2 (TREM2) (Wunderlich et al., 2013) or Alcadein (Hata et al., 2012). However, primarily focus has been set on Notch (De Strooper et al., 1999), which is important for the control of cell fate by regulating cell proliferation, survival, positioning and differentiation (Andersson et al., 2011; Kopan and Ilagan, 2009), and of course on APP processing (De Strooper et al., 1998). The special feature of the γ-secretase is that it cleaves intramembranous in a hydrophobic environment and thus belongs to the family of intramembrane cleaving proteases (i-CLiPs) (Beel and Sanders, 2008). These proteases all follow the principal of regulated intramembrane proteolysis (RIP), a process consisting of two consecutive cleavage events: first the ectodomain shedding

and then the intramembranous proteolysis and consequently the secretion of a protein fragment (Brown et al., 2000). It was shown by cryo-electron microscopy that the γ-secretase has a membrane-facing surface groove and routes for water access into the depth of the membrane-embedded region that is required for hydrolysis in the hydrophobic environment (Osenkowski et al., 2009). Interestingly, the γ-secretase cleaves its substrates not at a single position, but rather in a sequence of cleavage events at the so called ε-, ζ-, and γ-sites at intervals of two to three amino acids resulting in a final imprecise cleavage event (Qi-Takahara et al., 2005; Sastre et al., 2001; Takami et al., 2009; Weidemann et al., 2002). During the anti – amyloidogenic pathway, first, the α-secretase ADAM10 cleaves APP at the cell surface between amino acids 687 (lys) and 688 (leu) which refers to p17/p18 of the Aβ peptide (Esch et al., 1990; Sisodia et al., 1990; Wang et al., 1991). Due to this cleavage event, no Aβ will be generated. However, a soluble APPα (sAPPα) fragment is released. This event is followed by cleavage of the remaining C-terminal fragment 38 (CTF or C83 or CTFα) by the γ-secretase and the secretion of p3 (Haass et al., 1993), a small peptide supposed to have no relevant function or pathogenic effect. The remaining APP intracellular domain (AICD) that is released into the cytosol (Gu et al., 2001; Sastre et al., 2001) has been shown to have nuclear signaling functions (Cao and Sudhof, 2001; von Rotz et al., 2004).

However, besides the anti – amyloidogenic pathway, APP can also be processed in a different manner by two consecutive cleavage events, resulting in the release of the AD critical peptide Aβ. The pathway starts with the cleavage at the ectodomain N-terminal to the Aβ sequence between amino acids 671 and 672 by the β-site APP cleaving enzyme (BACE-1) and the release of sAPPβ. The remaining CTF99 (or CTFβ) is, likewise to the anti – amyloidogenic pathway, cleaved by the γ-secretase in varying positions, resulting in the secretion of Aβ peptides with a length of 36 to 43 amino acids and the release of AICD into the cytosol.

BACE-1 is an aspartyl protease that is highly expressed in brain and is, besides cleaving APP, responsible for myelination by cleaving neuregulin (Fleck et al., 2012; Willem et al., 2009). The secretase that undergoes several posttranslational modifications has a pH optimum in the acidic range. Thus, cleavage of APP could be expected to occur in either the TGN (pH 6) or in endosomes (pH < 6). However, due to results of several studies, it is most likely that BACE-1 cleaves APP in endosomes (Das et al., 2013; Koo and Squazzo, 1994). Strikingly, it has been shown that CTF99 accumulates in endosomes (Golde et al., 1992; Haass et al., 1992). Moreover, cells overexpressing APP lacking the NPxY motif, which is responsible for proper

internalization and translocation to endosomes, secrete decreased levels of Aβ (Koo and Squazzo, 1994; Perez et al., 1999). Additionally, via confocal microscopy it could be shown that activated neurons transport APP to BACE containing endocytic vesicles and show increased levels of CTF99 (Das et al., 2013).

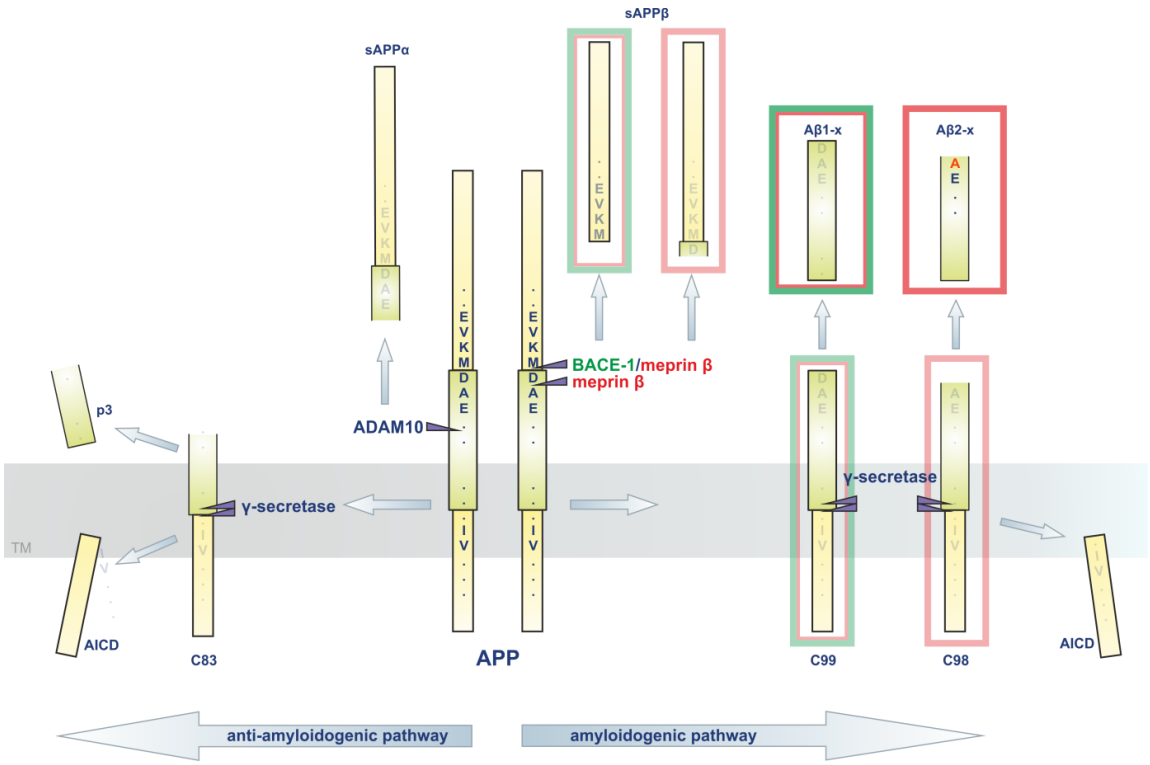

FIGURE 2 Processing pathways of APP

Two principal processing pathways for APP have been described. The non-amyloidogenic pathway consists of subsequential cleavage of ADAM10 and the γ-secretase. First, ADAM10 cleavage APP at the ectodomain and sAPPα is secreted. Further, the remaining CTF is cleaved by the γ-secretase releasing p3 and AICD. No Aβ is generated. During the amyloidogenic pathway BACE-1 cleaves N-terminally of Aβ. This work suggests that cleavage at this position can also be performed by meprin β and additionally in p2 of Aβ. Following γ-secretase cleavage Aβ is secreted and AICD liberated into the cytosol. Cleavage products related to BACE-1 cleavage are marked by green boxes, those related to meprin β cleavage by red boxes.

Recently, several studies described the presence of N-terminally truncated Aβ peptides in brain or cerebrospinal fluid (CSF) like Aβ2-42, pyroglutamate Aβ3-42 (AβpE3-42) or Aβ4-42 (Becker et al., 2013; Bibl et al., 2012a; Bouter et al., 2013; Jawhar et al., 2011; Wiltfang et al., 2001; Wirths et al., 2010). However, BACE-1 is incapable in generating these truncated peptides, since it only cleaves Aβ in p1 or p11 (Vassar et al., 1999). Moreover, it has been shown that inhibition of BACE only has an effect on cells generating Aβ1-x, but not on those generating N-terminally truncated Aβ (Citron et al.,

1996). These peptides might be generated by a subsequent cleavage of Aβ1-x by aminopeptidases like the aminopeptidase A (APA) (Sevalle et al., 2009) or by a direct cleavage of APP at another position by another protease. The metalloprotease meprin β has been described to be capable in generating Aβ2-10 by direct cleavage of APP in overexpressing cells (Bien et al., 2012).

3.1.3 AMYLOID β

Aβ is a natural cleavage product of the amyloidogenic processing pathway of APP. The peptide occurs in different variants having a length of 36 to 43 amino acids. This is a result of alternative cleavage sites. The γ-secretase for example can shed APP in different positions resulting in C-terminal truncated peptides (see section “APP processing”). The most prevalent form is Aβ40 followed by Aβ42. In the CSF of non-demented individuals approximately 50 % of detected variants are Aβ40, ~16 % Aβ38 and ~10 % Aβ42 (Bibl et al., 2012b). However, this naturally occurring peptide is associated with AD. An imbalance between production and clearance of Aβ might be one factor for triggering the disease. Yet, rather a shift in the pattern of generated variants and an increase in the ratio of Aβ42:Aβ40 than an increase in total Aβ levels might be a critical feature for FAD (Chavez-Gutierrez et al., 2012). The problem of this shift can be explained by the different properties of Aβ variants, concerning self-assembly and aggregation. The longer Aβ42 is much more prone to form neurotoxic aggregates than Aβ40 (Iwatsubo et al., 1994; Roher et al., 1993). Following, these soluble oligomers deposit as extracellular plaques consisting of mature amyloid fibrils that are morphological detectable correlatives of Aβ aggregates in AD (Glenner and Wong, 1984; Masters et al., 1985). These plaques occur long before first clinical symptoms of AD. They were shown to trigger the formation of dystrophic neurites and following the occurrence of neuritic plaques, the co-localizing occurrence of Aβ plaques and dystrophic neurites (Dickson, 1997; Wang and Munoz, 1995). The pathology starts in neocortical regions. Following, plaques can be found in allocortical regions like the entorhinal cortex, the hippocampus and cingulate gyrus, then in striatum, hypothalamus, thalamus and basal forebrain and at last in midbrain, medulla oblongata, cerebellum and pons (Thal et al., 1997; Thal et al., 2002). Although, plaque pathology can be histologically confirmed in brains of AD affected individuals, they are not specific for symptomatic AD, since non-demented individuals can also show the same histological phenotype (Arriagada et al., 1992; Price et al., 1991; Thal et al., 1997). Still, as published by the National Institute of Aging and the Alzheimer Association, they are all to be diagnosed with AD. However, non-demented are classified as individuals with “AD neuropathologic change” (Montine et al., 2012).

In the last years, more and more focus has been set on other species, either modified of N-terminally truncated Aβ. Various modifications have been described ranging from oxidation (Hou et al., 2002; Palmblad et al., 2002) to phosphorylation (Kumar et al., 2011; Kumar et al., 2012), nitration (Kummer et al., 2011), glycosylation (Halim et al., 2011) or pyroglutamation of Glu3 of Aβ3-40 (Russo et al., 2002; Wittnam et al., 2012). These modifications have been shown to have an effect on the properties of the peptide. The oxidation at Met35 for example impedes the formation of protofibrils and fibrils from monomers (Hou et al., 2002). Nitration and pyroglutamation both increase the aggregation of Aβ (Kummer et al., 2011; Schilling et al., 2004). But besides these modifications, an effect on Aβ properties could be also ascribed to a truncated N-terminus. Increased levels of Aβ2-42 were detected in AD brains (Wiltfang et al., 2001). This goes in line with results showing decreased levels of Aβ2-42 in CSF of AD patients (Bibl et al., 2012a). Since BACE-1 is not capable in directly generating these peptide, a suggested model for the emergence of N-terminal truncation is the subsequent cleavage of the N-terminus of BACE generated Aβ1-x by either Aβ degrading enzymes like insulin-degrading enzymes (IDE) or neprilysin or APA (Arai et al., 1999; Wang et al., 2006a; Wiltfang et al., 2001). However, another candidate directly generating N-terminally truncated Aβ independent of BACE might be much more likely. Already in 2011 it could be shown that APP serves as a substrate for the metalloprotease meprin β that generates N-terminal APP fragments (NTF) (Jefferson et al., 2011). These fragments were also detected in human brain homogenates suggesting that this interaction not only occurs in overexpressing cell systems, but probably also under endogenous levels in the human brain. In 2012, N-terminally truncated Aβ2-40 peptides generated by meprin β, dependent on subsequential cleavage of the γ-secretase, but independent of BACE-1, were detected in supernatants of overexpressing cells. Interestingly, increased mRNA levels of the same protease were measured in AD brain homogenates in the same study (Bien et al., 2012).

3.1.4 AMYLOID CASCASDE HYPOTHESIS

Many results of studies on AD point to the idea that Aβ might be the central and primary trigger in AD (Glenner and Wong, 1984). This hypothesis is supported by several findings:

1. Trisomy 21 patients, that have a triplicate of chromosome 21 that carries the gene for APP, are likely to develop AD (Rovelet-Lecrux et al., 2006).
2. Individuals that show mutations in APP, PS1 or PS2 that lead to increased levels of Aβ42, will be affected by AD (Wu et al., 2012).

3. Carriers of the APP A673T mutation that protects from β-site cleavage and thus leads to decreased levels of Aβ are protected from developing AD and show a lower risk for cognitive decline (Jonsson et al., 2012).

The hypothesis states that due to relative increased levels of aggregation prone Aβ42 in the brain, either due to mutations in PS1/2 or APP in cases of FAD or due to a failure of Aβ clearance mechanisms, an accumulation and aggregation of these peptides affect the synaptic efficacy and directly injure the synapses and neurites in the brain. Soluble oligomers deposit as diffuse plaques and meanwhile an inflammatory response via astrocyte and microglia activation is initiated that causes an altered neuronal ionic homeostasis and oxidative injury. This in turn and soluble aggregates of Aβ trigger the activation of glycogen synthase kinase-3 beta (GSK-3β) (Koh et al., 2008) and other kinases that lead to a hyperphosphorylation of the microtubule stabilizing protein tau (Otth et al., 2002) that loses its affinity for microtubules (Mazanetz and Fischer, 2007) and forms neurofibrillary tangles (NFT) (Goedert et al., 1988; Lee et al., 1991). Finally, a synaptic and neuronal dysfunction, a severe loss of neurons and neurotransmitter deficits lead to dementia.

3.1.5 Familial Alzheimer´s Disease

Only the minority, approximately 5 % of the total number of AD cases, can be assigned to familial AD (FAD). In contrast to SAD, in most cases first symptoms of the disease can already occur in the 30s or 40s. This congenital form of early-onset AD (EOAD) can be ascribed to mutations in one of three genes: APP on chromosome 21, presenilin-1 (PS1) on chromosome 14 or presenilin-2 (PS2) on chromosome 1. All of these mutations lead to increased levels of Aβ. Most frequent are mutations in the PS1 gene with 75-80 %, followed by the APP gene with 20-25 % and the PS2 gene with less than 5 % (reviewed in Wu et al., 2012). In 30-50 % of autosomal dominant AD cases, mutations in these genes are responsible for the disease and thus, 0.5 % in AD in general. However, concerning APP, not only missense mutations (Fig. 3) but also the duplication of the gene, which is the case for Trisomy 21, is sufficient to cause AD (Rovelet-Lecrux et al., 2006; Sleegers et al., 2006). The genetics of late-onset AD (LOAD) appear to be more ambiguous, since only an allelic variation of the Apolipoprotein E (Apo E), the allele ε4, could be identified to be a risk factor for AD as the frequency of this allele in AD patients is 2-3 times higher than in healthy controls. Although the outbreak of the disease is at a much earlier age, the clinical symptoms remain the same compared to SAD. However, it has been shown that genetic factors change the spatial patterns of Aβ deposits to a greater deposition of Aβ in the form of

clusters of diffuse deposits in FAD, whereas a greater proportion of diffuse deposits may be converted to primitive deposits in SAD (Armstrong, 2011).

3.1.5.1 APPSWE

The APP Swedish double mutation (APPswe) has first been characterized in 1992 (Mullan et al., 1992). It was found in two large, probably related Swedish families both showing high risk of EOAD. The amino acid substitutions K670N (lysine to asparagine) and M671L (methionine to leucine) are located directly N-terminal to the β-cleavage site and alters the processing of APP leading to tremendous consequences in those who carry the mutation. Cells transfected with APPswe have been shown to secrete 6-8 times more Aβ, predominantly Aβ40 and Aβ42, than cells transfected with APP wt (Cai et al., 1993; Citron et al., 1992) due to an increased affinity of BACE-1 for that mutation. Since Aβ accumulation is predictable in the presence of that double mutation, it has been used in many murine AD models, such as 5xFAD mice, carrying mutations in the APP and presenilin 1 (*PSEN1)* genes (APP K670N/M671L (Swedish), APP I716V (Florida), APP V717I (London), PSEN1 M146L and PSEN1 L286V) (Oakley et al., 2006), J20 mice, carrying mutations only in the APP gene (K670N/M671L (Swedish) (Mucke et al., 2000) and the APP V717F (Indiana), or the 3xTg mice, carrying mutations in the APP, PSEN1 and the microtubule-associated protein tau (MAPT) genes (K670N/M671L (Swedish), MAPT P301L and PSEN1 M146V) (Oddo et al., 2003).

3.1.5.2 APPLON

The London mutation in APP is one of the first described mutations in the APP gene causing early-onset FAD. Two non-related families with affected individuals have been described carrying the mutation that results in a substitution from valine to isoleucine and is located at p717 and therefore in the transmembrane domain within the Aβ sequence in close vicinity N-terminal to the γ-secretase cleavage site (Goate et al., 1991). A transgenic mouse carrying the human APPLon gene shows high levels of Aβ1-42 and a deposition of amyloid at the age of 12 month. First memory deficits occur between 3 and 6 month (Moechars et al., 1999). Moreover, it was demonstrated that induced pluripotent stem cells (iPSC) overexpressing APPLon generate increased levels of Aβ38 and Aβ42 (Muratore et al., 2014). Additionally, Muratore and colleagues analyzed the co-localization of APPLon or APP wt to the endosomal marker EEA1 in overexpressing differentiated forebrain neurons via immunofluorescence which was increased for the FAD causing mutant. These results explain the likewise described increased BACE-1 cleavage product since active BACE-1 can be found in acidic compartments like early endosomes. However, since that mutation is distant from the

β-cleavage site it was of interest of this work if it can also affect the cleavage properties of meprin β in a manner to change the pattern of the ratio of generated Aβ variants.

3.1.5.3 PROTECTIVE MUTATION APP A673T

The A673T mutation has first been described by Jonsson and colleagues in 2012 (Jonsson et al., 2012). The substitution of the hydrophobic alanine to the hydrophilic threonine at position 673 of APP lies within the Aβ sequence at p2 (Aβ A2T) and thus, in immediate vicinity to the β cleavage site. The peculiarity of this APP mutant is that it is so far the only known mutation which protects from cognitive decline in the elderly and even more protects from AD. Coding variants of 1,795 Icelanders have been tabulated to screen for low-frequency variants which have an impact on the risk of developing AD. The single nucleotide polymorphism (SNP) which results in the substitution has been found to occur more likely in the healthy control group in the elderly than in the AD group. Moreover, it was shown that the cognitive decline in individuals at age 80-100 was dampened in carriers versus non-carriers. Due to the position of the substitution an impact on β-secretase cleavage has to be considered. Indeed, the analysis of BACE-1 mediated APP cleavage products of overexpressing HEK293T cells revealed that less cleavage occurs for APP A673T compared to APP wt. A decrease in sAPPα levels as in Aβx-40 and Aβx-42 levels has been shown. Simultaneously, sAPPβ levels were decreased in APP A673T, suggesting an impact of the mutation on BACE-1 cleavage efficiency. In follow-up studies evidence has been provided that not an impaired affinity of BACE-1 on APP A673T is the reason for decreased cleavage, but rather a modulation in the catalytic turnover rate (V_{max}) (Maloney et al., 2014). However, it has been proposed that not only impaired BACE-1 cleavage has protective effects. It has suggested that APP not only acts as a precursor for Aβ peptides but that it also appears to be a receptor for TGFβ2. It was described that TGFβ2 is a neuronal-death inducing ligand of APP that activated a death pathway via heterotrimeric G protein G(o), c-Junk N-terminal kinase, NADPH oxidase, and caspase 3 or related caspases (Hashimoto et al., 2005). The impact of this pathway has been shown to be more severe for mutants of APP that are associated to FAD than for wt APP. Interestingly, it has been demonstrated that the APP A673T mutant again shows protective effects concerning this Aβ independent neurotoxicity, since TGFβ2 did not induce cell death in neuronal cells overexpressing APP A673T (Hashimoto and Matsuoka, 2014). Different species of Aβ varying in length show different characteristics concerning their aggregation propensity and their toxicity (Bouter et al., 2013). For example, it has been shown that the longer variant Aβ1-42 shows a higher disposition for aggregation than Aβ1-40 and is thus more toxic and more meaningful for

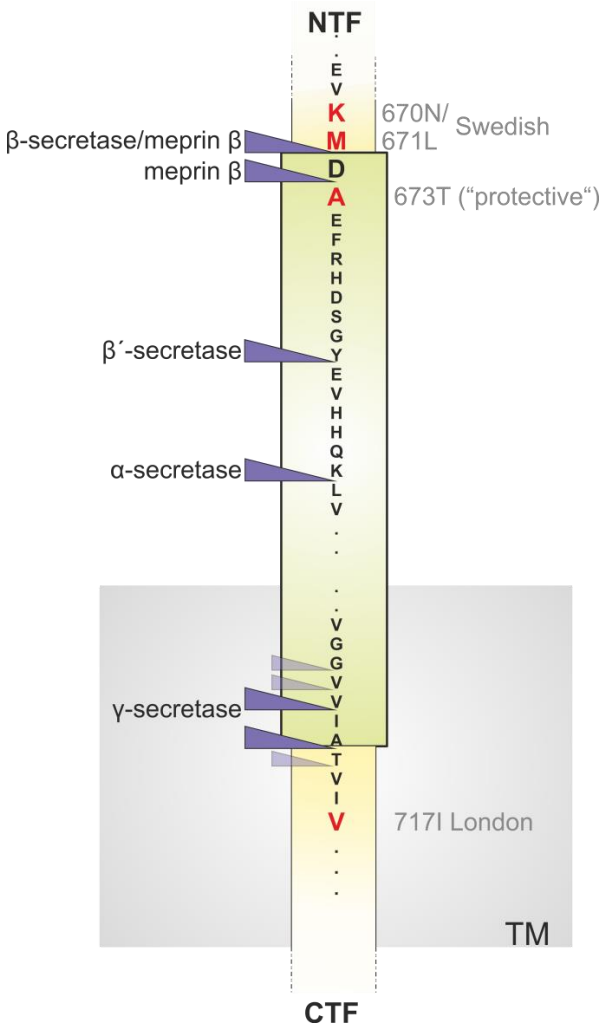

FIGURE 3 FAD associated mutations in the APP sequence

Besides mutations in the PS1 or PS2 genes, several mutations in the APP sequence can affect the processing of the protein. Depicted are the Swedish double mutation (K670N/M671L) and the London mutation (V717I), leading to increased Aβ1-40 and Aβ1-42 or only increased Aβ1-42 levels, respectively. In contrast, the recently identified "protective" mutation (A63T) decreases Aβ levels.

AD pathogenesis. But not only the length of the peptide is crucial for its characteristic, also single substitutions in the sequence appear to have an influence. Mutations at position 673 in APP and thus p2 in Aβ have been analyzed in context to their aggregation behavior. Here, it was observed that Aβ A2V shows an accelerated aggregation, whereas Aβ A2T displays a delayed aggregation (Benilova et al., 2014). Maloney and colleagues showed that this decreased aggregation can only be observed in Aβ1-42 A2T, but not in the shorter variant Aβ1-40 A2T (Maloney et al. 2014). Moreover, they detected a decreased microglial phagocytosis of Aβ1-42 A2T compared to Aβ1-42 wt. All these effects of a single substitution led to study the effect of this mutation on meprin β mediated cleavage of APP in this work.

3.1.6 γ-Secretase modulators

One therapeutical target in AD is the reduction of Aβ and thus the γ-secretase. However, as described above, the γ-secretase not only cleaves APP, but also Notch that has regulatory functions in neurogenesis, cell fate and cell communication. Thus, the inhibition of the γ-secretase has deleterious effects (reviewed in De Strooper, 2014). To circumvent this problem another strategy that still targets the γ-secretase has been developed. Non-steroidal anti-inflammatory agents (NSAIDs) like ibuprofen have been shown to influence the cleavage properties of the γ-secretase (Weggen et al., 2003). These γ-secretase modulators (GSM) do not block Aβ generation or lower the levels of total Aβ peptides but rather selectively decrease the production of specific AD critical Aβ variants. Moreover, levels of CTFs and other cleavage products of γ-secretase remained unaltered. Different kinds of GSMs were established: acidic, non-acidic and triterpenoid natural product derived GSMs. Acidic GSMs lower levels of Aβ1-42 and increase levels of Aβ1-38 (Page et al., 2008). Non-acidic GSMs decrease Aβ1-40 and Aβ1-42 levels and increase Aβ1-37 and Aβ1-38 (Kounnas et al., 2010). Triterpenoid GSMs decrease levels of Aβ1-38 and Aβ1-42 (Hubbs et al., 2012; Loureiro et al., 2013). However, the effect of GSMs on N-terminally truncated Aβ variants has not been studied so far and was thus studied in this work.

3.2 Meprins

3.2.1 Structural differences and similarities of meprin α and meprin β

Meprins (metallo-endoprotease from renal tissue) are zinc-endopeptidases that belong to the astacin family and metzincin superfamiliy and play an important role in development, physiological and pathological processes. They are phylogenetically related to matrix metalloproteases (MMP). They were discovered more than 35 years ago and were first found to be highly expressed in kidney and intestine (Beynon, 1981). There are two phylogenetically related subunits: meprin α and meprin β. They are ~40 % identical in their amino acid sequence (Fig. 4) and form disulfide-bonded homo- and hetero-oligomers. Membrane bound heterooligomers consisting of both subunits however, have only been detected in rodents (Bertenshaw et al., 2003), but not in humans, which was shown to occur unlikely, due to its crystal structure (Arolas et al., 2012). Further oligomerization is mediated by non-covalent interactions. Homooligomers of meprin α form the largest secreted proteases known, in a size of 1 to 6 MDa.

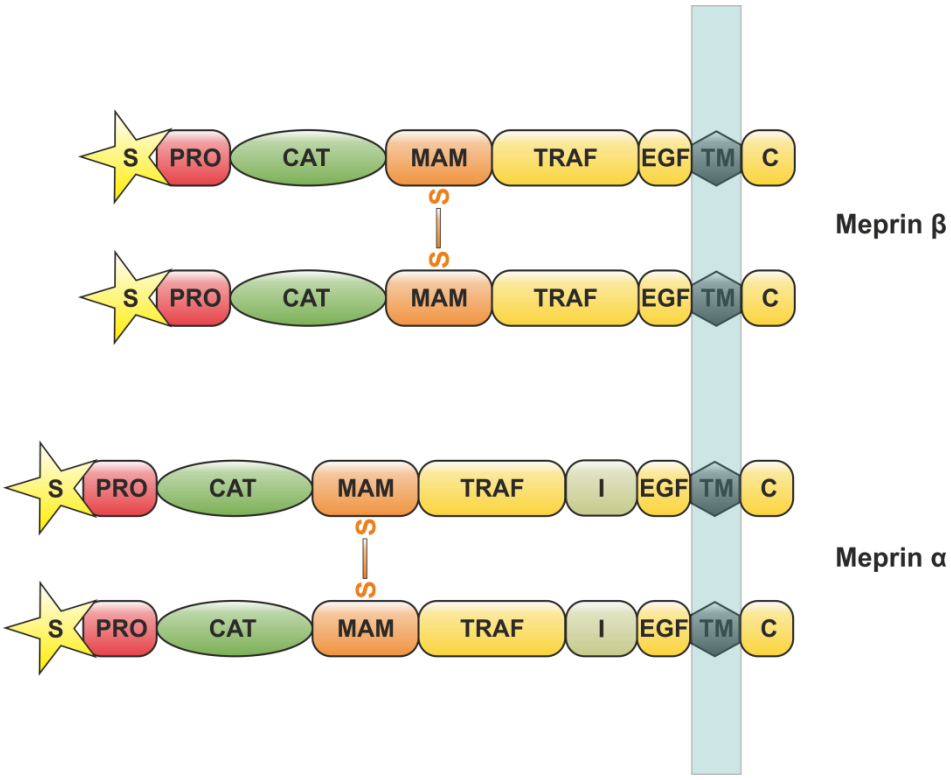

FIGURE 4 The metalloproteases meprin α and β

Both meprins share structural and domain similarities. Both contain a N-terminal propeptide, an astacin-like protease domain (CAT), a MAM (meprin A5 protein tyrosine phosphatase μ) domain and a TRAF (tumor-necrosis-factor-receptor-associated-factor). Disulfide bridges between the MAM domains of two proteins lead to dimerization. While meprin α dimers are shed by furin at their inverted domain and form non-covalently oligomers meprin β that lacks that domain, predominantly remains surface bound as a dimer.

Both meprins share structural and domain similarities. First, they have a N-terminal signal peptide that directs the protein to the endoplasmic reticulum (ER). Since meprins are expressed as inactive zymogens, they have a N-terminal propeptide, which needs to be cleaved off for proteolytic activity. This is followed by an astacin-like protease domain (CAT). The MAM (meprin A5 protein tyrosine phosphatase μ) domain and the TRAF (tumor-necrosis-factor-receptor-associated-factor) domain mediate protein-protein interactions. The dimerization of meprins is yielded by disulfide bridges between the MAM domains of two proteins. It has been shown that only one disulfide bridge is sufficient to form a dimer (Arolas et al., 2012). C-terminal to the TRAF domain lies the EGF (epidermal growth factor) domain, a transmembrane domain and a small C-terminal cytosolic tail. The major difference between both meprin subunits is the inserted domain between the EGF and the transmembrane domain that only occurs in meprin α. This small domain includes a furin cleavage site and thus meprin α can be

released from the cell surface after furin cleavage. Released meprin α dimers then form homooligomeric complexes in size of 1-6 MDa in the ER. Thus, meprin α only stays membrane bound when forming hetero oligomers with meprin β, which primarily remains surface bound since it is lacking the inserted domain. However, it can also be shed and released from the surface by ADAM10/17. This shedded form of meprin β has been shown to cleave only certain substrates, other than the membrane bound meprin β.

3.2.2 Expression, regulation and functions of meprin

The highly glycosylated meprin β is expressed as an inactive zymogen. Pancreatic trypsin and kallikrein-related peptidases (KLK) 4, 5 and 8 have been identified as activators for soluble meprin β (Ohler et al., 2010). However, only the transmembrane serine protease matriptase-2 (MT2) so far is capable in activating membrane bound meprin β, since the propeptide appears to be shielded due to its proximity to the plasma membrane (Jackle et al., 2015). Fetuin-A has been shown to be an endogenous inhibitor for meprin α and β (Hedrich et al., 2010). Also the fetuin-A homologue nephrosin has been shown to be capable in inhibiting both subunits. However, these and other synthetic inhibitors, like the potent hydroxamate actinonin (Kruse et al., 2004), lack in specificity.

In the 1980s meprins first have been found in intestine after an unexpected proteolytic activity has been found in intestines of patients after pancreas surgery (Sterchi et al., 1982). The same metalloprotease has been isolated and characterized from the mouse kidney in 1981 (Beynon et al., 1981). There it has been found to be localized in high concentrations at the brush boarder membrane of proximal tubule cells where it represents 5 % of all membrane proteins (Craig et al., 1987). An increased as well as a decreased expression of meprins has been associated with kidney diseases (Beynon and Bond, 1983). Moreover, nine SNPs in the *MEP1B* gene were found to alter the transcription of trafficking of meprin β, thus leading to diabetic nephropathy in Pima Indians (Red Eagle et al., 2005). Furthermore, meprins show a high expression in leucocytes of the lamina propria of human inflammatory sites, epithelial cells of the intestine and enterocytes of the small intestine, where it is in proximity to the mucin networks (Lottaz et al., 1999). There it has been found to play a role in the release of anchored small intestinal mucus (Schutte et al., 2014). However, cleavage of the gel-forming and major mucus component MUC2 mucin can only be cleaved by shedded meprin β.

Moreover, meprins have been suggested to play a role in the movement of macrophages to inflammatory sites, since they showed a decreased ability to move to those sites in meprin deficient mice (Crisman et al., 2004). Apparently, meprins play a crucial role in inflammation and inflammatory diseases like Crohn´s Disease (CD), where meprin mRNA levels are decreased (Vazeille et al., 2011) or inflammatory bowel disease (IBD) by modulating the immune environment by processing and activating proinflammatory cytokines like interleukins (IL), such as IL-1β (meprin α and β), IL-18 (meprin β) (Banerjee and Bond, 2008; Herzog et al., 2009; Li et al., 2014) or IL-6 (meprin α and β) (Keiffer and Bond, 2014).

Meprin α and β are constitutively expressed in skin, however they are localized in different layers (Becker-Pauly et al., 2007). The α subunit is expressed in the stratum basale, whereas the β subunit is expressed in the stratum granulosum where it induces the terminal differentiation of keratinocytes (Ohler et al., 2010) and might therefore be involved in cornification (Broder and Becker-Pauly, 2013). Moreover, both subunits are procollagen proteinases and induce the collagen fibril assembly (Broder et al., 2013).

Recently, it has been shown that meprin β mRNA levels are increased in AD brains (Bien et al., 2012). The same study and others also showed that the AD critical APP can serve as a substrate for meprin β (Jefferson et al., 2011). The further characterization of the interaction and interplay of both proteins was substance of this thesis.

3.2.3 MEPRIN SUBSTRATES AND CLEAVAGE SPECIFICITY

Via PICS (proteomic identification of protease cleavage site specificity) and TAILS (terminal amine isotopic labeling of substrates) the cleavage specificity of meprin could be characterized. Meprin β has been shown to prefer negatively charged amino acids in P1’ position. This is also true for meprin α, however, this preference was shown to be less pronounced (Becker-Pauly et al., 2011). Cleavage events in native protein confirmed the specificity, since both subunits showed an increased preference for aspartate and glutamate. No other proteases, despite the astacins BMP-1 (bone morphogenetic protein-1) and ovastacin, showed this cleavage specificity. The same study showed that meprin β is capable in cleaving completely acidic peptide sequences, which is a unique feature of this protease. The following table shows *in vivo* and *in vitro* substrates for meprin β.

TABLE 1 Substrates of meprin β (Proteins in *italic* have been validated *in vitro*.)

Substrates of meprin β	
Neuropeptide Y	(Bertenshaw et al., 2001)
GRP-(14–27)	(Bertenshaw et al., 2001)
gastrin	(Bertenshaw et al., 2001)
$sCCK8_{NH2}$	(Bertenshaw et al., 2001)
secretin	(Bertenshaw et al., 2001)
glucagon	(Bertenshaw et al., 2001)
cerulein	(Bertenshaw et al., 2001)
osteopontin	(Bertenshaw et al., 2001)
orcokinin	(Bertenshaw et al., 2001)
gastrin 17	(Bertenshaw et al., 2001)
peptide YY	(Bertenshaw et al., 2001)
kinetensin	(Bertenshaw et al., 2001)
IL-1β	(Herzog et al., 2005)
IL-18	(Banerjee and Bond, 2008)
E-cadherin	(Huguenin et al., 2008)
proKLK7	(Ohler et al., 2010)
APP	(Jefferson et al., 2011)
ADAM9	(Jefferson et al., 2012)
ADAM10	(Jefferson et al., 2012)
ADAMTS-1	(Jefferson et al., 2012)
BMP-1	(Jefferson et al., 2012)
MMP1	(Jefferson et al., 2012)
MMP7	(Jefferson et al., 2012)
PCSK9	(Jefferson et al., 2012)
IL-6	(Keiffer and Bond, 2014)
Procollagen III	(Broder et al., 2013)
MUC2	(Schutte et al., 2014)

3.2.4 MEPRIN β AND APP

Via a proteomics study, APP was recently identified as a potential substrate for meprin β (Jefferson et al., 2011). Here, it was shown that meprin β generated non-toxic N-terminal APP fragments. These fragments could be also found in human brain lysates of AD patients and healthy controls. Ongoing studies showed that meprin β is capable

in generating N-terminally truncated Aβ2-40 (Bien et al., 2012) suggesting a cleavage adjacent to the usual BACE-1 cleavage site. In this work, the interaction of meprin β and APP and its localization was investigated in more detail. Moreover, the relevance of mutations within the APP sequence was analyzed and the *in vivo* relevance of the metalloprotease characterized.

4 AIM OF THE STUDY

The importance of the metalloprotease meprin β in APP processing has become more obvious in recent studies. The protease has been first described to be highly expressed in kidney and intestine (Sterchi et al., 1982), but also in skin (Becker-Pauly et al., 2007). Different functions have been ascribed to meprin β like the induction of the terminal differentiation of keratinocytes (Ohler et al., 2010) or the cleavage of procollagen that induces collagen fibril assembly (Broder et al., 2013), but it has been also described to have a role in inflammation (Banerjee and Bond, 2008; Herzog et al., 2009).

In a proteomics based analysis APP has been found to be a potential substrate for meprin β that generates N-terminally APP fragments which could be detected in human brains (Jefferson et al., 2011). This protein is highly associated with Alzheimer´s Disease (AD) since sequential cleavage by the β-secretase BACE-1 and the γ-secretase results in the release of amyloid β (Aβ). Different characteristics, like aggregation behavior or toxicity, have been ascribed to different variants of the peptide that differ in their length. The arising of an imbalance of the normal ratio of Aβ forms is believed to be a primary event in AD. Interestingly, it was found that meprin β, which prefers acidic amino acids like glutamate or aspartate in P1´ position, is capable to function as a β-secretase and cleaves the N-terminus of Aβ between amino acids 671 and 672 of APP, but also adjacent to this position between amino acids 672 and 673 to generate N-terminally Aβ2-x *in vitro* (Bien et al., 2012), which has been shown to have a high aggregation propensity and a seeding effect on other variants (Schonherr et al., 2016).

Aim of this study was to characterize this cleavage event in more detail and to analyze the physiological role of meprin β with regard to a potential role in AD. Since increased mRNA levels have been detected in brains of AD patients, one question of this work was if this increase can also be detected on protein level, and if so, if this increase is also reflected in the ratio of different Aβ species or an increase in variants that are generated by meprin β. To further determine the *in vivo* role of the protease, it was of interest to analyze different APP fragments, which accrue during APP processing, in brains of wild type versus meprin β knockout mice.

Since BACE-1 cleavage of APP has been described to likely occur in acidic microdomains (Das et al., 2013) one aim was to study the subcellular co-localization of APP and meprin β via confocal fluorescence microscopy in overexpressing cells.

Moreover, the focus was set on the cleavage behavior of meprin β in dependence to different mutations in APP that are associated with FAD, but also the recently described protective APP A673T mutation (Jonsson et al., 2012).

5 MATERIAL AND METHODS

5.1 MATERIAL

5.1.1 CHEMICALS

30% Acrylamide 37.5:1 Bis-Acrylamide	National Diagnostics, Atlanta, USA
40% Acrylamide 19:1 Bis-Acrylamide	BioRad, Munich, Germany
40% Acrylamide 29:1 Bis-Acrylamide	National Diagnostics, Atlanta, USA
Agar	Carl Roth, Karlsruhe, Germany
Agarose-A-Beads	Thermo Fisher, USA
Ammoniumpersulfate (APS)	Sigma-Aldrich, Taufkirchen, Germany
B27-supplement	Thermo Fischer, USA
Bicine	Carl Roth, Karlsruhe, Germany
Bis-Tris	Carl Roth, Karlsruhe, Germany
Bovine Serum Albumin (BSA)	Sigma-Aldrich, Taufkirchen, Germany
Bromphenol blue	Roth, Karlsruhe , Germany
Calcium chloride ($CaCl_2$)	Merck, Darmstadt, Germany
DAPT (N-[N-(3,5-Difluorophenacetyl)-L-alanyl]-S-phenylglycine t-butyl ester)	Sigma-Aldrich, Taufkirchen, Germany
Desoxynucleotide-tri-phosphate (dNTP)	NEB, Frankfurt, Germany
Dimethylsufoxide (DMSO)	Sigma-Aldrich, Taufkirchen, Germany
DRAQ5™	Biostatus Limited, Leicestershire, UK
Dry-milk (fat-free)	VONS, USA
Dulbecco´s Modified Eagle´s Medium (DMEM)	Invitrogen, Karlsruhe, Germany
Dynabeads® M-280 Sheep Anti-Mouse IgG	Thermo Fisher Scientific, Waltham, Massachusetts, USA
Ethanol	Carl Roth, Karlsruhe, Germany
Ethidiumbromide (EtBr)	Sigma-Aldrich, Taufkirchen, Germany
Ethylenediaminetetraacetic acid (EDTA)	Carl Roth, Karlsruhe, Germany
Fetal Calf Serum (FCS)	Invitrogen, Karlsruhe, Germany
GlutaMAX™	Life Technologies, Darmstadt, Germany
Glycerol	Carl Roth, Karlsruhe, Germany
Glycine	Merck, Darmstadt, Germany
HEPES	Invitrogen, Karlsruhe, Germany

Hydrochloric acid (HCl)	Carl Roth, Karlsruhe, Germany
Immobilon^{TM} Western HRP Substrate Reagents	Millipore, Schwalbach, Germany
Isofluran	Forene® Abott, Wiesbaden, Germany
Isopropanol	Carl Roth, Karlsruhe, Germany
L-Glutamine	Invitrogen, Karlsruhe, Germany
Lipofectamine®2000	Invitrogen, Karlsruhe, Germany
Magnesium chloride ($MgCl_2$)	Carl Roth, Karlsruhe, Germany
Methanol	Carl Roth, Karlsruhe, Germany
MES-SDS electrophoresis buffer	Carl Roth, Karlsruhe, Germany
Neurobasal medium	Thermo Fisher, USA
Nitrocellulosemembrane	Hartenstein, Würzburg, Germany
Nonidet-P40	Roche, Mannheim, Germany
Opti-MEM	Invitrogen, Karlsruhe, Germany
Paraformaldehyde (PFA)	Sigma-Aldrich, Taufkirchen, Germany
Phosphate buffered saline (PBS)	Life Technologies, Darmstadt, Germany
Polyornithine	Sigma-Aldrich, Taufkirchen, Germany
Polybrene	Sigma-Aldrich, Taufkirchen, Germany
Ponceau S	Sigma-Aldrich, Taufkirchen, Germany
Potassium chloride (KCl)	Sigma-Aldrich, Taufkirchen, Germany
Prolong® Gold antifade reagent	Invitrogen, Darmstadt, Germany
Protease inhibitor cocktail tablets, EDTA free	Roche, Mannheim, Germany
Roti Load® (4x protein loading buffer)	Carl Roth, Karlsruhe, Germany
Sodium azide (NaN3)	Carl Roth, Karlsruhe, Germany
Sodium chloride (NaCl)	Carl Roth, Karlsruhe, Germany
Sodium dodecyl sulfate (SDS)	BioRad, Munich, Germany
Sodium di-hydrogen phosphate (NaH_2PO_4)	Merck, Darmstadt, Germany
Sodium hydroxide (NaOH)	Merck, Darmstadt, Germany
Sodium pyruvate	Invitrogen, Karlsruhe, Germany
Sucrose	Sigma-Aldrich, Taufkirchen, Germany
Synthetic Aβ peptides	VCPBIO, China
TEMED (N,N,N+,N+-Tetramethylendiamine)	BioRad, Munich, Germany
Tris-acetate	Carl Roth, Karlsruhe, Germany
Tris-base (Tris-OH)	Carl Roth, Karlsruhe, Germany
Tris-hydrochloride (Tris-HCl)	Carl Roth, Karlsruhe, Germany
Triton-X100	Sigma-Aldrich, Taufkirchen, Germany
Trypsin/EDTA	Invitrogen, Karlsruhe, Germany

Tween-20	Carl Roth, Karlsruhe, Germany
Urea	Applichem, Darmstadt, Germany
β-Mercaptoethanol	Roth, Karlsruhe

5.1.2 ANTIBIOTICS

Ampicillin	Sigma-Aldrich, Taufkirchen, Germany
Blasticidin	Sigma-Aldrich, Taufkirchen, Germany
Puromycin	Alexis, Loerrach, Germany
Penicillin/Streptomycin(Pen/Strep)	Invitrogen, Karlsruhe, Germany

5.1.3 KITS

BCA™ Protein Assay Kit	Pierce, Bonn, Germany
High Pure Plasmid Isolation Kit	Roche, Mannheim, Germany
Nucleo Bond® Xtra Midi Kit	MachereyNagel, Düren, Germany
Nucleo Spin® PCR Clean-up and Gel Extraction Kit	MachereyNagel, Düren, Germany

5.1.4 ANTIBODIES

TABLE 2 Primary antibodies (CT = C-terminal; NT = N-terminal; mab = monoclonal antibody; pab = polyclonal antibody)

Antigen	Name	Species	Type	Dilution	Reference/Supplier
Aβ	1E8	mouse	mab	1:150 (WB)	(Schieb et al., 2011)
Aβ	6E10	mouse	mab	1:300 (IF) 1:100 (IP)	Covance
Aβ	IC16	mouse	mab	1:500 (WB) 1:100 (IP) 1:300 (IF)	Hybridoma cell line
α-tubulin	α-tubulin	mouse		1:5000 (WB)	Sigma-Aldrich
APP, CT	CT15	rabbit	pab	1:5000 (WB)	(Sisodia et al., 1993)
APP, NT	22C11	mouse	mab	1:1000 (WB)	Millipore
β-Actin	β-Actin	rabbit	pab	1:5000(WB)	Sigma-Aldrich
BACE-1	BACE-1	rabbit	pab	1:1000 (WB)	Sigma-Aldrich
cis-Golgi	GM130	mouse	mab	1:300 (IF)	BD Biosciences
c-myc	9E10	mouse	mab	1:500(WB)	Hybridoma cell line
early endosome	EEA1	rabbit	pab	1:500 (IF)	Abcam
ER	PDI	mouse	mab	1:500 (IF)	BD Biosciences
meprin β	MEP1B	goat	pab	1:3000 (WB)	R&D Systems

meprin β	MEP1B	rabbit	pab	1:1000 (WB)	(see section 10.2.1)
Phospho-Thr	P-threonine	rabbit	pab	1:1000 (WB)	Cell-Signaling

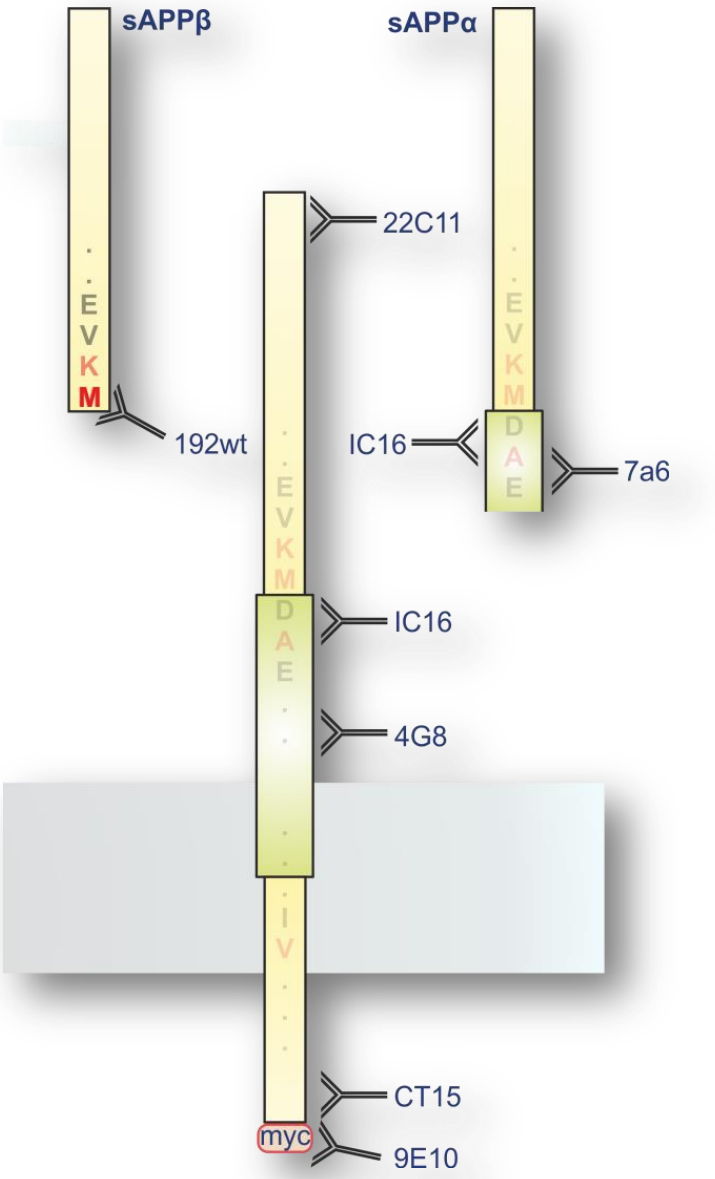

FIGURE 5 Antibody binding sites of APP and APP fragments

Antibody binding sites are illustrated. Note that 192wt antibody only recognizes the shorter sAPPβ variant mainly generated by BACE-1 (and partially meprin β) cleavage and not one amino acid longer variant generated by meprin β.

TABLE 3 Secondary antibodies

Antigen	Conjugate	Dilution	Reference/Supplier
Goat-anti-rabbit IgG	HRP	1:5000 (WB)	Sigma-Aldrich
Donkey-anti-mouse IgG	HRP	1:5000 (WB)	Dianova
Rabbit-anti-goat IgG	HRP	1:3000 (WB)	Sigma-Aldrich
Goat-anti-rabbit IgG	Alexa-Fluor546	1:1000 (ICC)	Invitrogen
	Alexa-Fluor546	1:1000 (ICC)	Invitrogen
	Alexa-Fluor546	1:1000 (ICC)	Invitrogen
	Alexa-Fluor488	1:1000 (ICC)	Invitrogen
	Alexa-Fluor488	1:1000 (ICC)	Invitrogen

5.1.5 LABORATORY HARDWARE AND EQUIPMENT

Agarose gel documentation imager	INTAS, Göttingen, Germany
Agarose gel electrophoresis chamber	Biometra, Göttingen, Germany
Anthos platereader 2010	Anthos Labtec, Salzburg, Austria
BioPhotometer plus UV/vis	Eppendorf, Hamburg, Germany
Cell culture dishes (6cm,10cm)	TPP, Trasadingen, Switzerland
Centrifuge Hereus Fresco	Kendro, Langenselbold, Germany
Centrifuge Hettich Universal 32	Hettich, Tuttlingen, Germany
Centrifuge Sorvall RC5B	Kendro, Langenselbold, Germany
CO_2 incubators	New Brunswick, USA
Coverslips	Marienfeld, Lauda-Königshofen, Germany
Cryo freezing container	Nunc, Wiesbaden, Germany
Cryo vials	Nunc
Flatbed shaker Infors	Bolmingen, Switzerland
Freezer -20°C	Liebherr, Germany
Freezer -80°C	Heraeus, Hanau, Germany
Fridge +4°C	Privileg, Germany
Glassware	Schott, Mainz, Germany
Heating block	Grant, Berlin, Germany
Incubator (bacteria)	Binder, Tuttlingen, Germany
Laminar flow	Nunc, Wiesbaden, Germany
LAS 3000 FujiFilm	Fuji, Japan
LAS-3000mini	Fujifilm, Duesseldorf, Germany
Light-optical microscope	Wilovert, Wetzlar, Germany
Light-optical microscope	OLYPMPUS, Hamburg, Germany
LSM710 Confocal Microscope	Zeiss, Jena, Germany
Magnetic stirrer	Heidolph, Kehlheim, Germany

Microwave	Micromaxx
Mini Protein III, Western Blotting System	BioRad, Munich, Germany
MiniTrans-Blot® Cell	Biorad, Munich, Germany
Optima™ TLX Ultracentrifuge	Beckman Coulter, USA
Optiplex 960 PC	Dell, USA
Pasteur pipettes	Carl Roth, Karlsruhe, Germany
pH-meter	inoLab, Weinheim, Germany
Pipettes (0.1- 1000 µl)	Eppendorf, Hamburg, Germany
Pipettor AccuJet	VWR, Darmstadt, Germany
T3 Thermocycler	Biometra, Göttingen, Germany
Trans-Blot® SD Semi-dry transfer	Biorad, Munich, Germany
Vortex-Genie 2^{TM}	Bender & Hobein AG
Waterbath GFL1086	GFL, Burgwedel, Germany

5.1.6 SOFTWARE

ADAP
Adobe Photoshop CS3
Chromas 2.33
Clonemanager
CorelDRAW X6/7
EndNote X5
GraphPadPrism 4/5
ImageJ 1.44, NIH
Microsoft Excel 2010
Microsoft Office 2010
Multi Gauge V3.0
SECentral7.0
ZEN2008

5.1.7 ANIMALS

C57BL/6 wild type mice were purchased from Jackson Laboratories (Bar Harbor, Maine, USA). *Mep1b*$^{-/-}$ mice (strain C57BL/6) were kindly provided by Christoph Becker-Pauly (Institute of Biochemistry, Christian-Albrechts University, Kiel). Mice were kept under a 12 h light cycle with food and drinking water ad libitum in the respective animal facilities. Mice were housed, anesthetized and sacrificed according to the European and German guidelines for the care and use of laboratory animals.

5.2 Cell Biological Methods

All cells were maintained under sterile conditions in a qualified S1/S2 laboratory. All equipment was cell culture qualified.

5.2.1 Cultivation of immortalized cell lines

All cells were maintained and passaged under sterile conditions in DMEM complete (Dulbecco's modified eagle's medium supplemented with 10% fetal calf serum (FCS); 5% pyruvate; 1% penicillin streptomycin) supplemented with 10% FCS; 5% pyruvate, 1% penicillin streptomycin) in an incubator at 37°C and 5% CO^2 in 10 cm dishes. Cells were passaged every second day. Adherent cells were detached by trypsinization and resuspended and seeded in fresh culture medium in an appropriate dilution depending on each cell line.

5.2.2 Cell lines

TABLE 4 Immortalized cell lines used in this study

Cell line	origin	Cell type	Cultue medium
HEK293T	human	Embryonic kidney cells	DMEM complete
GP2-HEK293T	human	Embryonic kidney cells	DMEM complete
N2a	mouse	Neuroblastoma cells	DMEM complete
MEF	mouse	Murine embryonic fibroblasts	DMEM complete

5.2.3 Cryoconservation of immortalized cells

For cryoconservation, cells were typsinized and pelleted at 1200 rpm for 4 min. Cells were resuspendend in 1 ml culture medium containing 10% dimethyl sulfoxide (DMSO), transferred to a cryotube and subsequently put on ice for 10 min. Afterwards, cells were stored at -80°C or in a liquid nitrogen tank.

5.2.4 Revitalization of cryoconserved cells

Cells were quickly thawed in a waterbath at 37°C and then diluted in 10 ml fresh culture medium. To eliminate DMSO, cells were pelleted and resuspended and seeded on a culture plate in fresh culture medium.

5.2.5 Transient transfection via the polyethylenimine (PEI) method

HEK293T cells were seeded in 6-well plates at a density of 300'000 cells/well. 24 h post seeding they were transfected by adding 1 µg DNA and 4 µl PEI in 60 µl serumfree medium per well. 4 h post transfection the medium was refreshed with either fresh or compound supplemented medium and stored in the cell incubator for respective incubation time. For all transient transfections the vectors pLHCX or pLBCX were used.

5.2.6 TRANSIENT TRANSFECTION VIA THE CALCIUM PHOSPHATE METHOD

HEK293T cells were seeded in 6-well plates at a density of 300'000 cells/well for transfection 24 h later. 8.3 µl of 2.5 M $CaCl_2$ was mixed with 75 µl H_2O, before adding 2 µg in total of plasmid DNA. Then, 83 µl of 2x HEPES (4-(2-hydroxyethyl)-1-piperazineethanesulfonic acid) buffer was added under air bubbling for 10 sec. The transfection batch was incubated for 20 min at room temperature. Meanwhile, cell medium was refreshed and afterwards, DNA mixture was added. After a 4 h incubation at 37°C and 5% CO_2, the DNA mixture containing medium was exchanged with fresh or compound supplemented medium and cells were set back to the cell incubator for 24 h. For the transfection of GP2-293T cells in 10 cm dishes (see below), six fold volume was used containing 10 µg of pVSV-G and 10 µg target DNA.

5.2.7 STABLE TRANSFECTION

Stably overexpressing cells were generated via lentiviral transfection. Lentiviruses are used to introduce genes into an *in vitro* system since they are capable to integrate their genome into the genome of non-dividing cells. Due to safety reasons, lentiviral vectors do not carry all required information for their replication. Thus, a packaging cell line that stably expresses the genes *gag*, encoding for capsid, and *pol*, encoding for the reverse transcriptase, is required. Here, GP2-HEK293T cells were used. The *env* gene encoding for the envelope protein of the vesicular stomatitis virus (VSV) which is further required for the generation of viral particles, is delivered by transfection of the pVSV-G plasmid. Additionally, the plasmid containing the target DNA, which is marked by the presence of the ψ (psi) sequence to be packaged into the viral particle, is transfected.

For this purpose, GP2-293T cells were seeded on a pre-coated 10 cm dish in a manner to yield 60-80 % confluency on the next day. To aim higher transfection efficiency 25 µM chloroquine was added to the cells on the next day. 2 h later, cells were transfected with the 10 µg pVSV-G plasmid and 10 µg of the respective pLHCX/pLBCX construct via the calcium phosphate transfection method. 4 h post transfection, media was refreshed, and henceforward, kept under S2 conditions. The media was again refreshed 24 h later and reduced to 5 ml to concentrate secreted virus particles. On the next day, the medium of GP2-293T cells was collected and dead cells were removed by centrifugation for 4 min at 1200 rpm. 2 ml of viral supernatant was added to target cells at a density of 50 % confluency in 500 µl fresh growth medium supplemented with 25 µg/ml polybrene. 24 h later, viral medium was exchanged with fresh medium and cells were set under antibiotic selection for two weeks to assure elimination of non-transfected cells.

5.2.8 Antibiotic selection of stably overexpressing cells

All retroviral vectors that were used for stable transfection of cells encode an antiobiotic resistance gene. Here, pLHCX, encoding for the hygromycin B resistance gene, and pLBCX, encoding for the blasticidin restitance gene, were used. Thus, to eliminate non-transfected cells, cells are incubated in medium supplemented the respective antibiotic for two weeks. For HEK293T cells 130 µg/ml hygromycine B or 7 µg/ml blasticidin was used, respectively.

5.2.9 Treatment with γ-secretase modulators

Transiently or stably APP wt overexpressing HEK293T cells were transiently co-transfected with empty vector, meprin β or BACE-1. 4 h post transfection medium was refreshed with 1.2 ml/well medium for 6-well plates and 4.5 ml/dish medium for 6 cm dishes, containing 200 nM GSK γ-secretase modulator, 200 nM Merck γ-secretase modulator or DMSO as vehicle control in an equal volume to modulators.

5.2.10 Preparation of primary cortical cultures

Primary cortical neurons were obtained from prenatal (E15) C57BL/6 wild type or *Mep1b*$^{-/-}$ mice. For this purpose, females were anesthetized with isofluran and sacrificed by neck fracture. The uterus was dissected and transferred into PBS in a 10 cm dish. Following, embryos were prepared out of the amnion and decapitated in a 6 cm dish in ice cold PBS and then brains were prepared from the heads in a 4 cm dish filled with ice cold HBSS and cortical tissue was carefully flattered with tweezers. For trypsinization the cortical tissue was transferred to 10 ml warm trypsin and incubated for 20 min on a shaker. After a following centrifugation step at 1200 rpm for 2 min, trypsin was discarded and the pellet carefully resuspended in neurobasal medium. The suspension was then filtered through two nybolt gaze into 10 ml of neurobasal medium. After additional pelleting at 1200 rpm for 5 min, the cells were resuspended in 10 ml warm neurobasal medium and then counted with a Neubauer counting chamber. The dissociated neurons were then seeded at a density of 63,000 cells/cm^2 on polyornithin (Sigma) precoated 6-well culture dishes (1:100 in PBS, 30 min) and maintained in 2 ml Neurobasal/B27 media (Gibco) supplemented with Glutamax (Gibco) per well.

TABLE 5 Media for the preparation of primary neurons

Media for preparation	supplemented with
500 ml Neurobasalmedium	10 ml B27 supplement (50 x) 5 ml Glutamax (100 x) 5 ml PenStrep
Trypsin 1 x in PBS	
HBSS	
PBS	
Polyornithin	

5.2.11 Adenoviral infection of primary cortical neurons

To overexpress APP695 in murine primary cortical cells, the cells were infected with a recombinant adenovirus expressing human APP695 at a concentration of 100 pfu/cell for 6 hours in DIV1. For this purpose, 1 ml of conditioned medium was removed from each well and stored at 37°. Afterwards, the virus was added in 1 ml of fresh Neurobasal/B27 media to 1 ml of the remaining conditioned medium and set on 37°C and 5% CO_2. After 6 h the virus containing medium was replaced with 1 ml of the stored conditioned medium and set back to the incubator. Supernatants and cells were collected 24 h post infection. All contaminated material was handled and disposed according to S2 safety instructions.

5.3 Protein biochemical methods

5.3.1 Cell lysis and protein extraction

24 h post transfection or compound treatment, HEK293T cells were lysed in NP-40 lysis buffer (500 mM Tris, pH 7.4, 150 mM NaCl, 5 mM EDTA, 1% (v/v) Nonidet P-40, 0.02% (v/v) Sodium Azide), plus Complete Protease Inhibitor Cocktail (Complete, Roche) for 20 min at 4°C on ice. Cell debris was eliminated by subsequent pelleting by centrifugation at 20.000 x g for 20 min at 4°C in a microcentrifuge.

5.3.2 Preparation of murine brain lysates for co-immunoprecipitation

Brains were homogenated in a glass homogenizer in co-IP lysis buffer [20 mM TrisHCl (pH7.5), 150 nM NaCl, 0.5 % Triton, protease inhibitor cocktail (Complete, Roche)] and lysed for 20 min of ice. Afterwards, samples were centrifuged at 4°C for 20 min, full speed. The supernatants were transferred to a new vial and immediately use for (co-) immunoprecipitation.

5.3.4 PREPARATION OF HUMAN BRAIN TISSUE LYSATES

Brain homogenates were prepared by homogenizing samples in a glass homogenizer in radio-immunoprecipitation (RIPA) buffer [50mM Tris-HCl, pH 8.0, 150mM NaCl, 1% octylphenoxy polyethoxyethanol (IGEPAL), 0.1% Sodium dodecyl sulfate (SDS), 0.5% deoxycholate] containing 10mM NaF, 1mM β-glycerophosphate, protease inhibitor cocktail (Complete, Roche Applied Science), phosphatase inhibitor cocktail (PhosSTOP, Roche Applied Science) in a six-fold volume to weight ratio. After incubation for 30 min on ice, the homogenates were either centrifuged at 100'000 xg (55000 rpm in a TLA120.2 rotor in a Beckman's Optima TLX ultracentrifuge) at 4°C for 30 minutes or at 14'000 rpm (full speed) in a tabletop centrifuge at 4°C for 2.5 h. The supernatants were transferred into a new vial and either used immediately or stored at -80°C.

5.3.5 BCA ASSAY

To determine the concentration of proteins of cleared lysates, a bicinchoninic acid (BCA) assay was conducted. In an alkaline environment peptide bonds reduce Cu^{2+} ions from copper (II) sulfate to Cu^{+}. Following, two molecules of bicinchoninic acid chelate with each Cu^{+} ion forming a purple-colored product. Since this color change is proportional to the amount of protein, the protein concentration can be determined by measuring the purple product that absorbs light at a wavelength of 562 nm with a plate reader.

Here, 1 ml of a 50:1 dilution of solution A containing sodium carbonate, sodium bicarbonate, bicinchoninic acid and sodium tartrate in 0.1M sodium hydroxide and solution B containing 4% cupric sulfate was added to 50 µl of a 1:10 dilution of each sample and additionally to a standard series of defined concentrations of bovine serum albumin (BSA) (0 µg/ml, 100 µg/ml, 200 µg/ml, 300 µg/ml, 400 µg/ml and 500 µg/ml) and incubated for 30 min at 60°C. Samples and standard series were measured in a plate reader at 562 nm and evaluated with ADAP version 1.6 Anthos Labtec, Instruments.

5.3.6 DYNABEAD IMMUNOPRECIPITATION

The immunoprecipitation (IP) of Aβ peptides was performed using magnetic dynabeads M-280. In advance, magnetic dynabeads M-280 containing sheep-anti-mouse-IgG attached to their surface were activated over night with 6E10 antibody (Covance) or IC16 antibody (1:100) for murine samples, both recognizing residues 1-16 of the human Aβ sequence, according to manufacturer's protocol. For the precipitation of Aβ peptides of cell supernatants and following separation on 8 M urea gels, supernatants

were reduced to 1.2 ml/well in a 6-well plate after transfection to yield highly concentrated medium. 24 h post transfection supernatants were collected and normalized according to protein content of cell lysates. 200 µl 5-fold concentrated IP detergent buffer (50 mM HEPES pH 7.4, 150 mM NaCl, 0.5% (v/v) Nonidet P-40 (NP40), 0.05% (w/v) SDS and protease inhibitor cocktail (Complete, Roche) was mixed with 800 µl of supernatant. For the precipitation of Aβ from brain homogenates 2.5 mg of lysate was mixed to 5-fold IP detergent buffer. After addition of 25 µl pre-activated beads, samples were incubated for 15 h at 4°C and afterwards washed three times for 5 min with PBS, 0.1% BSA and once for 3 min with 10 mM Tris-HCl, pH 7.5. In between the washing steps the Eppendorf tubes containing the samples were set to a magnetic rack to separate beads from supernatant to aspirate the washing buffer in this manner. Separation from beads was performed through boiling samples at 95°C in 25 µl sample buffer (0.36 M Bis-Tris, 0.16 M Bicine, 1% (w/v) SDS, 15% (w/v) sucrose and 0.0075% (w/v) bromophenol blue). 15 µl of these samples were separated on 8 M urea gels.

5.3.7 De-Phosphorylation of Aβ precipitates

De-phosphorylation of Aβ-A2T precipitates was performed applying λ-phosphatase (New England Biolabs) after the last washing step of dynabead IP. 400'000 units λ-phosphatase were added in Protein NEBuffer for MetalloPhosphatase (1x) to each sample and incubated at 30°C for 45 min. Afterwards, samples were set to magnetic rack to separate beads from λ-phosphatase containing buffer, and finally eluted in 25 µl dynabead sample buffer.

5.3.8 Co-Immunoprecipitation of meprin β and APP from murine brains

Co-immunoprecipitation provides the opportunity to detect protein-protein interactions. Since during a regular IP, proteins that are interacting with the precipitated protein are also purified, western blots of precipitates can be tested with an antibody directed against the protein suspected to interact with the precipitated protein.

Here, whole brains of C57BL/6J wt mice and *Mep1b*$^{-/-}$ mice were lysed in co-immunoprecipitation buffer for 20 min on ice. Cell debris was eliminated by centrifugation at full speed. Per sample containing 10 mg of total protein each, 30 µl sepharose protein G beads, mixed with either 22C11 antibody (anti-APP) in a final dilution of 1:100 or meprin β antibody (see supplement 10.2.1) in a final dilution of 1:100 at a total volume of 800 µl, was added. Bead-antibody master mixes were prepared to avoid concentration differences between samples. Samples were incubated overnight at 4° on a rotation wheel. On the next day, samples were washed

three times with ice cold PBS. Then, precipitates were eluted by boiling at 95° for 5 min in 25 µl 2x Roti-load. Finally, beads were eliminated by centrifugation at full speed for 2 min. Precipitates were separated on a NuPAGE precast 4-12 % gradient gel.

5.3.9 SDS-PAGE

SDS polyacrylamide gel electrophoresis (SDS-PAGE) allows the separation of proteins and peptides by their molecular weight in an electric field (Laemmli, 1970). Before the electrophoretic separation samples were boiled for 5 min in SDS and β-mercaptoethanol containing sample buffer to denature secondary and non–disulfide–linked tertiary structures and to dissociate proteins into their subunits. Moreover, the SDS binds to proteins and thereby applies a negative charge to each protein proportional to its mass.

Here, either precast gradient gels (4-12% NuPAGE, Novex) or self-made 10 or 12% gels, prepared using Biorad Mini-PROTEAN electrophoresis glass plates with 1.5 mm thickness, were used. Gels were mounted in a Biorad Mini-PROTEAN or Novex electrophoresis system and SDS- or MES-running buffer was added, respectively. Samples were run at 120 V.

5.3.10 Urea gel

Usual SDS polyacrylamide gel electrophoresis separates proteins according to their size (see above). However, this method is not precise enough to differentiate between small peptides that only differ in the length of one amino acid, for instance different Aβ variants. Klafki and colleagues described a suitable alternative for this approach, as they added urea to the SDS-Page system (Klafki et al., 1996). By applying 8 M urea to the bicine/Tris SDS–PAGE system, electrophoretic separation of these small peptides is possible. Here, not only the protein size is crucial for separation; another important factor is the hydrophobicity. In the conventional SDS-PAGE system, SDS binds proportional to the number of amino acids of the peptide/protein and thus to its length. In the presence of urea, however, SDS binds proportional to the sum of the hydrophobicity consensus indices of the constituent amino acids (Kawooya et al., 2003). Hence, it is not only possible to separate peptides differing in length of one amino acid, but proteins/peptides show also an unusual electrophoretic mobility. The longer Aβ1-42 for example, migrates faster than the shorter Aβ1-40, since Aβ1-42 bears the hydrophobic amino acids isoleucine and alanine that are missing in Aβ1-40 (Fig. 6).

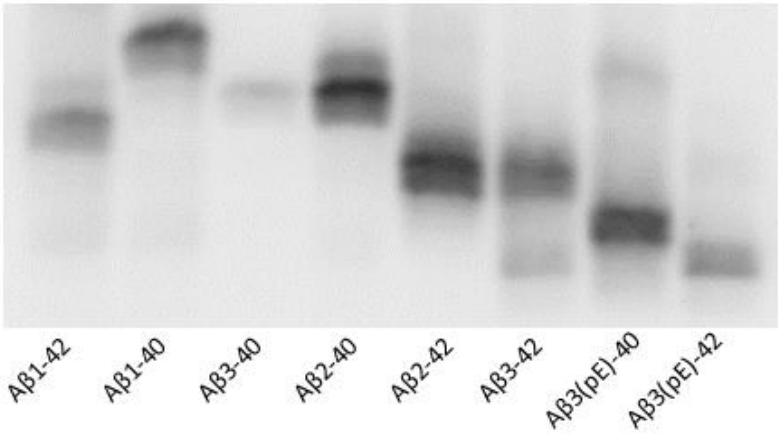

FIGURE 6 Running characteristics of Aβ variants on urea gels
Synthetic Aβ peptides are separated on an 8 M urea gel and semi-dry blotted on a PVDF membrane. Notably, variants bearing more hydrophobic amino acids migrate faster than shorter variants with less hydrophobic amino acids.

The urea bicince/Tris SDS-PAGE system is composed of a separation gel, a stacker gel and a comb gel.

Gels were prepared using Biorad Mini-PROTEAN electrophoresis glass plates with 0.75 mm thickness. After full polymerization, gels were mounted in a Biorad Mini-PROTEAN electrophoresis system and cathode buffer and anode buffer were added, respectively. Samples were run at 25 mA/gel and maximum voltage until dye front ran out of the gel.

Separation gel 8 M urea, 10%T 5%C acrylamide, 0.25% SDS	
urea [g]	4.8
separation gel buffer (1.6 M Tris/0.3 M H_2SO_4)[ml]	2.5
40% T 5.2%acrylamide (19:1) [ml]	2.5
10% SDS [ml]	0.25
H_2O_{dd} [ml]	1.01
10% APS [µl]	80
TEMED [µl]	10
Vol_{final} [ml]	10

Stacking gel 6%T 3%C acrylamide	
stacking gel buffer (0.8 M BisTris/0.2 M H_2SO_4) [ml]	1
40% T 5.2%acrylamide (29:1) [ml]	0.3
1% SDS [ml]	0.5
H_2O_{dd} [ml]	0.2
10% APS [µl]	10.5
TEMED [µl]	3.5
Vol_{final} [ml]	2

Comb gel 6%T 3%C acrylamide	
comb gel buffer (0.72 M BisTris/0.32 M Bicine/0.1% SDS) [ml]	1
40% T 5.2%acrylamide (29:1) [ml]	0.3
1% SDS [ml]	0.5
H_2O_{dd} [ml]	0.2
Bromphenol blue 1% (w/v) [µl]	10
10% APS [µl]	12
TEMED [µl]	4
Vol_{final} [ml]	2

(T = Total concentration of acrylamide and bisacrylamide monomer; C = bisacrylamide concentration)

5.3.11 WESTERN BLOTTING

Western Blotting is a technique to detect specific proteins/peptides of a protein mixture and to determine their levels after previous separation of proteins by size via SDS-PAGE. During this step proteins are transferred to a membrane for following immunodetection with antibodies. Usually applied membranes are polyvinylidene difluoride (PVDF) or nitrocellulose membranes which differ in protein binding capacities and binding interactions. While PVDF membranes have a high protein binding capacity, which makes detection of lowly expressed proteins feasible, they are also likely to show more background signal. Contrary, nitrocellulose membranes have a lower binding sensitivity, but also show lesser background signals. Protein transfer to the membrane is held in an electrophoresis chamber, either for wet blotting or semi-dry blotting. After the transfer the membranes were blocked in 5% non-fat dry milk in TBST (TBS; 0.01% (v/v) Tween-20) for 0.5 to 1 h to avoid unspecific binding of antibodies to the membrane. Blocked membranes were incubated with respective primary antibody at 4°C overnight and appropriate HRP-conjugated secondary antibody for 1 h at room temperature. Between incubation steps, blots were washed 3 x for 10 min with TBST. Secondary antibodies were detected via electrochemiluminescence (ECL) using the horseradish peroxidase (HRP) substrate Immobilon and were visualized with the FUJIFILM LAS-3000mini analyzer.

5.3.11.1 WET WESTERN BLOTTING

For wet western blotting, gel and membrane were arranged between sponges and two whatman filter papers, equibrilated in blotting buffer, and transferred in a blotting tank filled with blotting buffer via applying voltage of 70 V for 90 minutes vertical to the protein running direction on the gel.

Blotting buffer	
tris base	25 mM
glycine	1.92 M
methanol	20%

5.3.11.2 SEMI-DRY WESTERN BLOTTING WITH DISCONTINUOUS 3-BUFFER SYSTEM

The semi-dry western blotting method with discontinuous 3-buffer system was used to transfer samples containing Aβ peptides that were separated via urea gel to a PVDF membrane. For this approach filter papers are equilibrated in buffer A, B or C for 15 minutes. Since PVDF membranes are highly hydrophobic and are not wetted properly by aqueous buffers, they need to be activated by incubation with methanol for 5 minutes. Afterwards, methanol is washed off with H_2O_{dd} before and transferred to buffer B. For transfer, membrane and gel are both sandwiched between pre-equibrilated filter papers and placed between cathode and anode (see Fig. 7). The migration of protein from gel to membrane is achieved by applying a constant power of 47 mA/gel for 45 minutes.

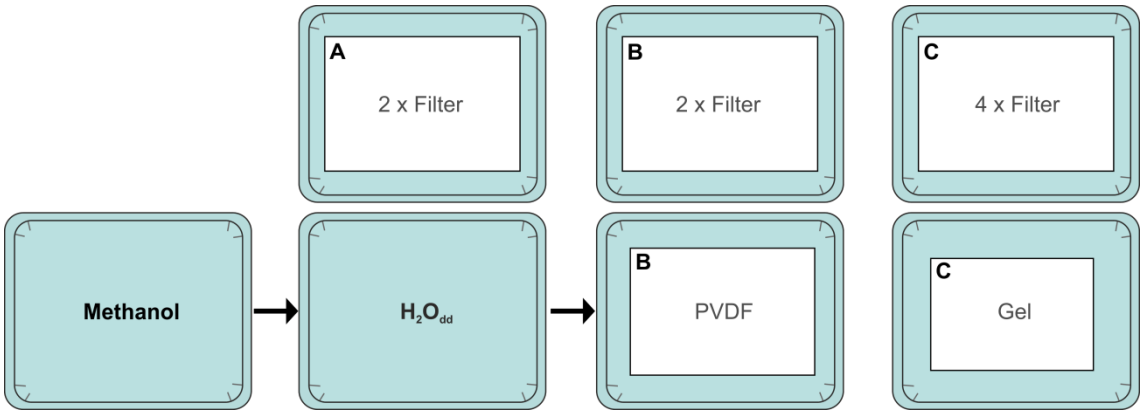

FIGURE 7 Preparation of a semi-dry western blot

Before blotting, filter papers need to be equilibrated for 15 minutes in blotting buffer A, B or C. The PVDV membrane is first activated with methanol, washed with H_20 and then also equilibrated in blotting buffer B.

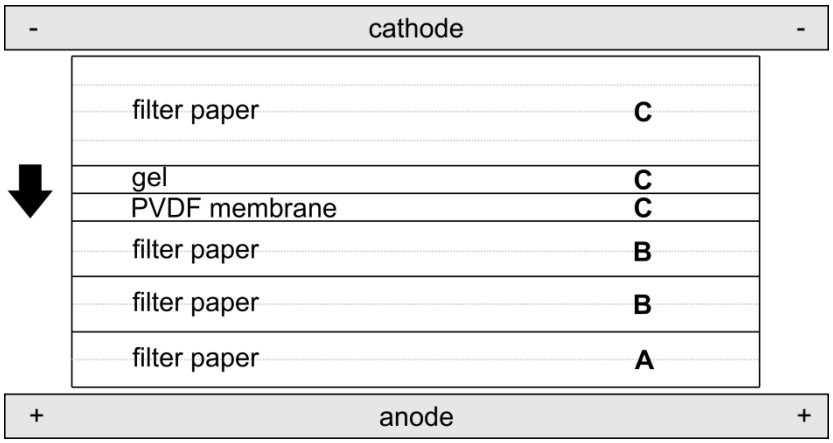

FIGURE 8 Stacking order of filter papers for semi-dry western blotting
Gel and PVDF membrane are sandwiched between filter papers between anode and cathode. First, filter papers equilibrated in buffer A are put on the anode, followed by filter papers equilibrated in buffer B, then membrane, gel and finally filter papers equilibrated in buffer C.

Cathode buffer

- **C**: 25 mM Tris 0,025% SDS with boric acid auf pH 9,0

Anode buffer

- **B**: 25 mM Tris 30% methanol pH 10,4
- **A**: 210 mM Tris 30% methanol pH 10,4

5.3.12 Densitometric analysis of western blots

The intensity of protein bands on western blots were analyzed with ImageJ 1.47c or Multi Gauge V3.0 software. Here, background signal values were subtracted from values of protein bands. Moreover, protein levels were normalized to actin or tubulin levels.

5.3.13 Enzyme linked immunosorbent assay (ELISA)

The enzyme linked immunosorbent assay (ELISA) is an antibody based method to detect proteins.

Samples were analyzed by the Aβ Triplex Immunoassay from Meso Scale Discovery using the sulfo-tagged 4G8 antibody for mouse Aβ detection. Aβ40 concentration was calculated using the MSD Discovery Workbench Software. The ELISA was performed together with Katrin Mosche of the laboratory of Prof. Lichtenthaler, DZNE Munich, Germany.

5.3.14 MATRIX ASSISTED LASER DESORPTION IONIZATION MASS SPECTROMETRY ANALYSIS (MALDI-MS)

MALDI-MS enables to determine molecule masses in a usual range of 5 to 100 kDa. Moreover, it can be used for the analysis of peptides and proteins.

For this approach, the analyte is co-crystallized with a matrix, consisting of low-molecular substances, such as dithranol, and spotted on a sample slide. Its radiation with a focused laser beam in the far red or UV ranges results in the vaporization of the matrix that strongly absorbs the energy and indirectly vaporizes the analyte. Since the matrix also serves as a proton donor and receptor, it additionally ionizes the analyte. However, the exact mechanism of ionization is yet unclear and still debated. After the ionization, molecules are linearly accelerated through a linear flight tube in direction to a detector that measures the time of flight (TOF). Their time of flight is dependent on their mass to charge (m/z) ratio. The acquired data can be used to identify peptides/proteins by comparison to protein databases.

5.3.14.1 Aβ PREPARATION FROM CELL CULTURE MEDIA FOR MALDI-MS MEASUREMENTS

Conditioned cell supernatants from 6 cm dishes of transiently transfected HEK293T cells treated with γ-secretase inhibitors in 4.5 ml (see above) were collected for Aβ immunoprecipitation (IP) and complete protease inhibitor cocktail was added. Dead cells were eliminated by centrifugation at full speed at 4°C. 400 µl of conditioned media was kept for Dynabead-IC16 IP and further Aβ analysis via urea gel. The remaining 4 ml were used for protein-G agarose bead Aβ IP. Agarose beads were activated with anti-Aβ IC16 antibody. Per 4 ml sample, 30 µl beads were mixed with 40 µl IC16 antibody and an amount of PBS was added to assure sufficient mixing in the vial for 2 h at room temperature on a rotation wheel. Afterwards, activated beads were washed three times with PBS. Then, 30 µl of IC-16 agarose beads (in suspension) were added to cell supernatants. After incubation on a rotation wheel at 4°C over night, beads were washed twice with PBS and afterwards twice with 50 mM ammonia-acetate (pH 7) to remove salt from the sample. In between washing steps PBS/ammonia-acetate was removed carefully by prior centrifugation at lowest speed for 2 min. For elution, beads were incubated twice for 1 min with 300 µl of 50 % acetic acid, centrifuged at 2000 rpm for 2 min and sample collected without beads. 600 µl of each sample of two elution steps was collected in one vial. The eluate was again centrifuged at 2000 rpm for 2 min and 550 µl sample was transferred to a new vial to assure complete elimination of agarose beads. Finally, the eluate was evaporated in a speed vac overnight and sent

to the laboratory of Dr. Lisa-Marie Münter from the Department of Pharmacology & Therapeutics of the McGill University, Montreal, Canada.

5.3.14.2 MALDI-MS MEASUREMENT

Samples were prepared for analysis by dried droplet method mixing 1 µl of sample with 1 µl of saturated sinapinic acid solution (dissolved in 33% acetonitrile in H_2O with 0.1% trifluoracetic acid). Samples were measured in positive ion mode using the reflector detector (Bruker UltraFlextreme). All MALDI-MS measurements were performed in the laboratory of Prof. Dr. Lisa-Marie Münter from the Department of Pharmacology & Therapeutics of the McGill University, Montreal.

5.3.15 SPLIT GFP COMPLEMENTATION ASSAY

For the analysis of specific proteins in cells by fluorescence microscopy, proteins can be tagged to fluorophores by cloning of respective constructs which can then be transfected and are expressed as fluorescing proteins. One familiar fluorophore to do so is the green fluorescent protein (GFP) which was first isolated from the jellyfish *Aequorea victoria.* The protein has a major excitation peak at a wavelength of 395 nm and a minor one at 475 nm and its emission peak is at 509 nm. The protein consists of a barrel structure, composed of eleven β-sheets. One approach to not only detect and localize tagged proteins via fluorescence microscopy but to also analyze the co-localization of specific proteins, the GFP protein can be splitted into two fragments (β-sheets 1-10 and β-sheet 11) and either one or the other fragment can be tagged to the two proteins of interest via cloning. One of both fragments alone does not show any fluorescence. Only when both proteins co-localize and both fragments of the GFP get into close proximity, the capability of fluorescing is regained. Here, one fragment was tagged to APP (β-sheet 1-10) and the other to meprin β (β-sheet 11) (cloning strategy described in molecular biological methods section) to study the co-localization of both proteins and to determine the localization of potential interaction. Both constructs were transfected into HEK293T cells and co-localization was analyzed by immunofluorescence microscopy with a confocal laser scanning microscope (LSM710).

5.3.16 IMMUNOFLUORESCENCE MICROSCOPY

Immunofluorescence microscopy allows the visualization of proteins either directly tagged to fluorophores or stained with antibodies conjugated to fluorophores. This enables such as the localization of proteins to different cell compartments or the co-localization of different proteins.

24 mm cover slides were placed in a 6-well plate and coated with polyornithin (1:2000 in PBS) for 30 min and afterwards washed twice with PBS. Thereafter, either HEK293T

cells or MEF cells were seeded on the cover slides for transfection with either fluorophore tagged proteins or untagged proteins, which were stained with secondary ALEXA antibodies. One day post transfection cells were fixed for 10 min with 4% paraformaldehyde (PFA) and afterwards washed twice with PBS. Except the cells for the purpose of cell surface staining, all other cells were permeabilized for 20 min with 0.5% triton in PBS and then again washed with PBS before blocked with 4% BSA in PBS for 1 h at RT. After an additional washing step cells were incubated with a primary antibody (see table above) for 1 h at RT. Then, cells were washed four times before the secondary antibody was added in a dilution of 1:500 for 1 h at 37°C in the dark. Finally, cells were again washed twice with TBS and then as the case may be incubated with 5 µM DRAQ5 for 3 min for nucleic staining. Cover slides were then mounted on microscopic slides with ProLong™ Gold antifade reagent. One day post staining procedure immunofluorescent Z-stack images were acquired using a LSM710, AxioObserver confocal laser scanning microscope and a Plan-Apochromat 63x/1.40 Oil DIC M27 objective, using the ZEN 2008 software (Carl Zeiss). In the results part representative layers of Z-stacks are shown.

TABLE 6 Constructs and antibodies for immunofluorescence microscopy

construct	**1st antibody**	**dilution**	**2nd antibody**
APP695ΔNPxYmyc-pLHCX	IC16	1:300	@mouse-Alexa546
APPmyc-pLHCX	IC16	1:300	@mouse-Alexa546
meprin β-pLBCX	MEP1B (R&D Systems)	1:300	@goat-Alexa488
pLHCX-APP695 split GFP11	-		-
pLHCX-meprin β split GFP1-10	-		-

TABLE 7 Antibodies used for compartment staining

compartment	**1st antibody**	**dilution**	**2nd antibody**
endoplasmic reticulum	PDI	1:500	Alexa546
cis-Golgi	GM130	1:300	Alexa546
early endosomes	EEA1	1:300	Alexa546

5.3.17 IMMUNOHISTOCHEMISTRY

Immunohistochemistry and analysis was performed together with Hermann Altmeppen of the Institute of Neuropathology, University Medical Center Hamburg-Eppendorf, Germany. Sections of paraffin-embedded samples of frontal isocortex of neuropathologically confirmed AD patients (n=21, mean age: 78 years, SD: 10 years),

non-demented control patients (n=17, mean age: 76 years, SD: 11.6 years) and of patients with either confirmed Lewy body dementia, Parkinson`s disease or Trisomy 21 as a “non-AD but neurodegeneration group” (n=10, mean age: 66 years, SD: 8.8) (source: University Medical Center HH-Eppendorf (UKE), use of these samples for research purposes is in agreement with ethical regulations of the State of Hamburg; patients were predominantly of Caucasian ethnicity) were stained with a Bielschowsky staining kit according to standard laboratory procedures. Immunostainings of Aβ (using monoclonal antibody 6E10; 1:100), meprin β (using rabbit polyclonal anti-meprin β antibody; 1:500), phosphorylated Tau protein (using monoclonal antibody AT8 (MN1020); 1:5000; Thermo Scientific) and α-synuclein (rabbit anti-synuclein (alpha), Zytomed Systems) were performed with a Ventana Benchmark XT system according to common protocols.

5.4 Molecular biological methods

5.4.1 Polymerase chain reaction (PCR)

Fragments of DNA can be amplified by PCR. In this work this method has been used for the cloning of DNA constructs. By using specific primers, not only the amplification of certain DNA fragments, but also a modification like the insertion of mutations (site-directed mutagenesis) or restriction sites can be achieved. Several components are required for the reaction:

- 1 µl template DNA
- 1 µl each forward and reverse primer
- 1 µl DNA polymerase
- 4 µl Desoxyribonucleosidtriphosphate (dNTPs)
- 5 µl buffer solution
- 37 µl H_2O

The PCR consists of several steps:

1. *Denaturation*: DNA is heated to 94°C to denature double stranded into single stranded DNA.
2. *Primer annealing*: Sample is set to 55-65°C for 30 sec. The exact annealing temperature depends on length and sequence of primers.
3. *Elongation*: At 72°C the polymerase synthesizes a new DNA strand complementary to the template strand and starts at the binding site of the primers.

4. *Final elongation*: 72°C for 15 min. This step ensures that any remaining single stranded DNA is fully extended.

The reaction takes place in a thermocycler and comprises 20 to 40 cycles. All PCRs were analyzed via agarose gel electrophoresis.

5.4.1.1 Cloning of split GFP constructs

The plasmid pcDNA3.1-APP695 CT split GFP11 was provided from Dr. Simone Eggert from the group of Dr. Stefan Kins of the University of Kaiserslautern and used as template to subclone the APP695 CT split GFP11 construct into a pLHCX backbone with a 5´HindIII and a 3´ClaI restriction site. The plasmid pcDNA3.1-APP695 CT split GFP1-10 was used as a template to subclone meprin β CT split GFP1-10 with a 5´MluI und 3`ClaI restriction site into pLHCX.

Following primers were used:

TABLE 8 Primer sequences for the cloning of split GFP constructs

Primer	Sequence
Fwd APP HA GFP11 HindIII	aagcttatgctgcccggtttggcactgctcctgc
Rev APP HA GFP11 ClaI	atcgatttaggtgatgccggcggcgttcacgtac
Fwd HindIII Mep for split GFP 1-10	aagcttatggatttatggaatctgtcttgg
Rev MluI Mep for split GFP 1-10	acgcgtaaaagcatgattttgcagagtcaaatt
Fwd MluI split GFP 1-10	acgcgtggtggttcgggtggtatgtccaaaggag
Rev ClaI split GFP 1-10	atcgatttattctataaatggacaccgatgggta

PCRs were run in a thermocycler with the following program:

Cycle	Temperature	Time	
1.	98°C	30 sec	
2.	98°C	15 sec	
3.	65°C	30 sec	31x
4.	72°C	1:30 min	
5.	72°C	5:00 min	

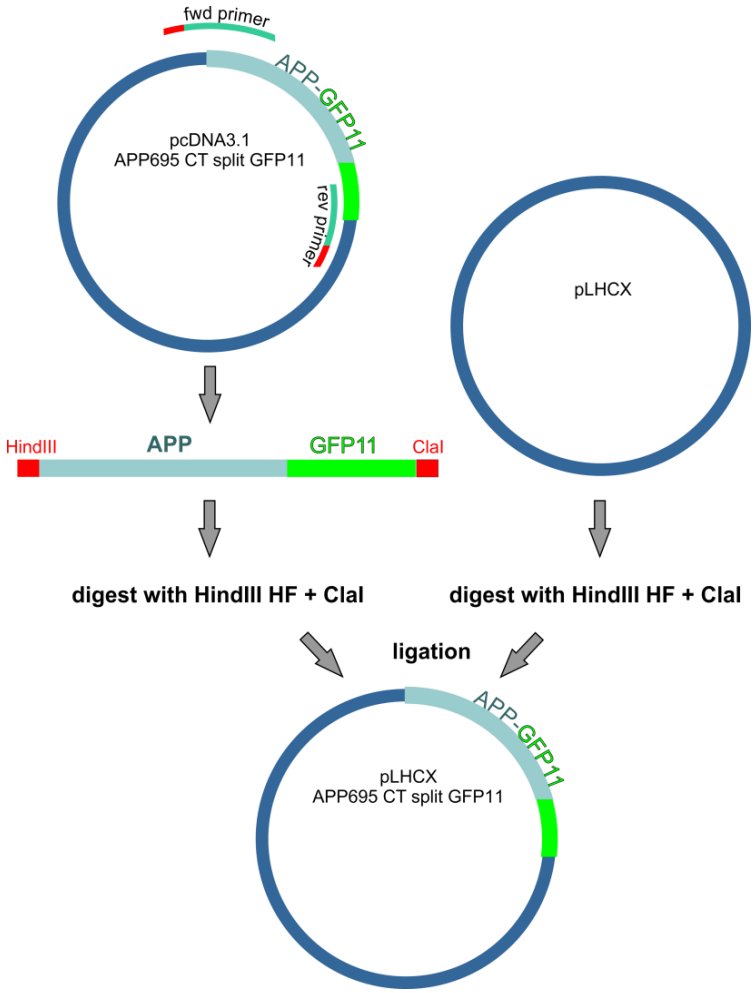

FIGURE 9 Cloning strategy of the APP695 CT split GFP11 construct

For the cloning of APP695 CT split GFP11 in pLHCX pcDNA3.1 APP695 CT split GFP11 was used as a template. Via PCR, APP split GFP11 insert was flanked with HindII and ClaI restriction sites. After digestion with HindII-HF and ClaI of the PCR product and empty pLHCX vector, both were ligated to obtain the desired construct.

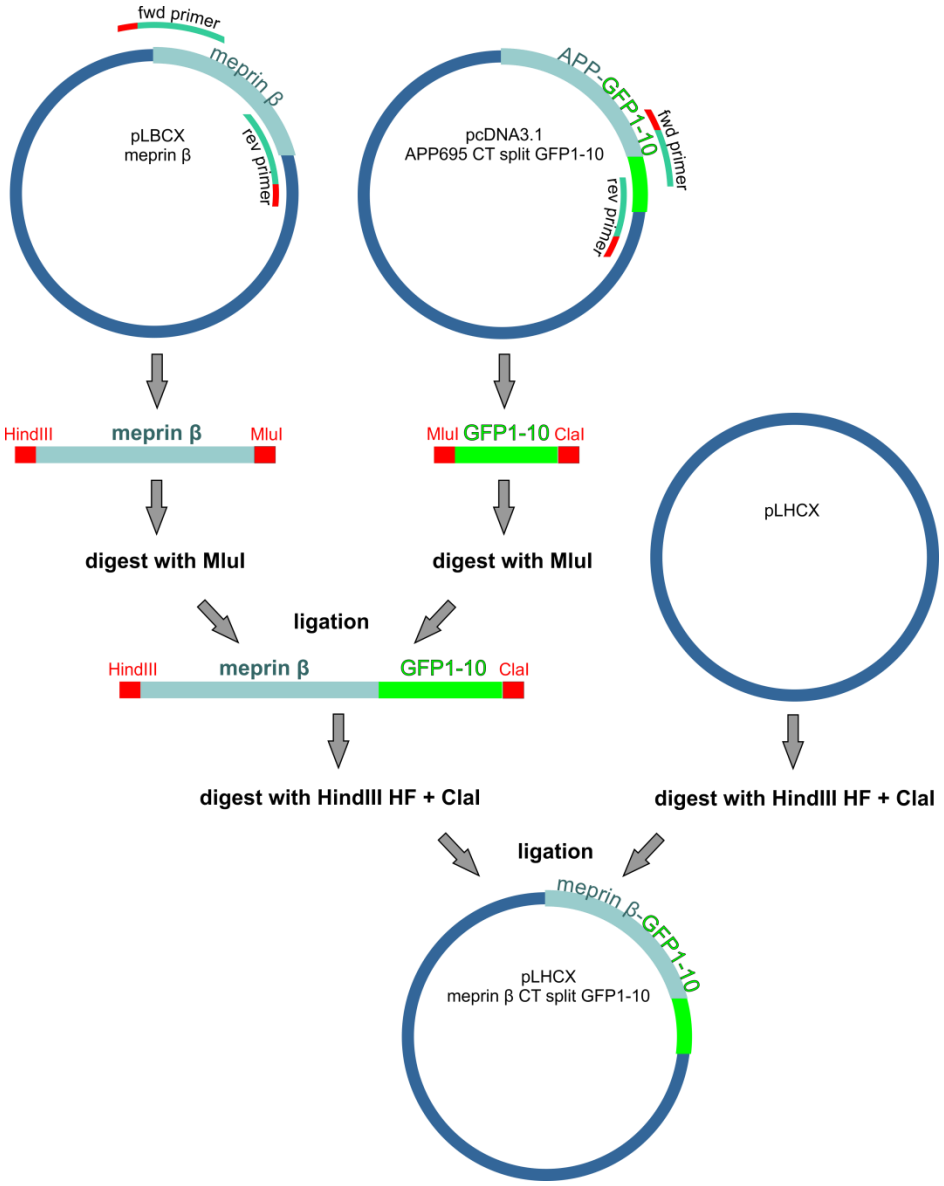

FIGURE 10 Cloning strategy of the meprin β CT split GFP1-10 construct

For the cloning of meprin β CT split GFP1-10 in pLHCX, pLBCX meprin β and pcDNA3.1 APP695 CT split GFP1-10 were used as templates. Via PCR, meprin β was flanked with HindII and MluI restriction sites and afterwards digested with respective enzymes. Additionally, GFP1-10 was flanked with MluI and ClaI restriction sites via PCR using pcDNA3.1 APP695 CT split GFP1-10 as a template. Meprin β and GFP1-10 were ligated and afterwards, the ligation product and pLHCX were digested with HindII-HF and ClaI. Then, both were ligated to obtain the desired construct.

5.4.1.3 GENOTYPING OF *MEP1B*$^{-/-}$ MICE

DNA was extracted of tissue biopsies of mice. The following primers were used for the genotyping PCR.

Primer	**Sequence**
Fwd	CCTGGCTGAATCCTGTCCCAA
Rev	CCTGGCTGAATCCTGTCCCAA
Neo	ACCGGTGGATGTGGAATGTG

The PCR was run in a thermocycler with the following program:

Cycle	**Temperature**	**Time**	
1.	95°C	10 min	
2.	95°C	20 sec	 35x
3.	60°C	30 sec	
4.	72°C	30 sec	
5.	72°C	7:00 min	
6.	10°	∞	

For analysis PCR samples were separated on a 2% agarose gel according to the standard protocol. After separation wild type mice showed specific bands at 200 bp, whereas homozygous *Mep1b*$^{-/-}$ mice showed a specific band at 220 bp and heterozygous mice accordingly specific band at 200 and 220 bp.

5.4.2 AGAROSE GEL ELECTROPHORESIS

Agarose gel electrophoresis enables the separation of DNA fragments according to their size by applying an electric field of 80 – 120 V to the gel. Due to its negatively charged phosphate backbone, DNA migrates to the cathode in a way that shorter fragments move faster through the gel than longer fragments. Depending on the size of expected DNA fragments, agarose is diluted in tris-acetate-EDTA buffer (TAE) to a final concentration of 0.5 to 2 %. Additionally, ethidium bromide (EtBr) or midori green stain is added to the gel, which both share to capability to bind DNA and can be visualized by exposure to ultraviolet light. Moreover, a 6 - fold sample buffer is added to each sample that contains glycerol to weigh down DNA sample to facilitate the loading into the gel pockets, and further bromphenole blue that enables to follow the running front on the gel. To analyze the size of DNA fragments, a DNA ladder containing DNA fragments of defined size, is added in one pocket. Separated DNA fragments could be visualized on a UV light table for excision and further clean-up at higher wavelength of

365 nm to prevent DNA damage, or, for documentation only, at lower wavelength of 312 nm.

In this work, 1 % agarose gels were used and a voltage of 100 was applied.

TAE buffer	
Tris-acetate	40 mM
EDTA (pH 8.0)	1 mM

5.4.3 DNA GEL AND PCR CLEAN-UP

The extraction of separated, as well as digested PCR fragments, in order to purify DNA from buffers, primers, enzymes or other contaminants, was performed using the NucleoSpin® Gel and PCR Clean-up kit (Macherey-Nagel) according to manufacturer´s protocol.

5.4.4 RESTRICTION DIGEST OF PCR FRAGMENTS

Restriction enzymes are endonucleases that recognize specific palindromic DNA sequences of four to eight base pairs (bp) in length, and cleave double stranded DNA at these so called recognition sites. These enzymes, which are categorized into four groups (Type I to IV) depending on their composition and cofactor requirements, naturally occur in bacteria and archeans and act as a defense mechanism against viruses. Each restriction enzyme generates either blunt ends, meaning that both DNA strands terminate in a base pair, or sticky ends, with 3’ or 5’ overhangs. They can be used for the cloning of DNA constructs since two DNA fragments, digested with the same restriction enzyme and are thus carrying the same sticky ends, can easily be ligated with a ligase. Here, either digests of purified PCR fragments for further cloning or control digests of cloning products were performed.

25 µl restriction batch	
NEB restriction enzyme	10 units (5 units each, if two enzymes are used)
DNA	1 µg
NEB buffer	1x

Incubation time	3 h
Incubation temperature	37°

5.4.6 Ligation of restricted PCR fragments

DNA ligases are capable of ligating PCR strains by forming an ester bond between the phosphate residue of one strain and the deoxyribose of the other. Here, the T4 ligase that naturally occurs in the T4 bacteriophage and enzyme is capable in ligating both, sticky as well as blunt ends was used for all ligations after restriction. Reaction batches of 30 µl total volume were prepared with a vector to insert ratio of 1:3.

30 µl ligation batch	
T4 ligase	400 units
T4 DNA ligase buffer	1x
Plasmid vector : DNA insert	1:3
H_2O_{dd} nuclease free	add to volume of 30 µl

5.4.7 Sequencing of DNA

All cloned DNA constructs were verified by sequencing and analysis by comparing the sequencing results to the desired sequence using the softwares SE central and Chromas. The sequencing was conducted by SEQ.IT GmbH & Co KG Kaiserslautern, Germany.

5.4.8 Cultivation of bacteria

The E. coli strain DH5α was used for the amplification of plasmids. DH5α were cultured in LB media or LB agar plates which were either supplemented with 100 µg/ml ampicillin or 50 µg/ml kanamycine, depending on which antibiotic resistance the respective plasmid was carrying.

LB medium	
1 % w/v	bacto-tryptone
0.5 % w/v	yeast extract
1 %	NaCl
1.5 %	agar (only for agar plates)

The pH was adjusted to 7.5 using NaOH. For agar plates 10 cm dishes were used.

To yield low amounts of DNA of inoculated single colonies, small scale cultures were prepared in 5 ml LB medium supplemented with the respective DNA and antibiotic and cultivated for 6 h at 37°C under vigorous shaking. Afterwards, DNA was extracted as described. Higher amounts of DNA could be produced by large scale cultures. For this purpose, bacteria of a previously cultivated pre-culture/small scale culture was diluted in a ratio of 1:1000 in 300 ml LB medium supplemented with appropriate antibiotic und cultivated at 37°C under vigorous shaking. DNA was again extracted as described.

5.4.10 Transformation of competent bacteria

Transformation means the insertion of exogenous DNA into competent bacteria. This naturally occurring process can be used for the amplification of DNA plasmids. In this work, either 7 µl ligation product or 1 µg DNA was added to 100 µl of competent DH5α bacteria, incubated on ice for 20 min and afterwards heat-shocked at 42°C for 45 sec. Then 500 µl LB medium was added to the suspension and incubated at 37°C for 1 h on a thermocycler. Finally, 100 µl of the suspension was plated on LB agar plates. These were incubated at 37°C on to let colonies grow.

5.4.11 Mini prep

For small scale preparation of plasmids after transformation, single clones were picked from LB agar plates and incubated in 5 ml LB medium supplemented with the respective antibiotic for 6 h at 37°C under vigorous shaking. Afterwards, DNA was prepared with the high pure plasmid isolation kit (Roche) under manufacturer´s instructions.

5.4.12 Midi prep

High scale preparations of plasmids after transformation were yielded by picking single clones from LB agar plates and culture these overnight at 37°C in larger volumes of LB media of 150-300 ml supplemented with the respective antibiotic after pre-culture in 5 ml for 6 h. On the next day, DNA was isolated using the kit endotoxin-free Plasmid DNA purification (Macherey-Nagel).

5.4.13 Determination of DNA concentration

DNA concentration was determined with a photometer by measuring the UV-absorption of the sample or passed light, respectively, at 260 nm, which is called optical density (OD) or extinction. For this purpose, diluted DNA is pipetted into a UV-light permeable cuvette that is set into the light path of the photometer. The concentration of DNA is calculated by the photometer with the detected OD value.

$$c\ (\mu g/ml) = A/(e*l)$$

c = concentration
A = absorbance at 260 nm
l = width of the cuvette which used to hold the solution, in cm, usually is 1cm
e = extinction coefficient (1 OD_{260} unit = 50ug/ml for double stranded DNA)

5.4.14 Quantitative real-time PCR (qPCR)

Via qPCR, the extent of the expression of a specific gene can be monitored. Therefore, first, RNA needs to be isolated from tissue or cells and is then

transcribed into cDNA. For this reverse transcription either oligo(dT) primers that are used to generate cDNA from poly(A)-tailed mRNA, random hexamer primers to generate cDNA from all RNA (tRNA, rRNA, mRNA) or gene specific primers are used. The generated cDNA is then used for real-time PCR, where the amount of DNA is measured after each PCR cycle (denaturation, 95°C, annealing, 60°C, extension, 72°C). The measurement of DNA amount is carried out via fluorescent dyes like SYBR green. These are added to the reaction and fluoresce upon binding to double stranded DNA. Thus, the increase of fluorescence is proportional to the number of generated PCR product molecules.

Here, RNA isolation was performed using TRI Reagent® (Sigma-Aldrich) according manufacturer´s protocol. RNA was synthesized to cDNA using the verso cDNA Synthesis Kit (Thermo Scientific) and using random hexamer primers following standard operating procedure of the manufacturer.

cDNA synthesis reaction batch	
5x cDNA synthesis buffer	4 µl
dNTP mix	2 µl
random hexamer primer	1 µl
RT enhancer	1 µl
verso enzyme mix	1 µl
RNA template	1 µl
H2O	Add to 20 µl

Afterwards, cDNA was used for qPCR. For the PCR reaction and fluorescence scanning the thermal cycler iCycler (Biorad) was used.

qPCR reaction batch	
2x ABsolute SYBR Green Mix	12.5 µl
H_20	11.3 µl
cDNA	1 µl
Primers (100 µM)	0.1 µl each

Primers specific for murine meprin β and for GAPDH as a housekeeping gene were used.

Primer	**Position**	**Sequence**
meprin β fwd	1903 - 1922	caagatggcagagctgagtg
meprin β rev	1951 - 1970	tcacacctttgcccatgta
GAPDH fwd	787 - 806	ggagaaacctgccaagtag
GAPDH rev	867 - 886	gacaacctggtcctcagtgt

The following running protocol was used:

Cycle	Repeats	Step	Temperature	Time
1	x 1	Step 1	95.0°C	15:00 min
2	x 35	Step 1	95.0°C	00:20 min
		Step 2	60.0°C	00:20 min
		Step 3	72.0°C	00:30 min
3	x 1	Step 1	95.0°C	01:00 min
4	x 1	Step 1	55.0°C	01:00 min
5	x 88	Step 1	60.0°C	00:08 min

The evaluation was performed using the ΔΔCt method. The Ct (threshold cycle) is the cycle number when the fluorescence signal causes a certain threshold, which is set to a level of a significantly increased fluorescence compared to the baseline signal.

$$\Delta\Delta Ct = \Delta Ct1_{(untreated)} - \Delta Ct2_{(treated)}$$

with $\Delta Ct1_{(untreated)} = Ct_{(gene\ of\ interest)} - Ct_{(reference\ gene)}$

and $\Delta Ct1_{(treated)} = Ct_{(gene\ of\ interest)} - Ct_{(reference\ gene)}$

The fold-increase in gene expression can be determined by calculating $2^{\Delta\Delta Ct}$.

6 RESULTS

6.1 THE PHYSIOLOGICAL ROLE OF MEPRIN β

6.1.1 A KNOCKOUT OF MEPRIN β LEADS TO INCREASED SAPPα SECRETION IN CORTICAL NEURONS

It was previously shown that meprin β is able to cleave APP and to generate Aβ peptides *in vitro* (Becker-Pauly et al., 2011; Bien et al., 2012; Jefferson et al., 2011). Moreover, Jefferson and colleagues showed that, besides Aβ, meprin β is also able to generate non-toxic N-terminal APP fragments (N-APP20/N-APP11) of the size of 20 kDa or 11 kDa in overexpressing cells and also in wt mice (Jefferson et al., 2011). These fragments were missing in *Mep1b*$^{-/-}$ mice. Even more interesting, the fragments could be additionally detected in human brain lysates. These results point that meprin β is an important element in APP processing. Thus, to study the physiological role of meprin β in APP processing in more detail was of further interest in this work. Since a difference in levels of N-APP fragments could be detected for wt versus *Mep1b*$^{-/-}$ animals, it was expected to see a similar effect on N-terminal soluble APP (sAPP) fragments that are generated by cleavage at the β-cleavage site. Therefore, endogenous APP processing in the brains of *Mep1b*$^{-/-}$ (n=6) mice compared to age-matched wt animals (n=6) was analyzed. Endogenous sAPPα and sAPPβ were detected in the soluble fractions and full-length APP was detected in membrane fractions of brain lysates. Levels of endogenous full-length APP remained identical (Fig. 2 A). However, levels of sAPP showed differences for *Mep1b*$^{-/-}$ versus wt mice. The release of endogenous sAPPα was increased in *Mep1b*$^{-/-}$ mice (Fig. 2 A, B). This suggests that there might be more APP substrate for ADAMs in the absence of meprin β and supports the involvement of endogenous meprin β in APP processing *in vivo*. The levels of sAPPβ were also slightly increased in *Mep1b*$^{-/-}$ mice (Fig. 11 A, C). However, the binding site of the antibody has to be considered. The selected 192wt antibody (Fig. 5) recognizes only the neo C-terminus of sAPPβ after BACE-1 (or minor meprin β) cleavage between M671/D672 (sAPPβ-M671). Therefore, it does not detect the one amino acid longer variant which is generated by meprin β cleavage between D672 and A673 (sAPPβ-D672). Thus these results basically reflect BACE-1 cleavage. Seemingly, the enhanced cleavage and sAPPβ-M671 generation by BACE-1 due to higher substrate availability in the absence of meprin β in the *Mep1b*$^{-/-}$, prevails the

lapse of meprin β generated sAPPβ-M671. Overall, these findings demonstrate that meprin β affects endogenous APP processing in the mouse brain.

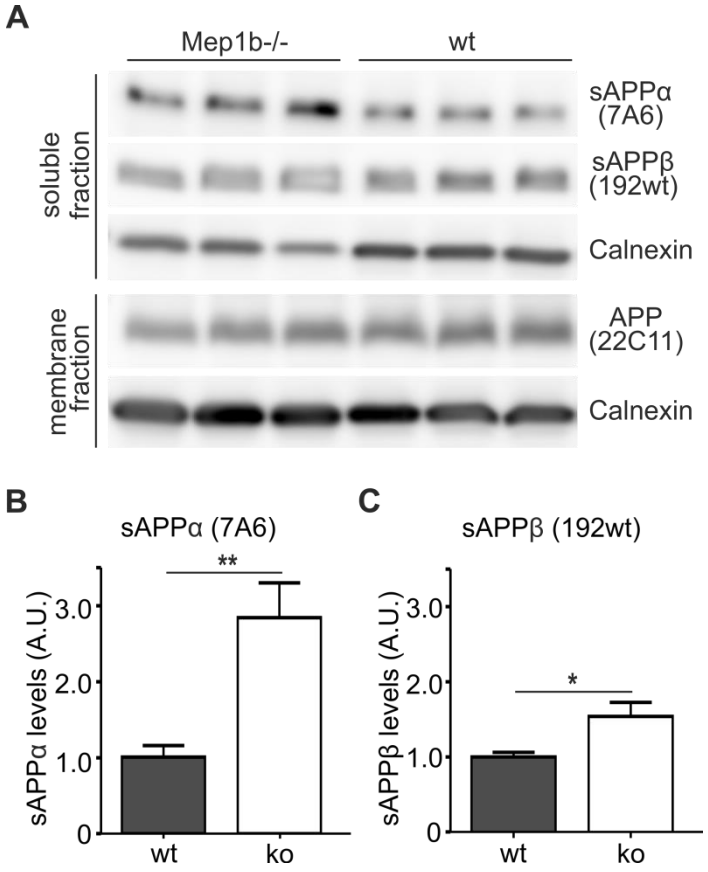

FIGURE 11 Increased sAPPα levels in meprin β ko mice

(A-C) Soluble and membrane fractions of brain lysates from meprin β ko (*Mep1b*$^{-/-}$) (n=6) and wt (n=6) mice were probed with antibodies specific for sAPPα (7A6), sAPPβ (192wt), full-length APP (22C11) and calnexin as loading controls (note that only representative n=3 for each is shown). (B) Note that endogenous sAPPα levels were increased in the absence of meprin β, indicating a changed APP processing profile in *Mep1b*$^{-/-}$ compared to wt mice. B and C are normalized to calnexin levels. Graphs show mean ± SEM (n=6); statistical significance: *<0.05; **<0.01; t-test. The analysis of soluble and membrane fractions of *Mep1b*$^{-/-}$ and wt brains was performed together with Katrin Moschke of the laboratory of Prof. Dr. Lichtenthaler, DZNE Munich, Germany.

6.1.2 Decrease of Aβ2-40 and increase of mature APP in primary neurons of meprin β knockout mice

Since differences in sAPPα levels were detected for wt versus meprin β ko mice, next the focus lied on the total endogenous Aβ in supernatants of primary cortical neurons

of the same mice. These were measured via ELISA assay. Here it could be shown that total Aβ40 levels show a trend to decrease (by about 13%) in meprin β ko neurons (n=6) compared to controls (n=6) (Fig. 12 A); however due to the antibody specificity and overall low Aβ levels, endogenous mouse Aβ2-40 could not be detected.

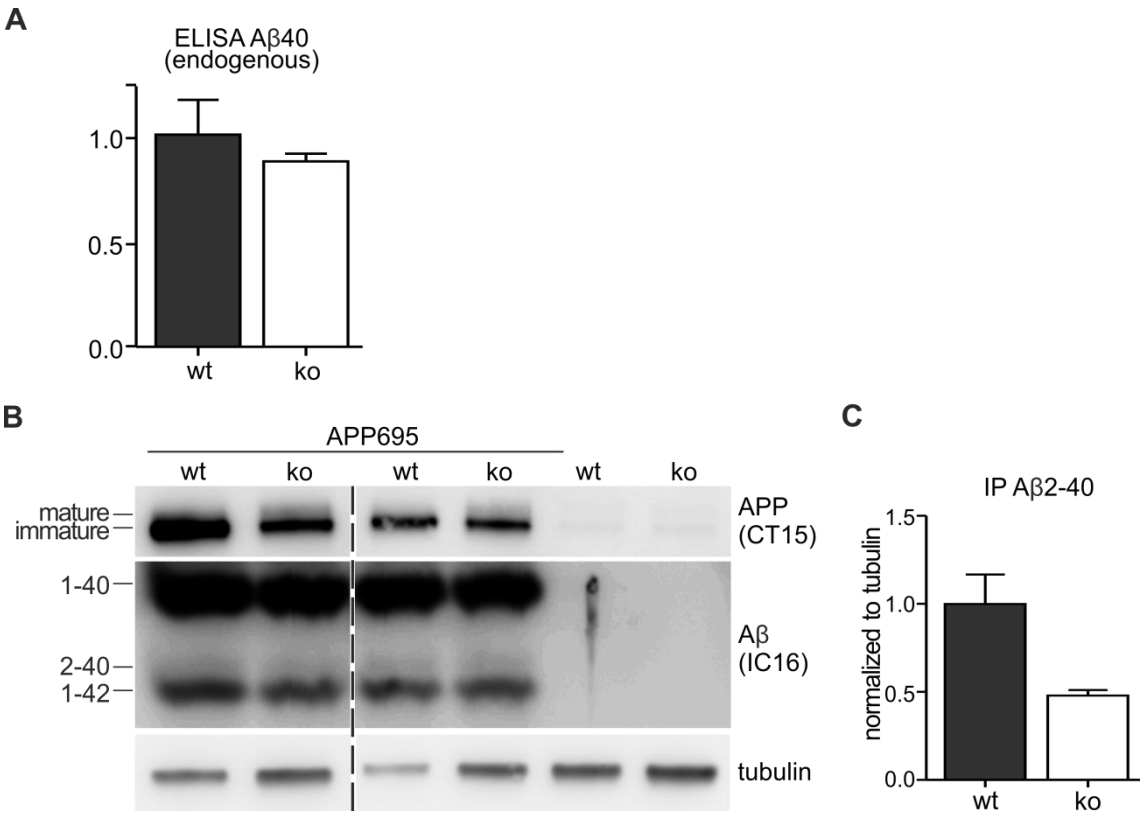

FIGURE 12 Decreased Aβ2-40 levels in primary neurons of meprin β ko mice
(A) Aβ40 levels of supernatants of primary cortical neurons of wt (n=3) and meprin ko mice (n=6) were detected via Meso Scale ELISA using sulfo-tagged 4G8 antibody. Meprin β ko mice showed approximately 13% less Aβ40 (normalized to total protein of lysates). (B) Urea gel of immunoprecipitated Aβ (using IC16 antibody) of supernatants of primary cortical neurons of wt and meprin β ko mice infected with a recombinant adenovirus expressing APP695. Lysates showed a decrease in mature APP for meprin β ko (CT15 antibody). (C) Quantification of Aβ2-40 levels (normalized to tubulin of lysates) of (B) showed a decrease of approximately 50% in meprin β ko neurons (n=2). ELISA measurements were performed together with Katrin Moschke, laboratory of Prof. Dr. Lichtenthaler, DZNE.

To circumvent this problem, primary cortical neurons of wt and *Mep1b*$^{-/-}$ mice were infected with a recombinant adenovirus expressing APP695. Aβ from cell supernatants was precipitated using IC16-activated dynabeads 48 hours post infection. The samples were separated on 8 M urea gels. The results showed that Aβ2-40 levels are decreased in meprin β ko neurons compared to wt of about 50% (Fig. 12 C, D).

Moreover, it could be observed that levels of mature APP are increased in neurons of meprin β ko mice compared to wt controls (Fig. 12 B). This is indicating that processing by meprin β of fully glycosylated APP occurs after posttranslational modification.

6.1.3 APP AND MEPRIN β INTERACT IN MURINE BRAINS

The results presented above clearly demonstrate that the absence of meprin β has a distinct effect on APP processing and the β-site cleavage. However, these results do not provide any evidence if meprin β directly sheds APP *in vivo* or whether the effect can be contributed to an indirect effect of meprin β on APP processing. A direct effect of meprin β on APP requires a co-localization in the same subcellular location. It was of major interest if both proteins interact. To address that question brain lysates of wild type mice and *Mep1b*$^{-/-}$ mice were precipitated for either APP using the 22C11 antibody or for meprin β using a polyclonal anti-meprin β antibody (see supplement 10.2.1). Both, APP precipitates as well as meprin β precipitates were then separated on the same 10 % SDS gel and then blotted on a nitrocellulose membrane that was following incubated with anti-meprin β antibody. As expected, the meprin β precipitate shows a band at 115 kDa, but only for wild type and not for the *Mep1b*$^{-/-}$ lysate (Fig. 13). Even if only to a lesser extent, a signal at the same height could also be detected for the APP precipitate and again, only in the lysate of the wild type but not of the *Mep1b*$^{-/-}$. This result might indicate a direct interaction for APP and the protease meprin β and shows that meprin β would be able to cleave APP and generate Aβ peptides. This interaction was further studied in this thesis.

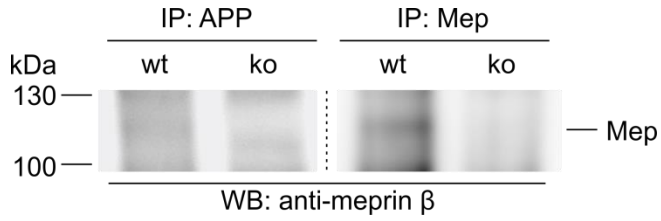

FIGURE 13 Interaction of APP and meprin β in murine brain

Brain lysates of *Mep1b*$^{-/-}$ and wild type mice were precipitated for either APP using the 22C11 antibody or for meprin β using a polyclonal anti-meprin β antibody. Precipitates were separated on 10 % SDS gels and blotted on nitrocellulose membranes and incubated with polyclonal anti-meprin β antibody. A band for meprin β at a height of 115 kDa could be detected in meprin β precipitates, as well as in APP precipitates for wild type but not for *Mep1b*$^{-/-}$. All precipitates were run on the same gel, but rearranged for better presentation (n=1).

6.1.4 MEPRIN β PROTEIN LEVELS ARE INCREASED IN SPORADIC AD

The metalloprotease meprin β has been previously described as an APP cleaving enzyme, reminiscent of β-secretase activity. Interestingly, it could be shown that mRNA levels of the protease are increased in AD brains (Bien et al., 2012). Therefore, it was of further interest to evaluate if this increase can be also detected on protein level.

Hence, brain sections of AD patients (n=21), healthy age-matched controls (n=17) and of a neurodegeneration but non-AD group (here, a section of a Lewy body disease (LBD) patient is depicted) (n=10) were immunohistochemically analyzed. For a precise analysis of sections and to confirm the respective pathology of AD, non-AD, but neurodegeneration or healthy control, different stainings were conducted. Sections were stained for phospho-tau, since hyperphosphorylation of tau is one major histopathologic characteristic in AD. As expected, the microscopic images only show positive phospho-tau staining for AD. Also Bielschowsky silver stain, which highlights senile plaques of AD, was performed. Here, senile plaques could be detected in AD sections, but not in the control groups. As expected, the anti-Aβ 6E10 staining was positive for AD cases, showing a high number of aggregates. To a much lower extent positive 6E10 staining could be also detected for LBD cases, since LBD can go along with amyloid pathology. Slices of LBD patients were also stained for α-synuclein.

Further, the number of meprin β positive neurons was evaluated. The generation and specificity of meprin β antibodies is described in the supplementary results part (see section 10.2.1). Moreover, upon immunohistochemical assessment, a subpopulation of neurons in cortical layers III to VI showed prominent DAB signal of soma and neurites in all samples and was thus defined as meprin β positive. These meprin β positive neurons were counted in three representative microscopic fields of approximately 1.87 mm^2 (taken along cortical layers III to VI) per patient. The mean value of meprin β positive cells, derived from these three pictures per patient (corresponding to n=1), was used for quantifications of experimental groups and statistical analysis. Immunohistological analyzes of sections of frontal cortex show for the first time increased meprin β protein levels of approximately 2.5-fold and an increased number of meprin β-positive cortical neurons in AD (n=21) compared to control brains of non-demented patients (n=17) and of a non-AD but neurodegeneration group (n=10) (Fig. 14 A, B) of approximately 50% and 40%, respectively (see supplementary results 10.2.2 for all cases). The morphometric analysis revealed a significant up-regulation of meprin β specifically in AD but not in the non-AD neurodegeneration group (Fig. 14 B).

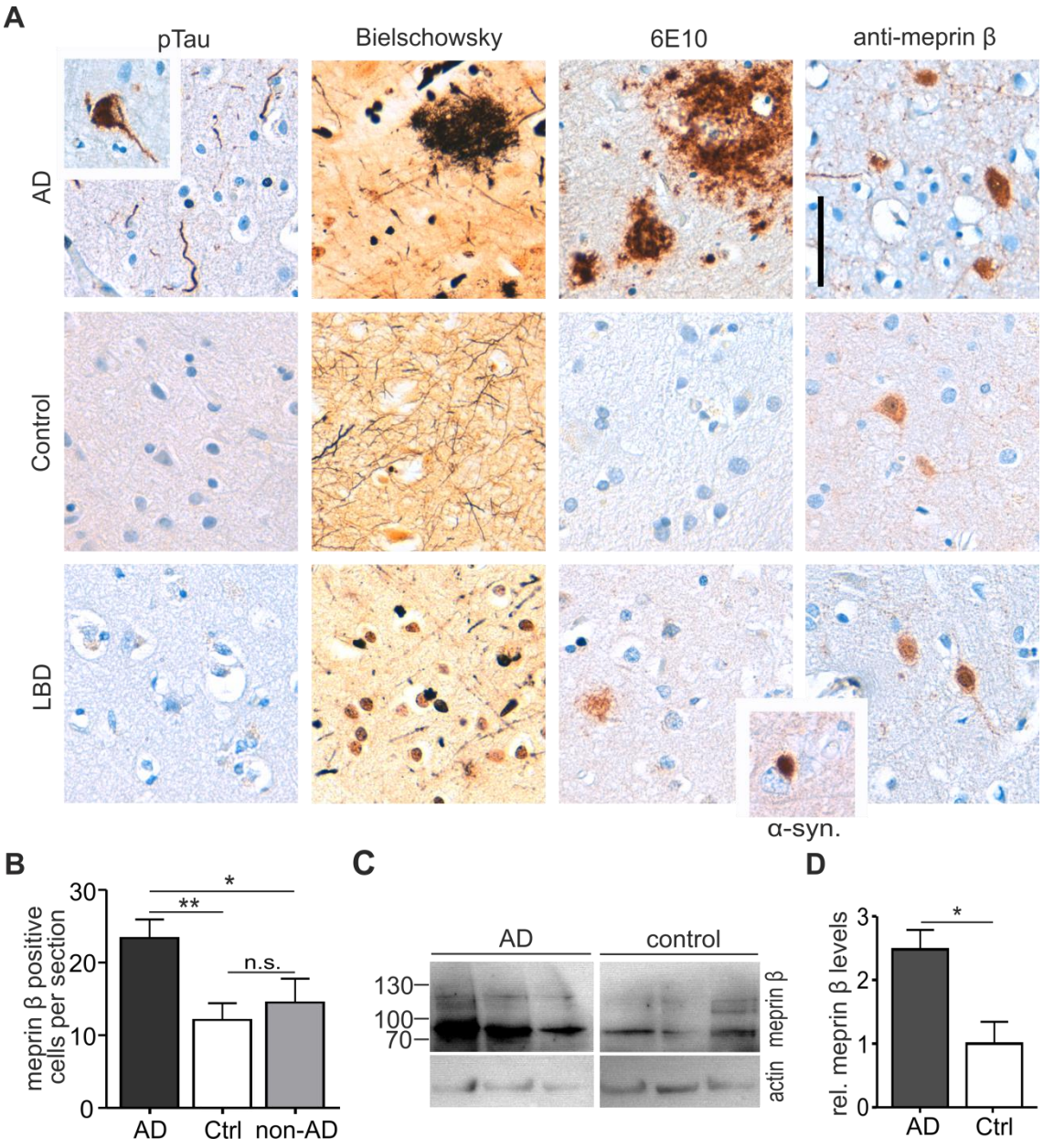

FIGURE 14 Increased meprin β levels in AD brains

(A) Immunostainings of human brain slices were performed with polyclonal anti-meprin β antibody (Supplementary Fig. 1). For detection of Aβ aggregates the monoclonal antibody 6E10 was used. Sections were also histologically stained with a phospho-tau antibody and Bielschowsky silver stain. Analyzes revealed more meprin β positive neurons in AD brains in concordance with increased Aβ generation and pTau staining. Slices of LBD patients were also stained for α-synuclein. Scale bars in overviews and magnified insets represent 100 µm. (B) Quantification of meprin β-positive neurons in cortical sections revealed a significantly higher number of meprin β positive neurons in AD compared to control brains from non-AD individuals (graph shows mean ± S.E.M. (n=21 AD, n=17 Control, n=10 non-AD neurodegeneration control; statistical significance: *<0.05, **<0.01; t-test). (C) Human brain lysates were probed with a

polyclonal anti-meprin β antibody (Supplementary Fig. 1) and actin as loading control. Meprin β and actin blots are from one gel. Control and AD samples were run on one gel, but are rearranged for better presentation. (D) Quantification of meprin β protein levels normalized to actin levels of AD versus control brains (graph shows mean ± S.E.M. n=3 AD, n=3 Control; statistical significance: *p=0.0323; t-test). The histological analysis was performed together with Dr. Hermann Altmeppen of the group of Prof. Glatzel, University Medical Center Hamburg, Germany. SDS PAGE and analysis of human brain lysates was performed together with Rielana Wichert of the laboratory of Prof. Becker-Pauly, CAU Kiel, Germany.

To further evaluate meprin β protein levels in brain, protein expression levels were analyzed from brain tissue of AD patients and healthy controls. Therefore, western blot analysis with brain tissue homogenates of sporadic Alzheimer´s disease patients (n=3) versus age matched non-demented controls (n=3) was performed. Meprin β levels were normalized to actin. Bands for meprin β at 120 kDa could be detected representing the membrane bound pro-meprin β, at 115 kDa, showing the membrane bound active meprin β and at 80 kDa, which shows the shedded meprin β. The biochemical analysis revealed significantly increased protein levels in AD versus control brain lysates (Fig. 14 C, D).

These results suggest that meprin β might play a crucial role in the pathology of AD. Moreover, the fact that the increase of the number of meprin β positive neurons and of meprin β protein levels in brain tissue is only the case for AD, but not for the non-AD neurodegeneration group, further highlights the specificity of the effect.

6.1.5 Increased ratio of Aβ2-40/1-40 in human frontal cortex of AD patients

During the last years, the appearance of N-terminally truncated Aβ variants and their role in AD have come to the fore. Some of these variants that are prone to aggregate and appear to be toxic to neurons are increased in AD. Since N-terminally truncated Aβ2-40 has been shown to be a characteristic consequence of meprin β cleavage it was of interest if this variant can be found in human frontal cortex and if the appearance of this variant correlates with AD. Although N-terminal truncated Aβ2-x peptides were already detected in the CSF and brain of AD patients (Wiltfang et al., 2001), there is so far no description of Aβ2-40 in human brain tissue. Thus, Aβ was precipitated with IC16-activated dynabeads from frontal cortex of six AD brains (n=6) and nine control brains (n=9). The precipitates were analyzed by separation on an 8 M urea gel. Besides Aβ1-40 and Aβ1-42, also Aβ2-40 could be clearly detected (Fig. 15 A). The ratio of Aβ1-40 to total Aβ levels, including Aβ1-40, Aβ2-40 and Aβ1-

42, and Aβ1-37, Aβ1-38 and Aβ1-39 that are expected to be represented as the three bands above the Aβ1-40 band, since the running properties on 8 M urea gels of these variants have been nicely assigned by Wiltfang and colleagues, were evaluated. As expected, the densitometric analysis showed that the Aβ1-40 level is decreased by approximately 40 % in frontal lobes of AD patients (Fig. 15 B). Moreover, the Aβ1-42/1-40 ratio was 4-fold increased (Fig. 15 C). Interestingly, the densitometric analysis also revealed a ~1.5-fold increase of the ratio of Aβ2-40/1-40 in AD compared to healthy controls (Fig. 15 D). To determine, whether this increase is significant, further samples need to be evaluated. It would be of interest, whether levels of these N-terminally truncated Aβ variants and meprin β protein levels correlate in AD frontal lobes.

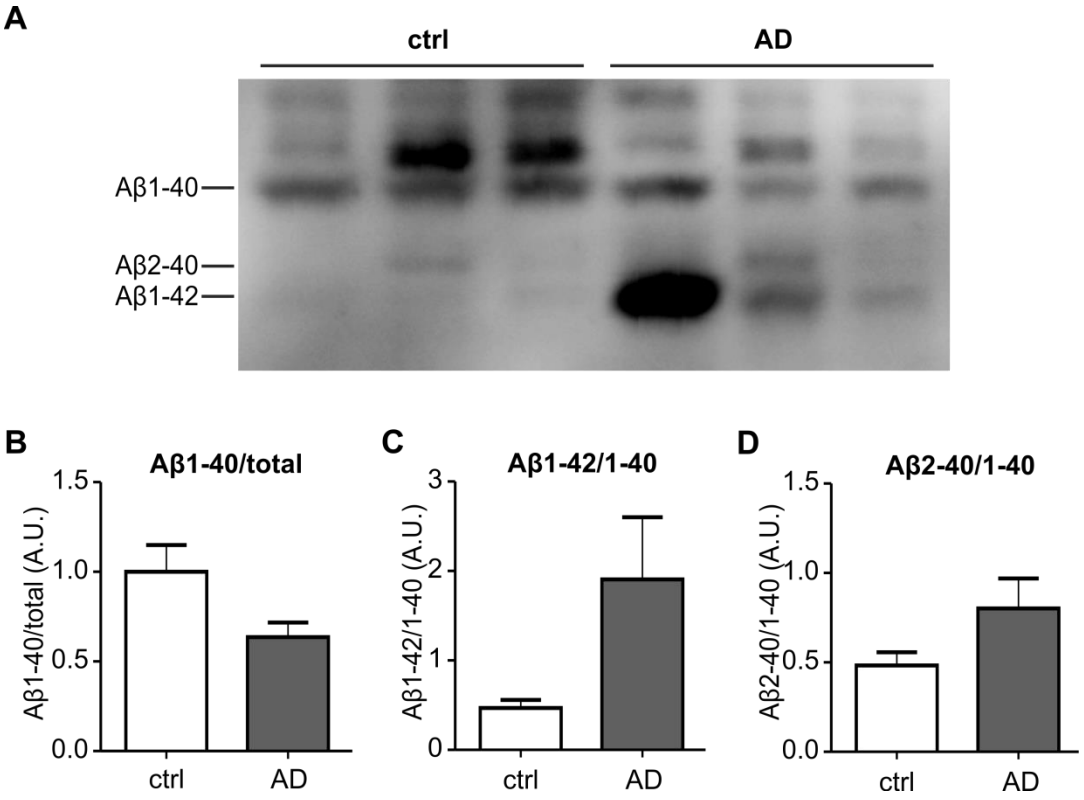

FIGURE 15 Increased Aβ2-40/1-40 ratio in frontal lobes of AD brains

Human brain homogenates of frontal lobes of AD (n=6) versus control cases (n=9) were precipitated for Aβ using IC16 antibody. Precipitated Aβ was separated on an 8 M urea gel. The blot was incubated with IC16 antibody (A). After densitometric analysis the ratios for Aβ1-40/total (B), Aβ1-42/2-40 (C) and Aβ2-40/1-40 (D) were determined.

6.1.6 N-TERMINALLY TRUNCATED Aβ2-40 IS EXISTENT IN THE HUMAN TEMPORAL CORTEX

The results presented above indicate that the Aβ2-40/1-40 ratio is increased in frontal lobe of AD brains. It was of further interest to additionally analyze other brain areas. Since meprin β mRNA levels in human brain are relatively high in the temporal lobe compared to other brain areas (Su et al., 2002; Su et al., 2004) it was analyzed if this increase has any effect on meprin β generated Aβ variants. Therefore, Aβ was precipitated of temporal lobes of six control cases (n=6) and six AD cases (n=6) with IC-16 activated dynabeads and then separated on 8 M urea gels. The blot nicely showed bands for Aβ1-40, Aβ2-40 and Aβ1-42, an unknown band slightly above Aβ2-40 and as described in the result part before, three bands above the Aβ1-40 band that are expected to represent Aβ1-37, Aβ1-38 and Aβ1-39 as described by Wiltfang and colleagues (Fig. 16 A).

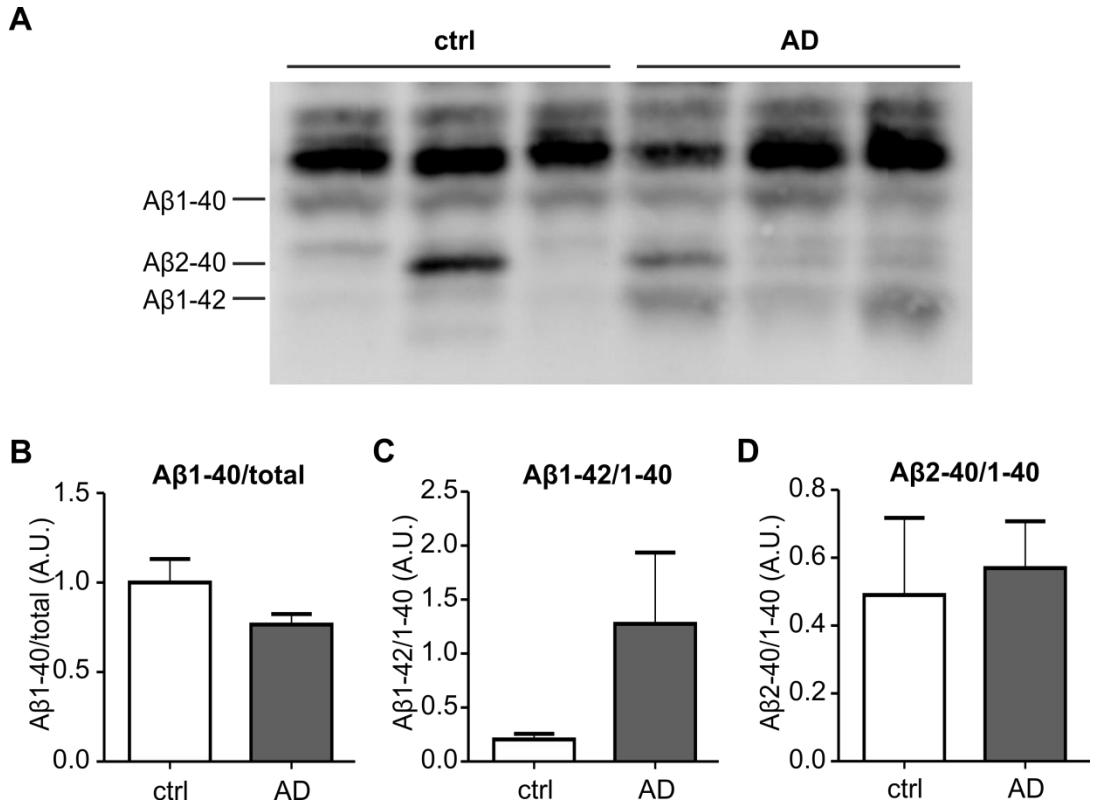

FIGURE 16 Aβ2-40 is present in temporal lobes of AD and control brains

Human brain homogenates of temporal lobes of AD (n=6) versus control cases (n=6) were precipitated for Aβ using IC16 antibody. Precipitated Aβ was separated on an 8 M urea gel and following blotted. The blot was incubated with IC16 antibody (A). After densitometric analysis the ratios for Aβ1-40/total (B), Aβ1-42/2-40 (C) and Aβ2-40/1-40 (D) were determined.

Comparable to the analysis of frontal lobes, the Aβ1-40/total ratio was decreased in AD cases by 20 % (Fig. 14 B). The ratio of Aβ1-42/1-40 was approximately 6.2-fold increased in AD (Fig. 14 C). No difference could be found for the Aβ2-40/1-40 ratio however, one outlier increased the mean of the control which is reflected by the high standard error of the mean (Fig. 14 D). Notably, this control case had not only a high level of Aβ2-40, but also of Aβ1-42, indicating that this case would have potentially developed AD at a higher age. Therefore, further cases need to be investigated to analyze meprin β generated Aβ variant in more detail.

6.2 Interaction of APP and meprin β

The effect of meprin β on the processing of APP and an increase of meprin β specific APP fragments has been published before (Bien et al., 2012; Jefferson et al., 2011) and further demonstrated in the first result part of this work. However, so far the focus on the direct interaction of both proteins has not been studied. Thus, in the following part this was of further interest.

6.2.1 APP and meprin β co-localize in the late secretory pathway or at the cell membrane

One way to study if the interaction of two proteins is feasible is to analyze if both proteins share a common localization in specific compartments. The co-localization can be determined by different approaches. One way for that analysis is the use of fluorescence microscopy.

It has been shown that meprin β has an acidic pH optimum, but also an additional proteolytic activity at basic pH (Bertenshaw et al., 2002). Therefore, different compartments come into consideration for APP cleavage by meprin β. Cleavage could occur in the late secretory pathway, at the cell surface or – like BACE-1 – in endosomes.

First, the cell surface was examined for co-localization of APP and meprin β. To visualize only surface localized proteins, cells were directly incubated with anti-Aβ IC16 antibody (Jager et al., 2009) and anti-meprin β antibody after fixation and blocking without permeabilization to ensure that antibodies do not penetrate into the cell. The confocal images nicely show a co-localization of both proteins at the cell surface (Fig. 17). As expected, the untransfected negative control and the controls of transfected cells that were only incubated with the corresponding secondary antibody,

did not show any surface staining (data not shown). These results consider the cell surface to be a co-localization spot.

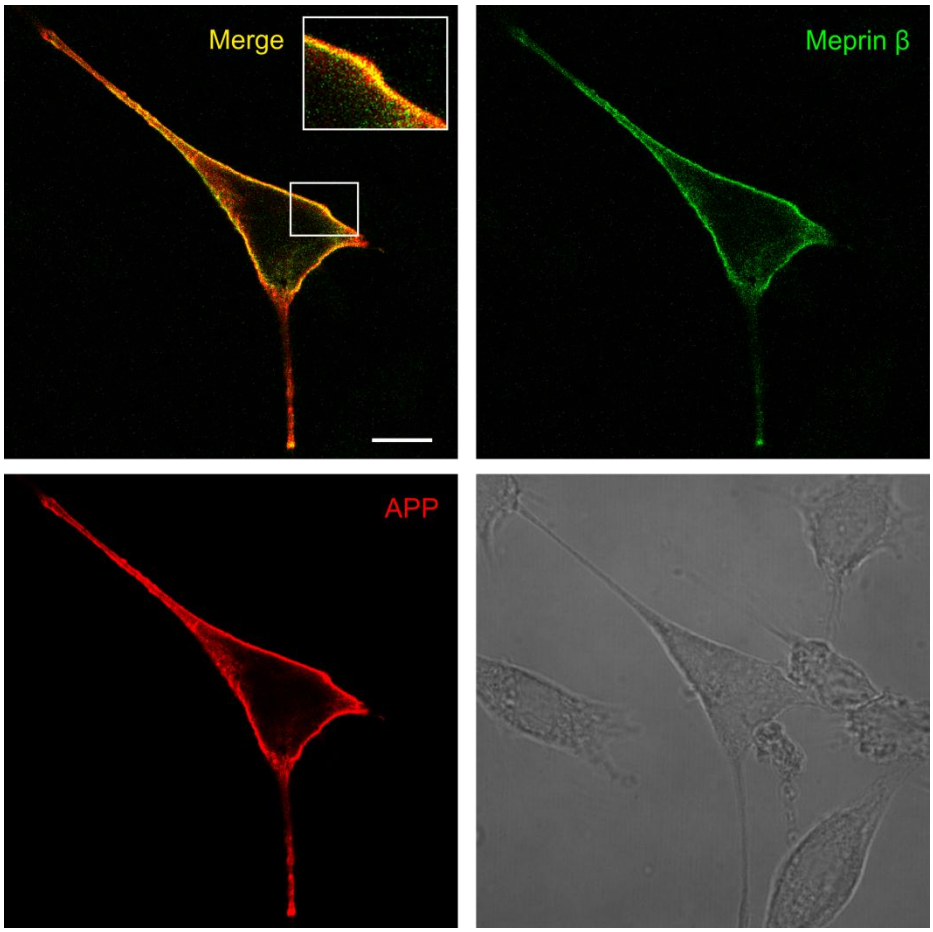

FIGURE 17 APP and meprin β co-localize at the cell surface in overexpressing MEF cells

MEF cells were transiently co-transfected with APP695ΔNPxY and meprin β. Surface staining was performed, using IC16 antibody for detection of APP and an anti-meprin β antibody. Secondary antibodies Alexa-Fluor546 and Alexa-Fluor488 were used, respectively. The confocal image shows co-localization of APP (red) and meprin β (green). Single channels are depicted aside. The right image shows the cell morphology as bright-field picture (Scale bar: 10 nm).

To further study the colocalization of APP with meprin β, a split GFP based complementation assay was performed. The fluorescent protein that is buildup of 11 barrels can be separated in two fragments via cloning which can be tagged to different proteins. The single fragment tagged to a protein and transfected into cells does not show any fluorescence. However, when both fragments attain close proximity, the fluorescence can be restored and is thus an evidence for the co-localization of these proteins. Here, HEK cells were co-transfected with APP and meprin β constructs that

are tagged with a fragment of the green fluorescent protein (GFP) (APP-GFP11, only bearing barrel 11 of GFP; meprin β-GFP1-10, only bearing barrel 1-10). Neither the GFP11 fragment nor the GFP1-10 fragment alone showed any fluorescence. However, fluorescence could be detected in cells that were co-transfected with both constructs indicating a co-localization of both proteins. To further identify the location of GFP fluorescence, a compartment staining for the *cis*-Golgi compartment, ER and early endosomes was performed. Of note, co-localization was mostly found in the secretory pathway within the *cis*-Golgi compartment (GM130 antibody) (Fig. 18 B), there was lesser co-localization within the ER (PDI) (Fig. 18 A), however hardly any in early endosomes (EEA1) (Fig. 18 C).

These results indicate that a direct interaction might be possible for APP and meprin β since a co-localization could be detected via immunofluorescence microscopy for both proteins. Potential locations for the interaction might be the cell surface or the late secretory pathway.

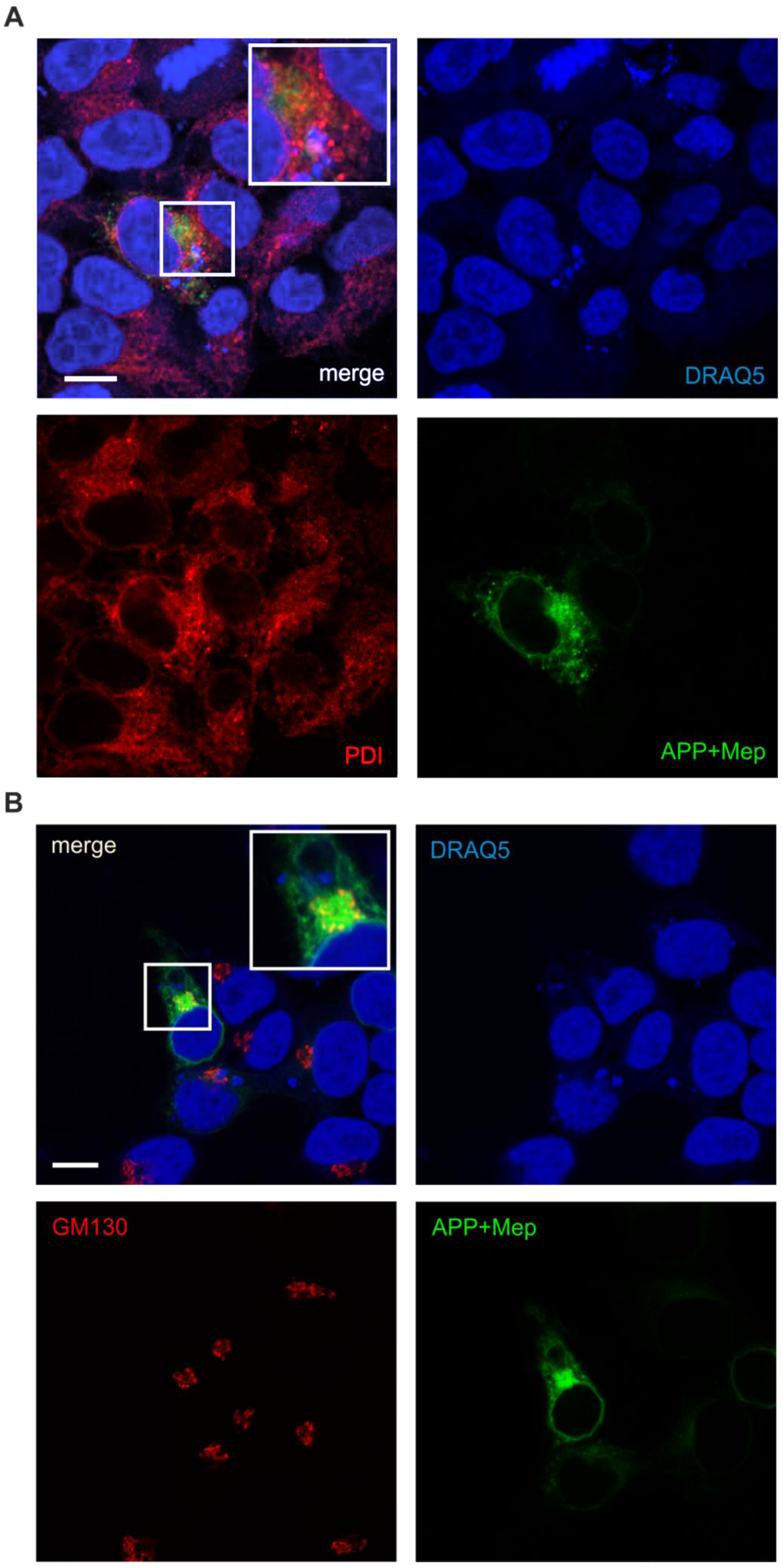
A
merge
DRAQ5
PDI
APP+Mep
B
merge
DRAQ5
GM130
APP+Mep

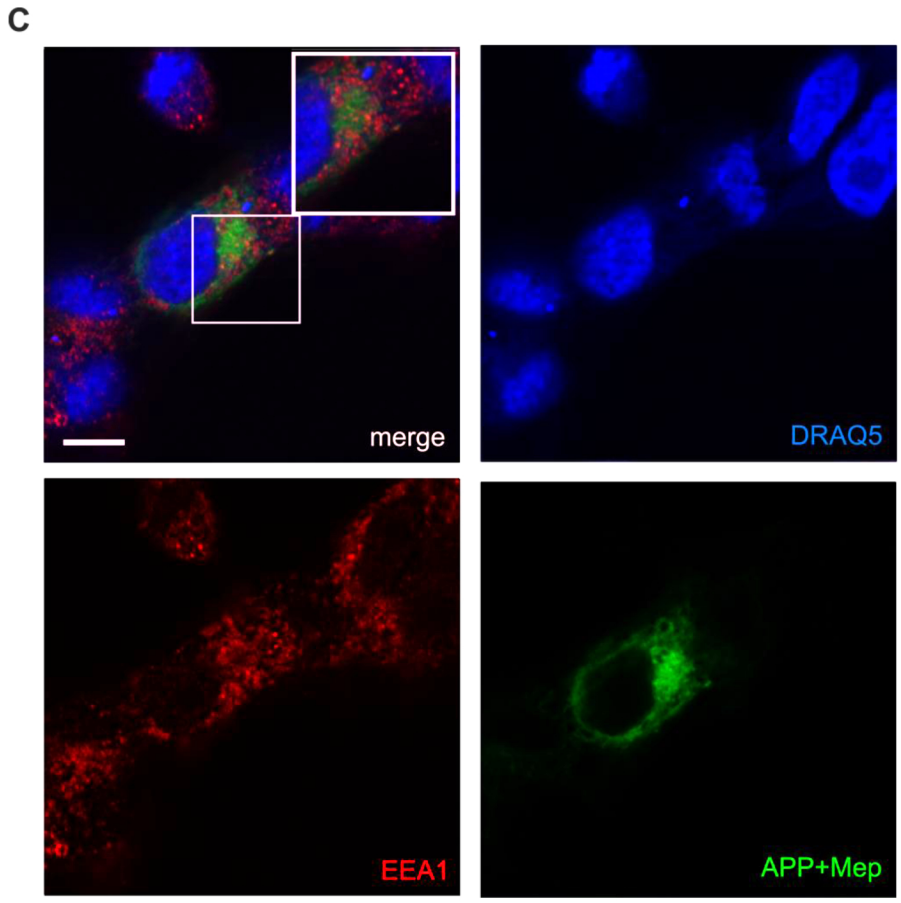

FIGURE 18 APP and meprin β co-localize in the cis-Golgi compartment in overexpressing HEK293T cells

(A,B,C) GFP fluorescence shows colocalizing APP and meprin β (depicted in green). (A) Only little colocalization of APP and meprin β can be found in the endoplasmic reticulum (PDI; depicted in red). (B) Colocalization was mostly found within the cis-golgi compartment (GM130; depicted in red). (C) Colocalization in early endosomes was hardly detectable (EEA1; depicted in red). (Scale bar: 10 nm).

6.3 MEPRIN β MEDIATED GENERATION OF Aβ IS INDEPENDENT OF BACE-1

With the discovery of the occurrence of N-terminally truncated Aβ peptides in brain and CSF, the question arose how these variants are generated. One way would be that BACE-1 cleaves at the usual β-cleavage site first and then subsequently or after γ-secretase cleavage and Aβ release, another peptidase/protease sheds of one more amino acids at the N-terminus of Aβ. Alternatively, another protease like meprin β instead of BACE-1 could directly cleave APP at the β-cleavage site in p2 of Aβ. In this

case the application of a BACE-1 inhibitor would not affect the generation of N-terminally truncated Aβ.

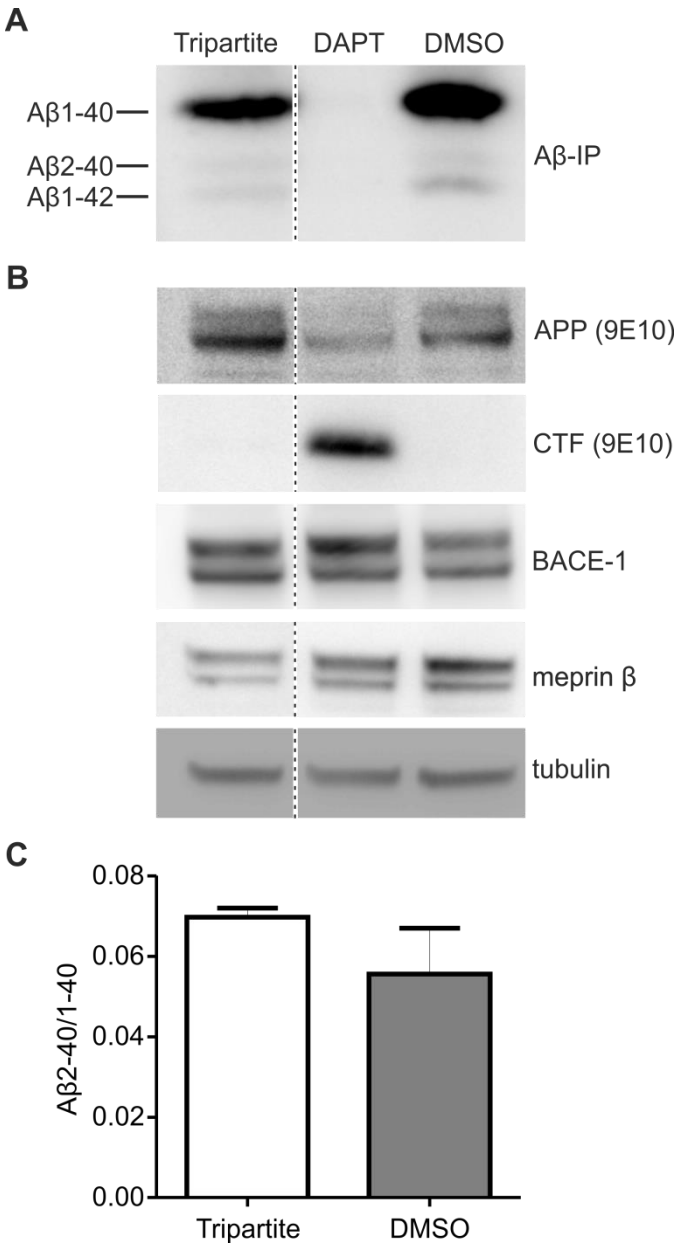

FIGURE 19 Meprin β cleaves APP independently of BACE-1

Stably overexpressing HEK293T APP cells were transfected with meprin β and BACE-1 and treated with tripartite BACE inhibitor (100 nM), DAPT (5 µM) or DMSO as vehicle control. Supernatants were precipitated for Aβ with IC16 activated dynabeads and separated on 8 M urea gels (A). Lysates were separated on 10 % SDS PAGE and checked for APP, BACE, meprin β and tubulin (B). After densitometric analysis the ratio of Aβ2-40/1-40 was evaluated (C). All samples were run on one gel but rearranged for better presentation (n=2).

To study this questions HEK293T cells stably overexpressing APP were transiently co-transfected with BACE-1 and meprin β. Post transfection, cells were treated for 24 h with 100 nM tripartite BACE-1 inhibitor, 5 µM DAPT γ-secretase inhibitor and DMSO as vehicle control. This experiment was conducted likewise before (Bien, 2012) however, Aβ-precipitates of cell supernatants were analyzed via MALDI-MS analysis. Due to the bad "flying" properties of Aβ1-42 during MALDI-MS an effect on BACE-1 generated Aβ1-42 could not be examined. Moreover, the ratio of Aβ2-40/1-42 has not been determined. Here, Aβ was precipitated from cell supernatants with IC-16 antibody activated dynabeads and afterwards, precipitates were separated on an 8 M urea gel. The analysis of the blot showed that generation of any Aβ variant is dependent of γ-secretase cleavage, since the application of the γ-secretase inhibitor DAPT completely abolished Aβ generation (Fig. 19 A). In comparison, cells that were only treated with the vehicle control DMSO secreted Aβ1-40, Aβ2-40 and Aβ1-42. Densitometric analysis of that blot revealed that the ratio of Aβ2-40/1-40 was ~0.05 (Fig. 19 C). Precipitates of cells treated with the BACE tripartite inhibitor still showed the occurrence of Aβ peptides. When applying the tripartite inhibitor a decrease of the Aβ1-42 level in comparison to the control was clearly visible, showing the efficiency of that inhibitor, since Aβ1-42 in mainly produced by BACE-1. Yet, supporting the results of Bien and colleagues, Aβ2-40 is still detectable in these samples, suggesting that the generation of meprin β generated Aβ is independent of BACE-1. Moreover, the Aβ2-40/1-40 ratio was slightly increased, compared to the control, even though the meprin β expression is lower than in the DAPT and the control sample (Fig. 19 B), suggesting that during inhibition of BACE-1 even more substrate is available for meprin β cleavage.

6.4 MEPRIN β MEDIATED APP CLEAVAGE IS INDEPENDENT OF THE OX2 AND THE KPI DOMAIN

The three different major isoforms of APP differ in the presence or absence of the KPI domain (APP751 and APP770) and the OX2 domain (APP770) (Sandbrink et al., 1997). The functions of these additional domains are not studied in detail yet, however recent results showed that the KPI domain presents an inhibitory capacity towards the serine protease matriptase-2 (MT2) by forming a complex with that protease (Beckmann, 2016). More interesting, results of the same study showed that in the absence of the KPI domain, as the case may be for APP695, MT2 is capable in cleaving APP and generating N-terminal truncated Aβ6-40.

To analyze if either the KPI domain or the OX2 domain affect APP cleavage by meprin β, HEK293T cells were transfected with APP695, APP751 or APP770 and meprin β. The cell supernatants were precipitated for Aβ that was following separated via urea SDS PAGE (Fig. 20 A). Additionally, lysates were separated via SDS PAGE and checked for APP and meprin β expression (Fig. 20 B). In cells that were only transfected with APP, Aβ1-40 and Aβ2-40 could be hardly detected after urea separation. Cells that were co-transfected with meprin β and either one of the APP isoform secreted high levels of Aβ variants in a similar pattern. The Aβ2-40/1-40 ratio was calculated and compared after densitometric analysis of the urea blot, since Aβ2-40 is the most prominent Aβ variant upon meprin β cleavage (Fig. 20 C). The analysis revealed that this ratio is significantly increased for cells co-expressing APP695 and meprin β compared to those cells solely overexpressing APP695. A similar Aβ pattern and an increased Aβ2-40/1-40 ratio could be observed for cells that were co-transfected with meprin β and either APP751 or APP770, however, the increase was not significant. Besides Aβ1-40 and Aβ2-40 all co-transfected cells showed a weak band for Aβ2-42 and even weaker for Aβ1-42.

These results suggest that the KPI domain has a rather small effect on APP cleavage by decreasing meprin β cleavage. If there are any indirect effects, since the KPI domain inhibits MT2 that in turn activates membrane bound meprin β (Jackle et al., 2015) still has to be determined.

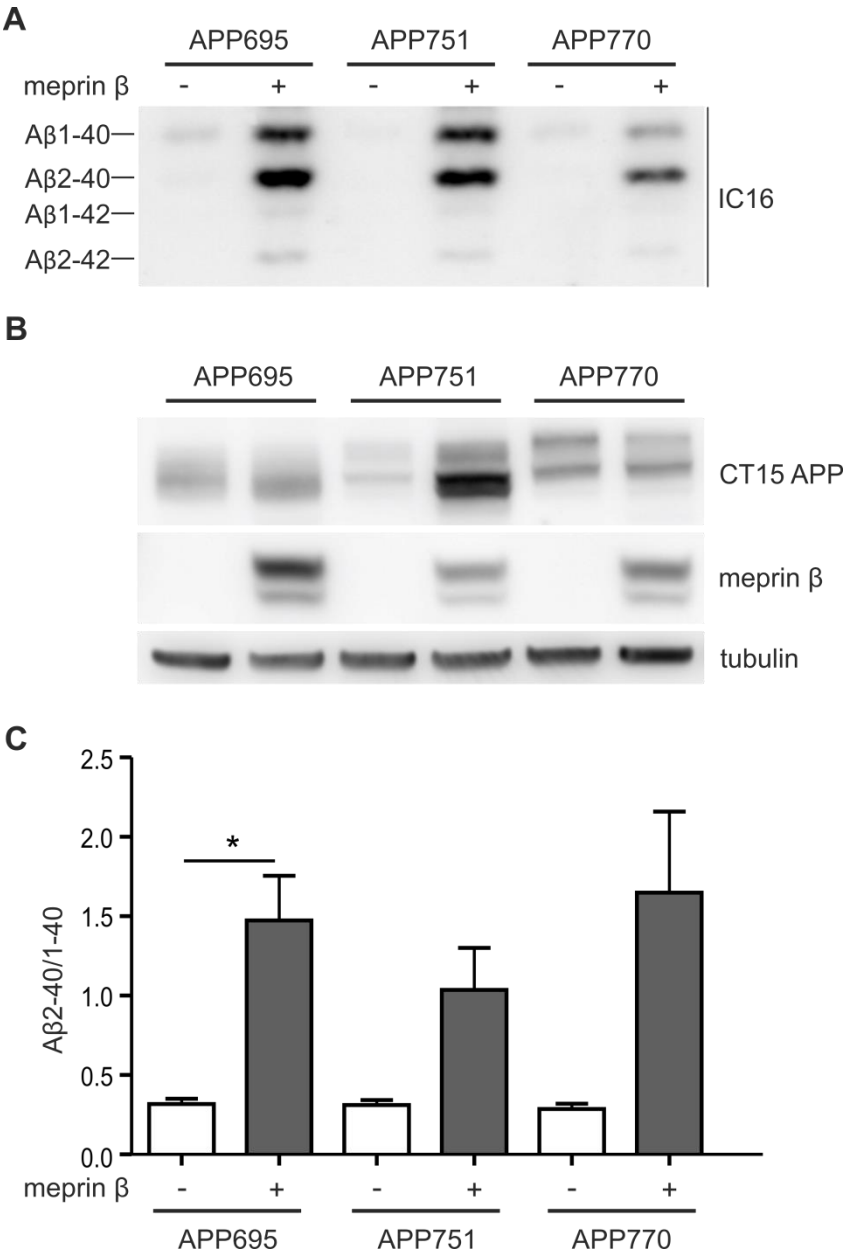

FIGURE 20 Neither the OX2 nor the KPI domain affect meprin β cleavage

HEK293T cells were transiently transfected with meprin β and APP695, APP751 or APP770. Supernatants were precipitated with IC16 activated dynabead for Aβ and subsequently separated on a 8 M urea gel (A). Additionally, lysates were separated on 10 % SDS PAGE and blotted and checked for APP (CT15 antibody), meprin β (R&D MEP1B antibody) and tubulin as loading control (B). The densitometric analysis of the urea gel showed a similar ratio of Aβ2-40/1-40 for all APP isoforms. Graph shows mean ± SEM (n=3); statistical significance: *<0.05; t-test.

6.5 Influence of γ-Secretase moldulators on meprin β associated Aβ variants

The application of γ-secretase modulators (GSM) is one therapeutical approach against AD. GSMs do not block Aβ, but selectively decrease the production of specific AD critical Aβ variants like Aβ1-42. To examine the effect on meprin β generated Aβ variants stably overexpressing HEK293T APP cells were transfected with either empty vector or meprin β. Post transfection cells were treated with two potent GSMs: the “GSK” GSM and the “Merck” GSM, both in a concentration of 200 nM for 24 h. Both are acidic GSMs that were already described by Hahn and colleagues (Hahn et al., 2011) and referred to as “compound 1” or “compound 2”, respectively. They were shown to decrease Aβ1-40 and Aβ1-42 levels and increase Aβ1-37 and Aβ1-38 (Hahn et al., 2003). Post treatment, cell supernatants were precipitated for Aβ using IC16-activated dynabeads and afterwards, precipitates were separated on urea SDS PAGE and blots were incubated with IC16 antibody (Fig. 21 A). The Aβ1-40/total ratio was only slightly decreased in cell supernatants of cells treated with GSMs (Fig. 21 B). As expected, the ratio of Aβ1-42/1-40 decreased after GSM treatment with both, the GSK and the Merck modulator (Fig. 21 C). Interestingly, by applying GSMs, the ratio of Aβ2-40/1-40 in meprin β transfected cells remained unaltered compared to cells without treatment, indicating that the treatment with these modulators has no effect on Aβ variants generated by meprin β (Fig. 21 D). Besides Aβ1-40, Aβ2-40, Aβ1-42 and Aβ2-42, further bands above the Aβ1-40 band could be detected (Fig. 21 A). These three bands above the Aβ1-40 band were proposed to represent Aβ1-37, Aβ1-38 and Aβ1-39 as Wiltfang and colleagues described these variants to run at this height.

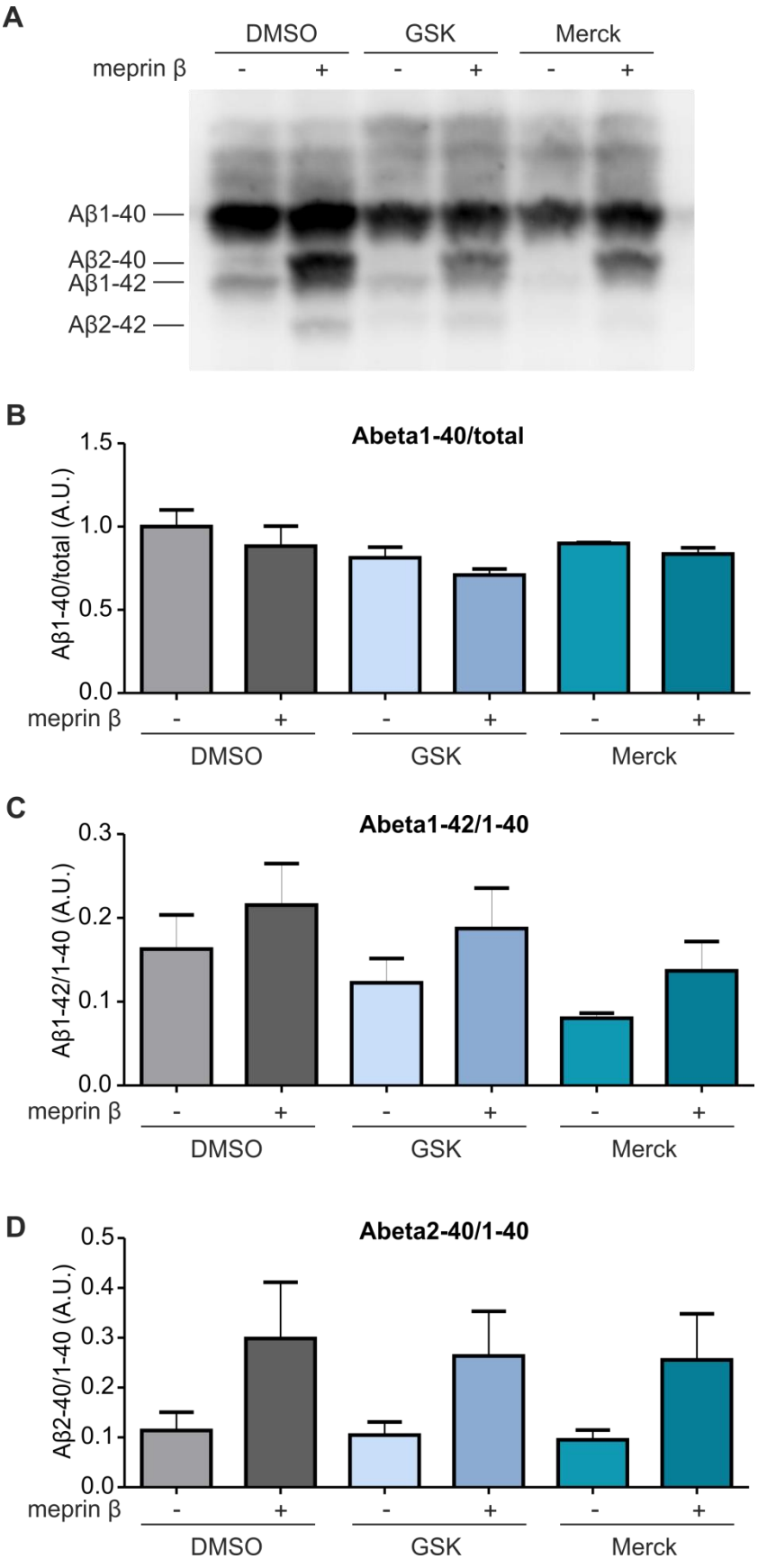

FIGURE 21 γ-secretase modulators do not affect levels of meprin β generated Aβ variants (see legend on next page)

(see figure on previous page) HEK293T APP cells were transfected with empty vector or meprin β and treated with DMSO (vehicle control), 200 nM GSK or 200 nM Merck modulator. Aβ was precipitated with IC16 activated dynabeads and separated on 8 M urea gels. The blot of the urea gel was incubated with IC16 antibody (A). The ratio of Aβ1-40/total (B), Aβ1-42/1-40 (C) and Aβ2-40/1-40 (D) was determined upon densitometric analysis of the urea gel. (n=3) ± SEM

To further determine if these variants are indeed present in these cell supernatants and further if Aβ2-37, Aβ2-38 and Aβ2-39 are present in meprin β transfected cells, Aβ was precipitated with IC16 conjugated agarose G beads. These precipitates were analyzed by MALDI-MS by Felix Östereich of the group of Dr. Lisa Münter of the McGill University, Montreal, Canada. Indeed, the analysis revealed that Aβ1-37 and Aβ1-38 are present in APP expressing HEK cells (Fig. 22). When these cells are co-transfected with meprin β, additionally Aβ2-37 and Aβ2-38 can be detected besides Aβ1-37 and Aβ1-38. These variants could be also found in cells that were treated with GSMs. If there is a shift in the ratio of these N- and C-terminally truncated peptides due to the application of GSMs has to be further evaluated by applying synthetic Aβ34 to the precipitates to calculate differences between the different samples. Moreover, it would be of further interest, to analyze the characteristic of the peptide variants in regard to aggregation propensity or toxicity.

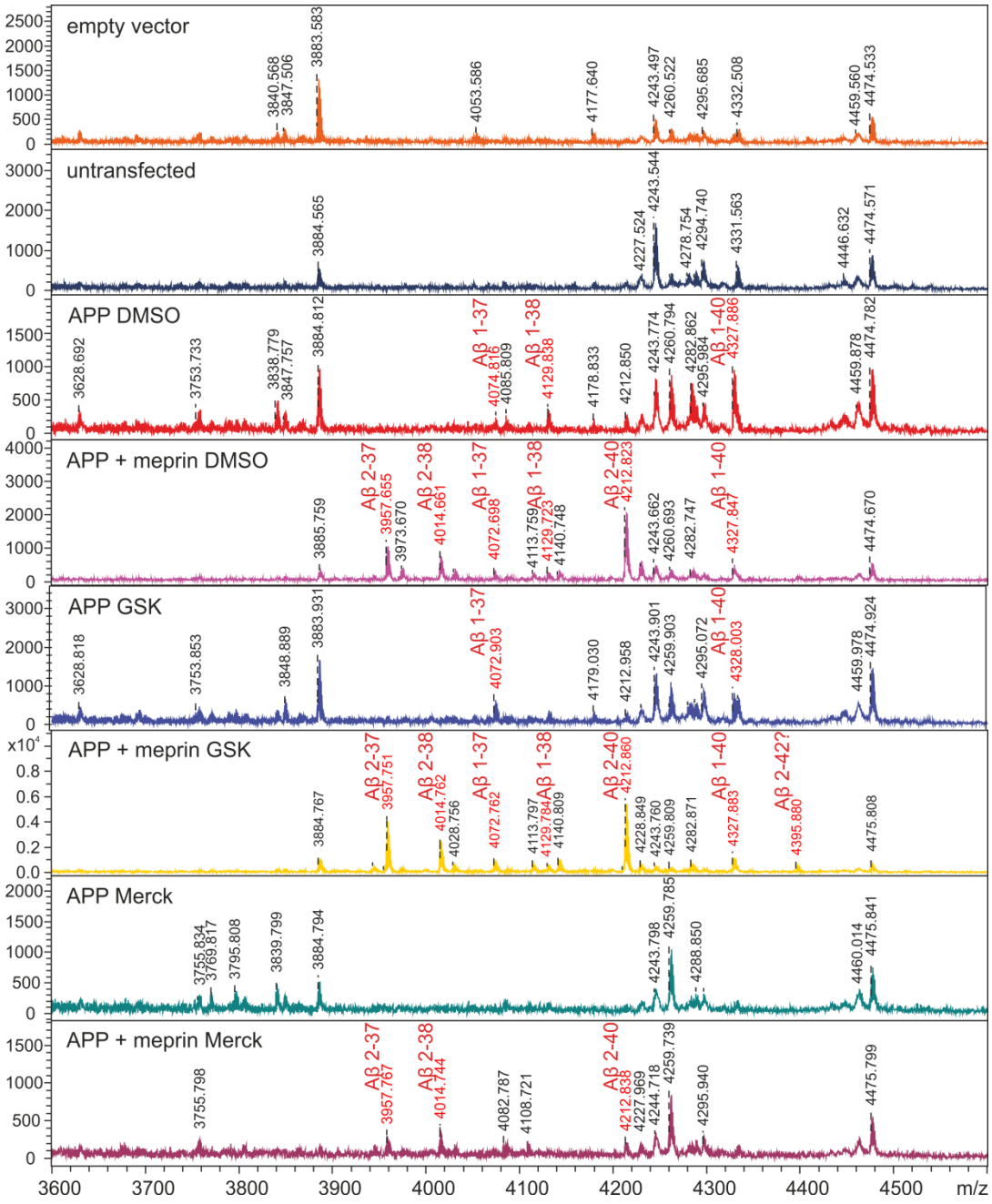

FIGURE 22 HEK293T APP cells secrete Aβ2-37 and Aβ2-38 before and after GSM treatment

HEK293T APP cells were transfected with empty vector or meprin β and treated with DMSO (vehicle control), 200 nM GSK or 200 nM Merck modulator. Aβ precipitates of cell supernatants were analyzed via MALDI-MS. The analysis showed that meprin β transfected cells generate Aβ2-37 and Aβ2-38 regardless of GSM treatment. MALDI-MS analysis was performed together with Felix Östereich, laboratory of Prof. Münter, McGill University, Montreal, Canada.

6.6 Influence of APP mutations linked to FAD on meprin β cleavage

In contrast to SAD, the outbreak of AD is well predictable to individuals that show a mutation in a risk gene for AD. This mutation either occurs on the genes for presenilin 1 or 2 or APP. It has been shown that these mutations lead to an increased generation of AD critical Aβ species. Besides increased γ-secretase cleavage, mutations that concern APP have been shown to also enhance BACE-1 cleavage. Thus, it was of special interest, if mutations within the APP sequence might also affect meprin β cleavage.

6.6.1 The "protective" APP A673T mutation is less prone to cleavage by meprin β

20 to 25 % of FAD cases are linked to mutations in the APP gene. All of these mutations have been shown to increase the generation of Aβ. However, a recently described APP mutation in position 673 (A673T) has been shown to protect against AD as well as against cognitive decline in the elderly independently of AD (Jonsson et al., 2012; Kero et al., 2013; Maloney et al., 2014). This mutation is located adjacent to the β-secretase cleavage site in the Aβ sequence at p2 and reduces Aβ generation by 40% *in vitro* (Jonsson et al., 2012). According to the findings reported above it can be suggested that the amino acid exchange (A673T) may also influence the affinity of meprin β towards APP. To investigate the influence of this mutation on meprin β cleavage of APP, a cleavage assay using recombinant enzyme and synthetic peptides including the A673T mutation was performed. HPLC and subsequent MALDI analysis revealed preferred cleavage of the wt over the A673T APP peptide by meprin β (Fig. 23 A, B). This is in agreement with other results that show that meprin β prefers alanine over threonine in P1' position (Becker-Pauly et al., 2011) and may explain reduced cleavage of APP A673T by meprin β.

To further clarify Aβ generation by meprin β from APP A673T *in vitro*, Aβ variants generated of APP wt or APP A673T by meprin β were compared (Fig. 23 C). Therefore, HEK293T cells were transfected with meprin β and APP wt or APP A673T and supernatants precipitated for Aβ. Precipitated Aβ peptides were separated on a urea gel. In APP A673T transfected cells no change in Aβ1-40 levels could be observed compared to those of APP wt. Furthermore, a distinct signal below the Aβ1-40 band could be detected, which could not be attributed to one of the Aβ marker peptides. It was assumed that this band is representing Aβ2-40 that could be shifted to different reasons analyzed and explained below (see 6.6.2 and 6.6.3). The

densitometric analysis revealed an approximately 70% decrease in the Aβ2-40/1-40 ratio (Fig. 23 D).

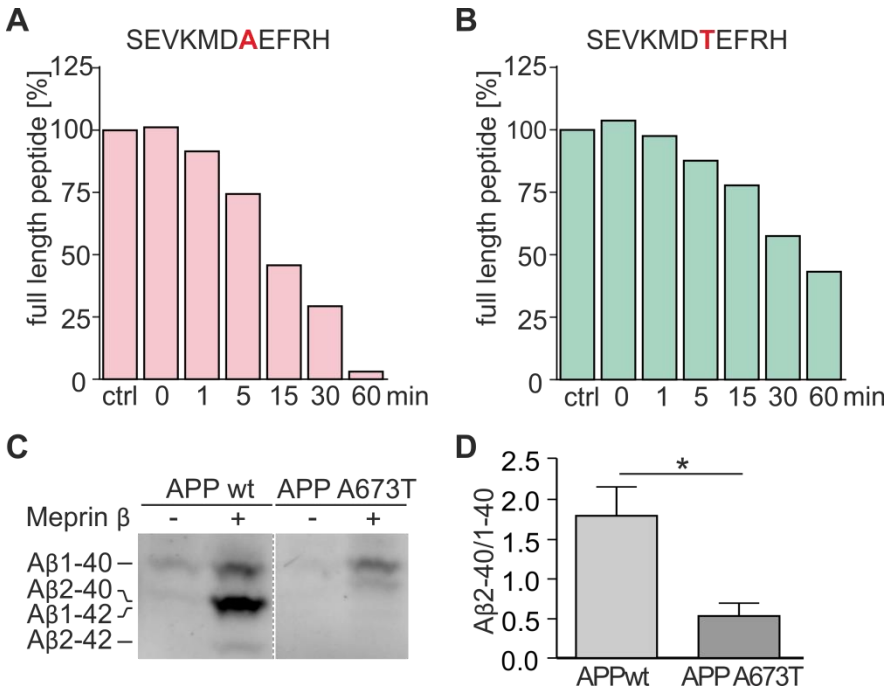

FIGURE 23 The APP A673T mutation protects from meprin β mediated cleavage
(A,B) 15 nM recombinant meprin β was incubated with synthetic APP peptides at 37°C. HPLC analysis showed that processing kinetics of APP A673T were decreased compared to wt APP. (C) Supernatants of HEK293T cells, transiently transfected with APP wt or APP A673T mutant and co-transfected with meprin β or empty vector were immunoprecipitated with anti-Aβ 6E10-Dynabeads, subsequently separated on an 8 M urea gel and probed with 6E10. The Aβ2-40 band, visible in samples transfected with APP wt and meprin β, is slightly shifted in samples transfected with APP A673T and meprin β. All samples were run on one gel but rearranged for better presentation. (D) A significant decrease of the Aβ2-40/1-40 ratio was observed in culture supernatants of cells co-transfected with APP A673T and meprin β compared to cells co-transfected with APP wt and meprin β (graph shows mean ± SEM (n=5); statistical significance: *, p=0.0317; t-test). HPLC analysis was performed together with Rielana Wichert, laboratory of Prof. Becker-Pauly, CAU Kiel, Germany.

6.6.2 The Aβ2-40AT Band is not Shifted Due to Phosphorylation

To further characterize this band the experiment above was repeated, however, this time using a different antibody to analyze urea separated Aβ-precipitates. Here, the 1E8 antibody was used that only recognizes Aβ peptides starting in p1 or p2, but not variants that are further truncated. The shifted band could still be detected, pinpointing the peptide to be starting in p1 or p2 (Fig. 24 A).

APP offers different sites for phosphorylation. The substitution from alanine to threonine would offer an additional phosphorylation site. To analyze if this peptide is representing Aβ2-40 but shifted due to a phosphorylation of the substituted threonine, samples were shifted band and an appearance of the familiar Aβ2-40 band.

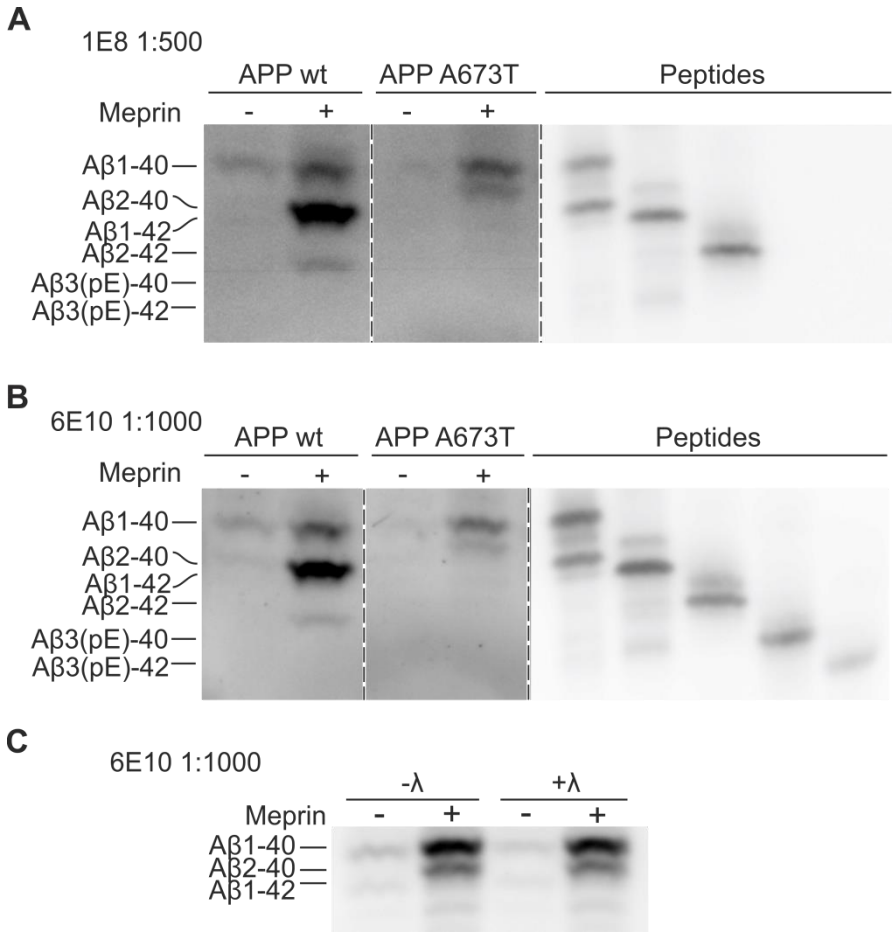

FIGURE 24 The Aβ2-40AT band is not shifted due to phosphorylation

HEK293T cells were transiently transfected with APP wt or APP A673T mutant and co-transfected with the empty vector or meprin β. 24 h post transfection supernatants were immunoprecipitated using Dynabeads conjugated with a 6E10 anti-Aβ antibody, subsequently separated on an 8 M urea gel and probed with 1E8 anti-Aβ1-x/2-x (A). The blot was reprobed with 6E10 anti-Aβ antibody. All samples were run on one gel but rearranged for better presentation. (B) A shift of the Aβ2-40 band caused by phosphorylation at the substituted threonine could be excluded by dephosphorylation with λ-phosphatase (New England Biolabs) after the last washing step of the immunoprecipitation. Samples were separated on an 8 M urea gel and probed with 6E10 anti-Aβ antibody that showed no change with or without phosphatase treatment (C).

However, the dephosphorylated sample showed the band at the same running height as without de-phosporylation that excludes a phosphorylation to be responsible for the

shift (Fig. 24 C). It is suggested that the band represents Aβ2-40 that is shifted due to changes in hydrophobicity, since the substitution leads to an elimination of the hydrophobic alanine and the inclusion of the hydrophilic threonine.

6.6.3 MALDI-MS ANALYSIS IDENTIFIES THE Aβ2-40AT BAND

To further validate that the before described band that only occurs after urea PAGE of Aβ precipitates of cells that were transfected with the APP A673T mutant and meprin β, but not with APP wt and meprin β is indeed Aβ2-40AT, but shifted in comparison to the wt Aβ2-40 due to decreased hydrophobicity since alanine is substituted to threonine, Aβ precipitates were further analyzed by MALDI-MS. Moreover, synthetic Aβ34 was added in equal concentrations to each precipitated, to provide the opportunity to compare the relative amounts of generated peptides of each sample. MALDI-MS data of precipitates of cells co-transfected with APP wt and meprin β showed distinct peaks for Aβ1-40 (labeled in orange) and Aβ2-40 (labeled in blue) (Fig. 25 A). Interestingly, in precipitates of cells co-transfected with APP A673T and meprin β, distinct peaks for Aβ1-40AT and, indeed for Aβ2-40AT could be detected (Fig. 25 B). When measuring the relative amounts of those peptides in relation to the additionally added synthetic Aβ34, in the case of APP wt transfected cells the ratio of Aβ2-40/Aβ1-40 was at ~3 (Fig. 25 C). In the case of APP A673T transfected cells this ratio was more than 3-fold decreased compared to the wt (Fig. 25 D). Even more interesting, the decrease of this ratio was only due to the decrease of Aβ2-40 levels in APP A673T transfected cells, since the level of Aβ1-40 was equally in both, APP wt and APP A673T transfected cell. These results strengthen the results of the urea PAGE based analysis of this thesis where a similar decrease in the Aβ2-40/1-40 ratio was described. This indicated, that the APP A673T mutation does not only protect form BACE-1 cleavage, as described by Jonsson and colleagues, but also protects from meprin β cleavage.

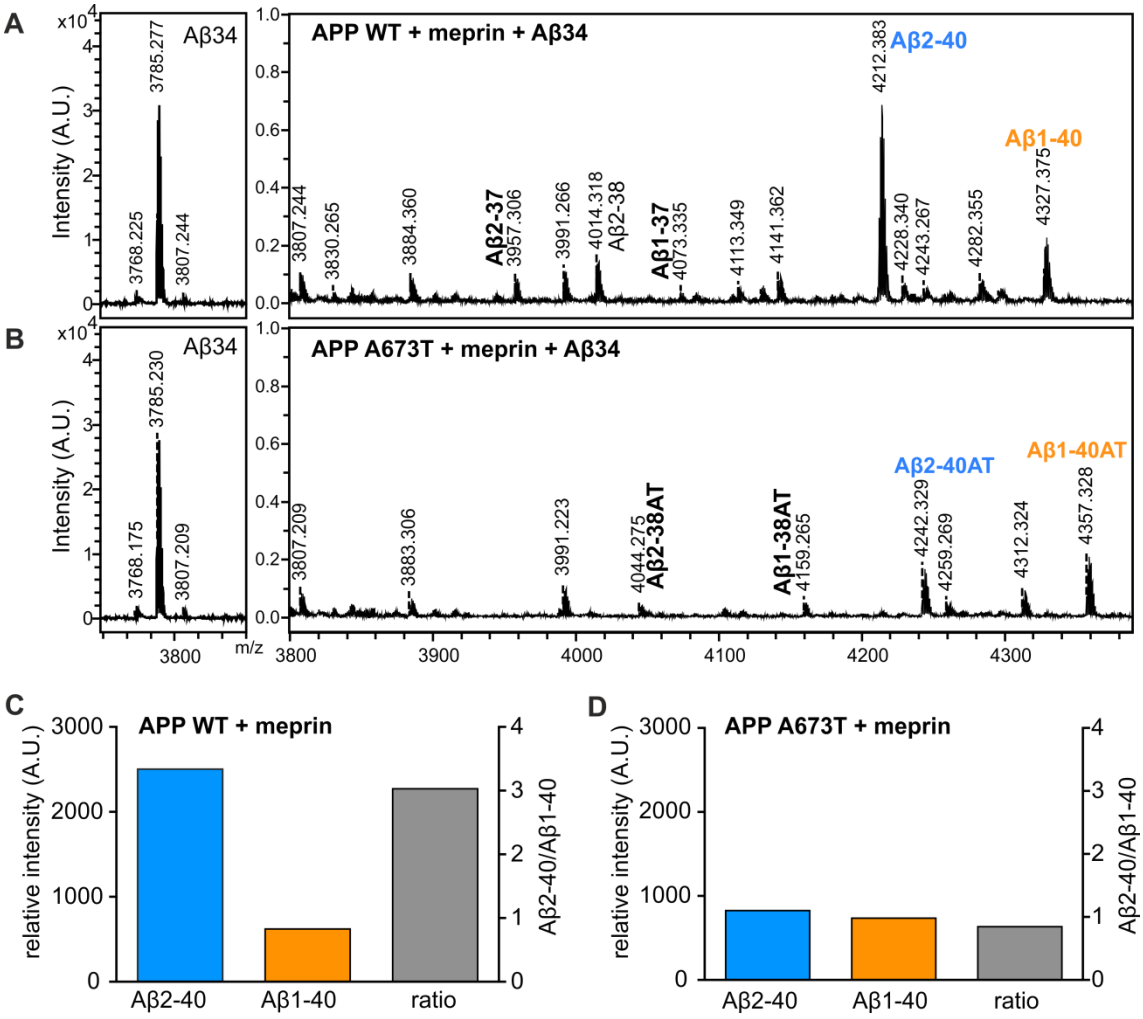

FIGURE 25 MALDI-MS spectra of secreted Aβ of HEK293T cells co-transfected with meprin β and APP wt or APP A673T

HEK293T cells were transiently co-transfected with meprin β and APP wt (A,C) or protective mutant APP A673T (B,D). Secreted Aβ was precipitated with IC16 for further MS-MALDI analysis. To normalize MS-MALDI measurements synthetic Aβ34 was added to each sample in equal amounts before measurement. (A) Mass spectrum shows peaks for wt Aβ2-40 and wt Aβ1-40. (B) Mass spectrum of samples transfected with mutated APP A673T shows peaks for Aβ2-40AT and Aβ1-40AT. (C,D) Normalization of Aβ2-40 and Aβ1-40 peaks to Aβ34 clearly shows that while Aβ1-40 levels are similar for wt (C) versus A673T (D), the levels of Aβ2-40 are approximately 3-fold increased in wt versus A673T. This is also reflected when comparing Aβ2-40/Aβ1-40 ratios, which is again approximately 3-fold increased in wt versus A673T. MALDI-MS analysis was performed together with Felix Östereich, laboratory of Prof. Münter, McGill University, Montreal, Canada.

6.6.4 APP$_{SWE}$ MUTATION AFFECTS MEPRIN β CLEAVAGE

Recently published results and the results of this thesis showed that meprin β overexpression results in increased levels of Aβ2-40. The degree of meprin β

generated Aβ1-40, however, is comparatively low. Therefore, the Aβ2-40/1-40 ratio was used as a measure for meprin β activity in the following analysis.

In contrast to BACE-1, meprin β exhibits the same increased affinity for APP wt peptides and those carrying the Swedish mutation (K670N/M671L) *in vitro* (Bien et al., 2012). However, here it is demonstrated that generation of the N-terminally truncated Aβ2-40/42 variants by meprin β from APP carrying the Swedish FAD mutation (APPswe) was almost completely abolished compared to APP wt controls (Fig. 26 A, B). To analyze whether other FAD mutations may affect meprin β activity in a similar fashion or whether only mutations localized closely to the N-terminus of the Aβ sequence influence meprin β cleavage specificity, the FAD causing London APP mutation (APPlon, V717I) was also investigated. Using APPlon it could be observed that the relative levels of Aβ in meprin β co-expressing cells are comparable to APP wt, indicating that changes close to the N-terminal sequence of the Aβ region may directly affect meprin β cleavage specificity. Additionally, the Swedish/London double mutation was tested. Again, no signal for Aβ2-40 could be detected which can be therefore attributed to the APPswe mutation. To further support this, data from a previously performed peptide cleavage assay was employed (Becker-Pauly et al., 2011), and analyzed with the help of a web-based tool (Schilling et al., 2011), if the change of methionine (APP wt) to leucine (APPswe) alters the preference of meprin β for certain amino acid residues around the cleavage site (Fig. 26 C, D). Indeed, while aspartate in P1 position (nomenclature by Schechter & Berger (Schechter and Berger, 1967)) is highly preferred in APP wt, this residue is clearly disliked at this particular position when leucine is set in P2, explaining the loss of Aβ2-40/42 generation by meprin β in APPswe.

Overall, it could be clearly shown that the amino acid composition around the β-site in APP affect meprin β cleavage preference. This is most striking for APPswe, which completely abolished Aβ2-40 generation.

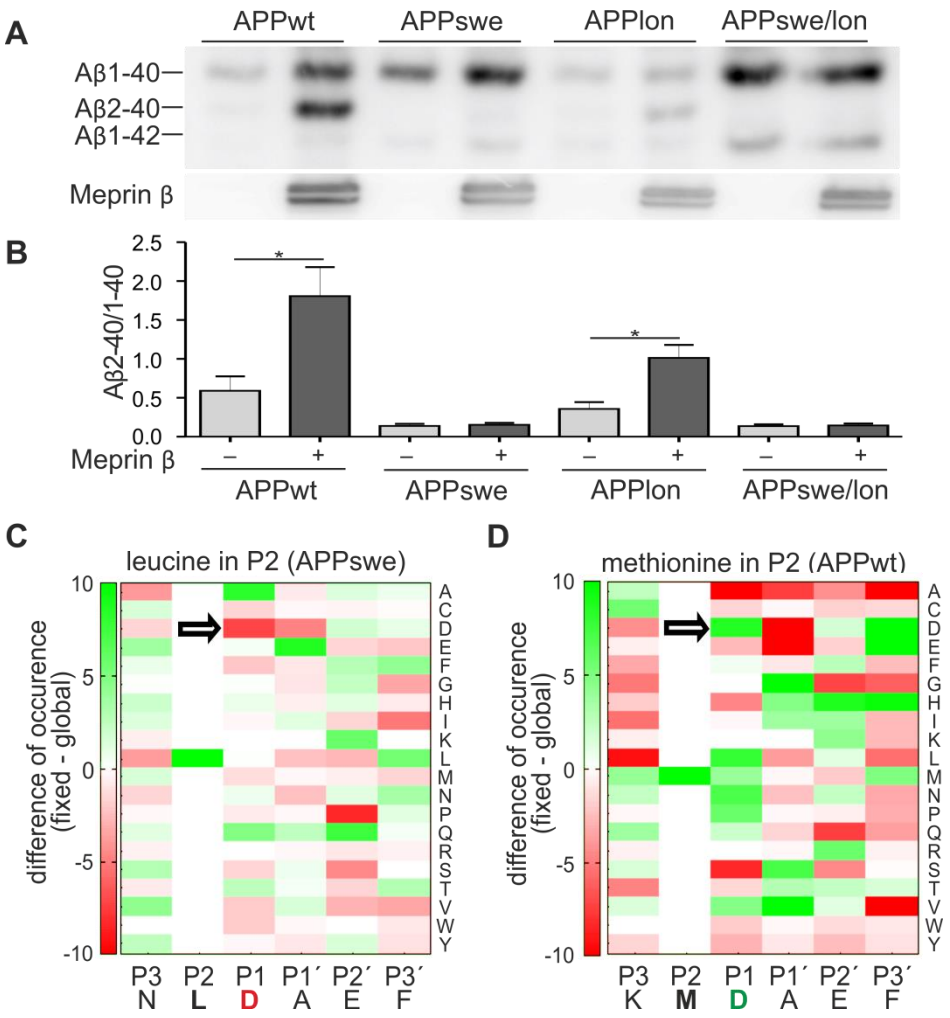

FIGURE 26 Meprin β cleavage is affected by mutations in APP.

(A,B) Western Blots of 8 M urea gels showed a distinct Aβ2-40 band in HEK293T cells transiently co-transfected with APP695wt or APPlon and meprin β. Supernatants were immunoprecipitated for Aβ using 6E10 antibody. Note that APPswe or APPswe/lon transfected cells, co-transfected with meprin β, did not show the Aβ2-40 band (graph shows mean ± SEM (n=4); statistical significance: *<0.05; t-test). (C,D) Subsite cooperativity determines the meprin β cleavage site in APP. Previously identified meprin β cleavage sites in peptides derived from HEK293T cell lysates (Becker-Pauly et al., 2011) were analyzed by a web-based tool (Schilling et al., 2011) to visualize changes in the preference for certain amino acid residue around the scissile bond (black line). Green color indicates high, red color low preference. Aspartate in P1 position is well preferred in APP wt, but disliked in APPswe. The meprin β cleavage site analysis was performed together with Prof. Becker-Pauly.

6.7 Preliminary Results

6.7.1 Increased meprin β mRNA levels upon Aβ treatment

The direct initiative causation for sporadic AD remained so far elusive. Though, the role of Aβ, to be more accurate, the imbalance of generation and clearance of Aβ and a shifted ratio of Aβ in the direction to more aggregation prone and toxic Aβ variants is acknowledged to be one primary event. However, how the amyloid cascade is commenced is still questioned. Yet, recently it has been shown that the activation of primary neurons by glycine stimulation leads to an increased co-localization of APP and BACE-1 due to APP transport to acidic and BACE-1 containing vesicles (Das et al., 2013). An increased chance for interaction of both proteins could following also lead to increased BACE-1 cleavage and thus increased Aβ generation.

Since this work shows that meprin β cleaves APP during the late secretory pathway or at the cell surface the activation of neurons is rather transporting APP away from subcellular compartments containing active meprin β. Thus, it was of interest if there are any other factors that lead to increase the meprin β mediated generation of Aβ. The first approach in that direction was the analysis of mRNA levels upon Aβ1-42 stimulation. Thus, N2a cells were treated with 0.5 µM and 5 µM Aβ1-42. 24 h post treatment RNA was isolated, cDNA was synthesized and following a quantitative qPCR was performed using primers for meprin β and GAPDH as housekeeping gene.

This first experiment may indicate that treatment of a neuronal cell line with Aβ1-42 leads to an upregulation of meprin β gene transcription (Fig. 27). Interestingly, the result shows that treatment with 0.5 µM Aβ1-42 led to a ~5-fold increase of mRNA levels compared to the vehicle control. However, by increasing the concentration of Aβ1-42 to 5 µM the effect on mRNA levels turned out to be reduced to a ~2-fold increase.

Yet, this experiment needs to be repeated to confirm the result. If the increased levels can be verified the results might indicate that an increased meprin β expression could be a downstream effect of BACE-1 mediated Aβ generation. Moreover, it would be of interest, if the increase in meprin β mRNA levels is specific to Aβ1-42 or if the same effect can be found for stimulation with other variants.

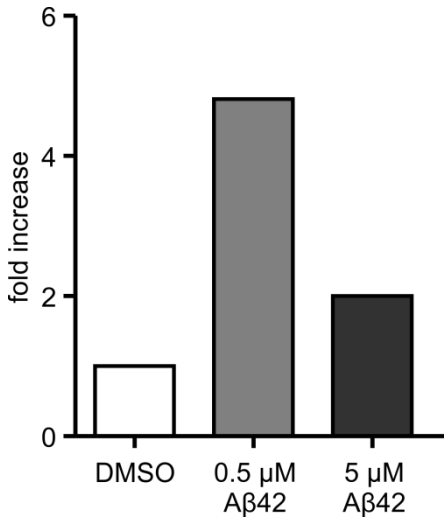

FIGURE 27 Increased meprin β mRNA levels in Aβ1-42 treated N2a cells

N2a cells were treated with 0.5 µM or 5 µM Aβ1-42. RNA was isolated 24 h post treatment, then cDNA was synthesized and following, qPCR was performed for meprin β. Increased meprin β mRNA levels could be detected upon Aβ1-42 treatment. (Housekeeping gene: GAPDH; n=1).

7 DISCUSSION

The amyloid cascade hypothesis postulates that the deposition of toxic variants of Aβ peptides in the brain, which are generated by sequential cleavage of APP by BACE-1 and the γ-secretase, is the central and initiating factor in the pathogenesis of AD. However, recent studies indicate that other proteases might contribute to this process since BACE cannot generate N-terminally truncated Aβ that has been shown to be present in CSF and brain of AD patients. The metalloprotease meprin β has been discussed to be one candidate protease for this cleavage event. The results of this thesis strengthen that idea and show that meprin β may indeed be a supporting actor besides the major β-secretase BACE-1.

7.1 MEPRIN β MAY HAVE A CONTRIBUTING ROLE IN AD PATHOGENGESIS

The proteolytic cleavage of the amyloid precursor protein and the accumulation of Aβ peptides in the brain are key events in the pathogenesis of AD (Haass and Selkoe, 2007; Hardy and Selkoe, 2002). It was shown that the deletion of BACE-1 in transgenic mice overexpressing APPswe abolishes Aβ generation in the brain (Cai et al., 2001; Dominguez et al., 2005; Luo et al., 2001; Roberds et al., 2001) and rescues behavioral and electrophysiological deficits (Dominguez et al., 2005; Ohno et al., 2004). However, several N-terminally truncated Aβ variants have also been described in the CSF and brains of AD patients and cannot be attributed to BACE-1 activity (Guntert et al., 2006; Lewczuk et al., 2004a; Lewczuk et al., 2004b; Maler et al., 2007; Murayama et al., 2007; Takeda et al., 2004; Vassar et al., 2014; Wiltfang et al., 2001). This suggests that proteases other than BACE-1 may be involved in the generation of N-terminally truncated Aβ peptides in the brain. Secretory proteases, such as insulin-degrading enzyme and neprilysin, might be involved in generating N-terminally truncated variants by degrading Aβ1-x (Wang et al., 2006a). The angiotensin converting enzyme (ACE) for instance might be one candidate to be responsible for the generation of Aβ8-x (Hu et al., 2001).

Only recently it could be shown that also the metalloprotease meprin β generates N-terminally truncated Aβ peptides *in vitro* (Bien et al., 2012). It was proposed that this protease may be a candidate for a cleavage event to generate Aβ2-40. Other N-terminally truncated Aβ peptides, such as the pyroglutamylated pE(3)-Aβ have already

been shown to correlate with AD pathogenesis what indicates a pivotal role of these peptides in AD (Mandler et al., 2014).

The *in vivo* relevance of meprin β-mediated APP shedding is indeed the most important issue. It has to be emphasized that under non-challenged conditions meprin β expression in the murine brain is relatively low, and therefore might only contribute to a small percentage to the physiological cleavage of APP in neurons. Here, BACE-1 activity is by far most relevant. However, in this work it could be shown with different approaches that meprin β partially contributes to APP processing. A different APP cleavage pattern in brains of meprin β ko compared to wt mice has already been shown, suggesting that meprin β is involved in N-terminal processing of endogenous APP *in vivo* (Bien et al., 2012). This study was aiming at investigating and evaluating the supposed endogenous cleavage of APP by meprin β in more detail. In this study, increased levels of endogenous sAPPα generation in meprin β ko mice were observed. sAPPα is generated through cleavage at the α-secretase cleavage site within the Aβ sequence by ADAM10 (Esch et al., 1990; Jorissen et al., 2010; Kuhn et al., 2010; Lammich et al., 1999; Postina et al., 2004; Sisodia et al., 1990). A similar increase in sAPPα levels has been observed in BACE-1 ko mice or after treatment of mice with BACE-1 inhibitors (Hussain et al., 2007; Luo et al., 2001; Nishitomi et al., 2006). Results of this work indicate that due to the absence of meprin β more substrate may be available for ADAM10 cleavage, since the levels of sAPPα are increased. One would expect that on the other site sAPPβ levels would decrease in meprin β ko mice due to decreased β-site cleavage. However, the 192wt antibody, which was used to detect sAPPβ, does only recognize the shorter sAPPβ-M671 variant, mainly produced by BACE-1 cleavage (and partially by meprin β) and not the longer sAPPβ-D672 only produced by meprin β. Therefore, it does not reflect the total sAPPβ load (Fig. 5) and an increase of the sAPPβ-M671 variant can be seen in meprin β ko mice, since the higher substrate availability for BACE-1 prevails the lapse of meprin β generated sAPPβ-M671.

Additionally, a decrease of approximately 13% of endogenous Aβ40 levels was detected in meprin β ko neurons compared to wt controls. However, the overall low Aβ levels and the lack of an appropriate antibody did not allow detecting Aβ2-40, the variant that has been previously detected in supernatants of APP and meprin β overexpressing cells via MALDI-MS. To circumvent this problem and to gain further insights into Aβ production of endogenous meprin β primary meprin β ko and wild type control neurons were infected with recombinant adenovirus expressing human APP695 and secreted Aβ was precipitated and analyzed on urea gels. A decrease of

approximately 50% of Aβ2-40 levels compared to wt neurons could be detected. The remaining Aβ2-40, which is also present in the ko, may be explained by other proteolytic events like N-terminal truncation of the full-length Aβ originally generated by BACE-1, through aminopeptidases like APA (Sevalle et al., 2009).

The effect of the lack of meprin β however, does not proof a direct involvement of the protease in APP processing. Indirect effects of meprin β could also lead to the observed changes in meprin β deficient mice, for example by an activating effect on BACE-1. In this case however, a direct interaction of APP and meprin β, as it has been shown before for APP and BACE-1 via co-immunoprecipitation (Huang et al., 2004), would not be required and would thus be rather unlikely. But interestingly, here a direct interaction could be indeed shown for meprin β and APP, which suggests a direct effect of meprin β on APP. Moreover, it was recently published that the incubation of recombinant active meprin β with recombinant BACE-1 does not show any activating effects on BACE-1 (Schonherr et al., 2016). Also, an activating role of meprin β on other proteases like BACE-1 still would not explain the generation of Aβ2-40, since, as already described above, BACE-1 does not generate N-terminally truncated Aβ2-40.

In this work, the focus has been set on the N-terminally truncated Aβ2-40 variant that has been shown to be generated by meprin β (Bien et al., 2012). The different naturally occurring Aβ variants that differ in length or due to modifications like nitration manifest different characteristics. For example, the longer Aβ1-42 is more prone to form neurotoxic aggregates than Aβ1-40 (Iwatsubo et al., 1994; Roher et al., 1993). Also, nitration increases the aggregation of Aβ (Kummer et al., 2011). So far, many studies have examined the characteristics of Aβ3-x, which can be N-terminally cyclized to pyroglutamate Aβ (pEAβ3-x) (Gunn et al., 2010; Guntert et al., 2006; Harigaya et al., 2000; Lai et al., 1995; Wittnam et al., 2012), as well as Aβ4-x (Bouter et al., 2013; Masters et al., 1985; Vassar et al., 2014) and Aβ5-x (Murayama et al., 2007; Portelius et al., 2013; Takeda et al., 2004). It was recently observed that also Aβ2-40 shows a high propensity to aggregate (Schonherr et al., 2016). Even more interesting, the same study showed that Aβ2-40 nucleates the aggregation of Aβ1-40 that usually exhibits a rather minor aggregation propensity. Even if meprin β expression levels are relatively low under physiological conditions and probably also in the initial phase of the disease, these results underline the importance of meprin β. Only low levels of meprin β could yet have detrimental effects, since already low levels of Aβ2-40 could have an initiating and perpetuating effect on aggregation of the overall Aβ load.

The results discussed above all hind to a role of meprin β in APP processing and the generation of Aβ2-40. To further elucidate the relevance of meprin β in AD pathogenesis it was of aim to directly focus on human brain samples. Only recently, it was shown that meprin β mRNA levels are increased in AD brains. However, it has to be considered that though mRNA levels are a good indicator of gene regulation, studies showed that there is not necessarily a correlation between mRNA and protein levels (Greenbaum et al., 2003), for example due to post-transcriptional modifications. For this reason frontal lobes of AD patients, healthy controls and a group of non-AD but neurodegeneration patients was immunohistochemically analyzed for meprin β. A significantly increased number of meprin β positive neurons could confirm the data for increased meprin β mRNA levels. Additionally, western blot analysis of human brain lysates (AD n=3, control n=3) were analyzed and revealed ~2.5-fold increased meprin β protein levels in AD. The band at 120 kDa represents the preform of meprin β, the band at 115 kDa shows the active form without the propeptide and the band at 80 kDa reflects the shedded meprin β (Fig. 14 C). The high levels of the shedded form can be explained by the upregulation of ADAM17 in apoptotic cells (Sommer et al., 2016) that is capable in shedding meprin β. The postmortem delay and time to freezing storage could account for this upregulation.

Thus, these results are in line with the previously observed meprin β mRNA levels by Bien and colleagues (Bien et al., 2012). Moreover, similar observations could be obtained for BACE-1 in different studies. By western blot analysis, Holsinger and colleagues showed a 2.7-fold increase of BACE-1 protein levels in the brain cortex of AD patients as compared to age-matched controls (Holsinger et al., 2002).These results were also confirmed by Fukumoto and colleagues who even measured a 14% increase of BACE-1 levels in the frontal cortex and a 15% increase in the temporal cortex of AD patients (Fukumoto et al., 2002).

Since the here illustrated results demonstrate that in murine brain the presence of meprin β has an effect on the processing of APP in a way that resulted from increased β-site cleavage Aβ2-40, the further shown increased meprin β levels in human AD brains would suggest a similar effect. In 2002 it could be shown that levels of Aβ2-42 are increased in brains of AD patients. This already might have been an effect evoked by meprin β cleavage (Wiltfang et al., 2001). Indeed, the analysis of precipitated Aβ from frontal lobe homogenates of AD patients and healthy controls additionally revealed the presence of Aβ2-40. To the author’s knowledge, this is the first time Aβ2-40 has been detected in the human brain. Further, an increase in the Aβ2-40/1-40 ratio for AD could be measured. Since meprin β mRNA levels are relatively high in temporal

lobe compared to other regions of the human brain (Su et al., 2002; Su et al., 2004) an increased meprin β activity and thus increased meprin β cleavage mediated APP fragments seemed likely. Therefore, homogenates of this region of human AD and healthy control brains were precipitated for Aβ. The analysis of the Aβ2-40/1-40 ratio did not reveal any significant changes for AD versus control. However, it has to be considered that one outlier in the control cases has high levels of Aβ2-40, but notably the same case still has increased levels of Aβ1-42. Thus, it might be presumed that this case would have been affected by AD later in life. Yet, more cases need to be analyzed to investigate if the Aβ2-40/1-40 ratio is increased in the temporal lobe of AD patients. Still, these first cases show a slight tendency in that direction and thus make it an interesting target for ongoing studies.

Overall, these results obtained by analyzing brains of meprin β ko mice and moreover of human AD brains, strongly support an involvement of the protease meprin β in the processing of APP.

7.2 Overexpressing cell culture based experiments reveal a direct effect and interaction of meprin β on APP processing

The interaction of BACE-1 with APP at the cell surface and in early endosomes has been demonstrated (Das et al., 2013; Kinoshita et al., 2003). As discussed above, it could be shown that the metalloprotease meprin β and its substrate APP interact in brain lysates of wild type mice. To further elucidate in which cellular compartment meprin β mediated Aβ generation occurs, an APP construct with impaired endocytosis due to a deletion of the tyrosine dependent sorting signal (NPxY motif; ΔNPxY) at the C-terminus (Bonifacino and Traub, 2003; Koo and Squazzo, 1994) was used. When APP is endocytosed most of the Aβ1-40/1-42 generation and BACE-1 activity is found in endosomes due to its acidic pH optimum as an aspartyl protease (Golde et al., 1992; Haass et al., 1992; Vassar et al., 1999). Meprin β, however, belongs to the astacin family of zinc endopeptidases and is mainly active at or near the cell surface as a membrane-bound enzyme. Recently, it could be shown that a hyperactive mutant of meprin β, which was exclusively localized at the secretory pathway and not secreted, resulted in enhanced APP shedding and Aβ generation (Arnold et al., 2015). Additionally, rat meprin β was shown to exhibit an acidic pH optimum with additional proteolytic activity at basic pH (Bertenshaw et al., 2002). Therefore, it is possible that meprin β cleaves APP in the late secretory pathway, at the cell surface or – like BACE-

1 – in endosomes. To exclude the endosomal pathway for meprin β, APPΔNPxY was used, which allows to normal post translational modification, maturation and transport to the cell surface.

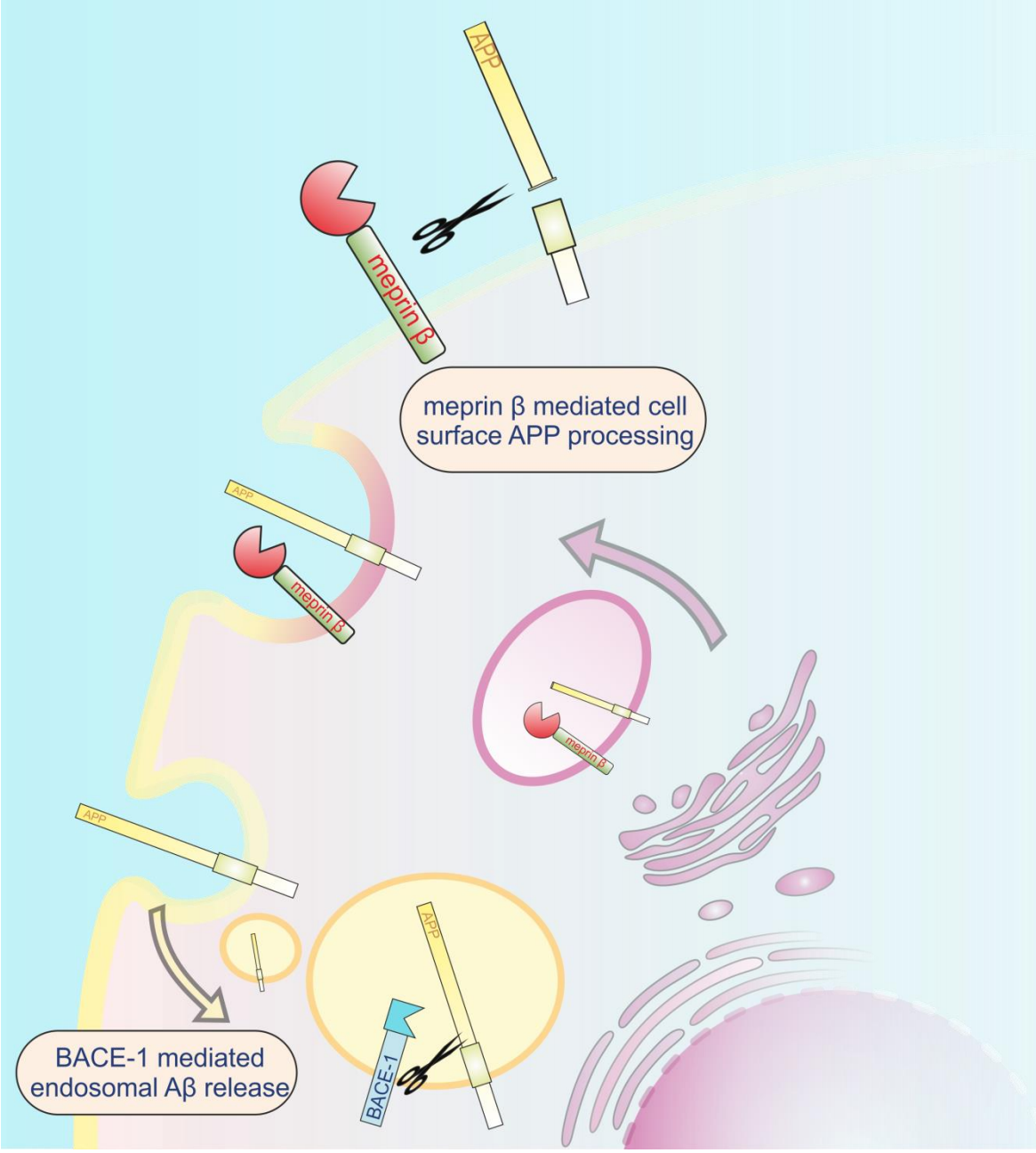

FIGURE 28 Schematic representation of the proteolytic cleavage of APP by meprin β

In contrast to BACE-1 cleavage that mainly occurs in endosomal compartments, here it was shown that the molecular interaction of APP and the metalloprotease meprin β takes place in the secretory pathway and at the cell surface.

However, internalization and degradation of APPΔNPxY is impaired and thus BACE-1 mediated Aβ generation is strongly reduced (Koo and Squazzo, 1994; Lai et al., 1995;

Perez et al., 1999). The processing of full-length APP and the generation of N-terminally truncated Aβ was analyzed in cells co-expressing APPΔNPxY and meprin β. Mature surface APP wt was almost completely vanished through cleavage of meprin β and this effect was even greater when endocytosis of APP was impaired. In contrast to BACE-1, meprin β was still able to cleave APP and to generate N-terminally truncated Aβ peptides when internalization of APP is decreased. Thus, these results demonstrate a spatial subcellular segregation of APP cleavage by meprin β from BACE-1 mediated APP cleavage. Still, most of the initial APP processing of the amyloidogenic pathway occurs in the endosomal compartment by BACE-1, but the N-terminally truncated Aβ2-40 and Aβ2-42 variants are generated at or close to the cell surface by meprin β. The immunofluorescent data of this work further confirms these results. Using a split-GFP based complementation assay combined with antibody stainings against transfected proteins, meprin β and APP/APPΔNPxY could be detected in close proximity prior to internalization. This supports the above described study, which showed that a hyperactive mutant of meprin β led to massive shedding of APP already within the secretory pathway, again pointing to a potential interaction of the two proteins before endocytosis (Fig. 28) (Arnold et al., 2015). Eventually, the spatial separation of meprin β cleavage and BACE-1 cleavage of APP is even going beyond the subcellular level. Only recently, it was shown that while primary chicken neurons only secrete very low levels of Aβ2-40, primary chicken astrocytes and microglia produce a higher portion of that species (Oberstein et al., 2015). Additionally, they showed that the Aβ2-40/1-40 ratio is increased in astrocytes and microglia compared to neurons that predominantly produced Aβ1-x. Since, so far, the here depicted histologically analysis of AD brains only focused on neurons, it would be of great interest to specifically focus on astrocytes and microglia to evaluate if these results are correlating with meprin β levels.

The total amount of APP in astrocytes is ~90% higher than in neurons (Rohan de Silva et al., 1997). This might suggest a tremendously increased Aβ generation in astrocytes compared to neurons. Still, neuronal cultures generate 7-fold more total Aβ than cultured astrocytes (Oberstein et al., 2015). It has to be considered that while in neurons the most abundant isoform appears to be the shorter variant APP695, it has been shown that in astrocytes 3-fold more KPI domain bearing isoforms are present (Rohan de Silva et al., 1997), which may represent a rate limiting factor in the production of N-terminally truncated Aβ. The KPI domain that is present in the longer APP751 and APP770, but not in the shorter isoform APP695 does not seem to reveal a prominent effect on meprin β mediated Aβ generation since the Aβ2-40/1-40 ratio does only slightly differ. For all isoforms an increase of the Aβ2-40/1-40 ratio can be

detected, when cells were co-transfected with meprin β. Yet, this increase was only significant for APP695. It was previously shown that the KPI domain decreases APP *cis*-dimer formation (Isbert et al., 2012). Potentially, meprin β, which is itself expressed as a dimer, slightly prefers APP dimers over monomers. Moreover, it has to be considered that recent results showed that the KPI domain exhibits an inhibitory capacity towards the serine protease matriptase-2 (MT2) by forming a complex with that protease (Beckmann, 2016). Interestingly, the same protease has been shown to be an activator of membrane bound meprin β (Jackle et al., 2015) Therefore, decreased levels of active MT2 in the presence of the KPI domain result in decreased meprin β activation and could thus lead to decreased APP cleavage. However, as mentioned before, only a small change in the Aβ2-40/1-40 ratio could be detected. Therefore, MT2 represents an interesting target to decrease levels of active meprin β to thereby lower levels of aggregation prone Aβ2-40.

The results described above suggest that meprin β directly interacts and cleaves APP and that the described effects are not due to an activating effect of meprin β on BACE-1. Vice versa, it has to be considered that APP is not the only substrate of BACE-1 and hence, it had to be excluded that meprin β is among other substrates of that secretase, which are for example neuregulin-1 (Hu et al., 2006; Willem et al., 2006) or the voltage-gated sodium channel β (VGSC β) (Kim et al., 2007; Wong et al., 2005). Here however, by applying BACE tripartite inhibitor to BACE-1 and meprin β overexpressing HEK293T cells, it could be excluded that BACE-1 cleaves/activates meprin β since in this case the Aβ2-40/1-40 ratio would be decreased. The observed slight increase of that ratio however, further supports the independent role of meprin β and shows even more that in the absence of active BACE-1 more substrate is converted by the metalloprotease. Interestingly, this is in line with the results of Oberstein and colleagues that revealed a decrease of Aβ1-40, but no change in Aβ2-40 levels in primary chicken astrocytes upon treatment with two different BACE-1 inhibitors (Oberstein et al., 2015).

Besides BACE-1, another therapeutic target in AD is the γ-secretase. Yet, this secretase does not only cleave APP but also Notch that is involved in neurogenesis, cell fate and cell communication. The knockout of Notch1 has been shown to block T cell development in mice (Radtke et al., 2000; Radtke et al., 1999). The treatment with γ-secretase inhibitors leads to unintended consequences (reviewed in De Strooper, 2014; Searfoss et al., 2003; Wong et al., 2004). This problem can be probably bypassed by the application of GSMs, which have no effect on the total Aβ load. GSMs rather specifically decrease levels of Aβ1-42 and slightly of Aβ1-40 levels but increase Aβ1-37 and Aβ1-38 levels (Weggen et al., 2003). However, here it could be shown that

in overexpressing cells two tested GSMs did not affect the Aβ2-40/1-40 ratio. Thus, considering the aggregation and seeding characteristic of Aβ2-40, the Aβ aggregation problematic in AD would probably not be eliminated. In meprin β co-transfected cells, additionally Aβ2-37 and Aβ2-38 could be detected. These variants were also present in GSM treated cells. The characteristics and importance of these peptides thus needs to be analyzed in future studies. Concluding, the application of GSMs might not completely solve the issue of the disposal of aggregating Aβ and might be further analyzed with an eye on toxic Aβ variants other than Aβ1-42.

7.3 APP MUTATIONS ASSOCIATED TO FAD AFFECT MEPRIN β CLEAVAGE

Several mutations within the APP sequence have been shown to have an impact on BACE-1 cleavage affinity on APP. The recently described APP mutation A673T that has been shown to protect against AD as well as against cognitive decline in the elderly independent of AD was analyzed. The mutation is located at position two of Aβ (Aβ-A/T) and has been shown to reduce BACE-1 mediated Aβ generation by 40% using synthetic peptides as substrates (Jonsson et al., 2012). Moreover, a significantly decreased Aβ production in human APP A673T-overexpressing primary neurons has been observed (Benilova et al., 2014; Maloney et al., 2014). Additionally, a decreased aggregation propensity of Aβ-A/T could be measured, which is showing the complexity of the protective effects of the substitution. Thus, here, the meprin β mediated cleavage of APP A673T in cell culture and in a peptide cleavage assay was studied and revealed a significant decrease of ~70% in the Aβ2-40/1-40 ratio compared to wt APP. This result could be confirmed by analyzing Aβ precipitates by MALDI-MS. The decreased cleavage of meprin β in the presence of the A673T substitution is consistent with the data of the cleavage assay which focused on the cleavage preference of meprin β by using recombinant enzyme and synthetic peptides including the mutation and analysis via HPLC and subsequent MALDI. Here, a preference of alanine over threonine in P1' position could be detected (Jonsson et al., 2012).

Besides other modifications, Aβ can be phosphorylated at serine residue 8 and 26 or at tyrosine residue 10. Phosphorylated Aβ has been shown to be present in AD brains (Kumar et al., 2011). Moreover, the phosphorylation at serine residue 8 increases the formation of oligomeric Aβ and is moreover, resistant to degradation by the insulin degrading enzyme (IDE) (Kumar et al., 2011; Kumar et al., 2012). The protective APP mutation bears a substitution of alanine to threonine at the N-terminus of Aβ at position

2 which would offer an additional phosphorylation site. Aβ precipitates of HEK293T cells co-transfected with protective APP A673T and meprin β that were separated on urea gels showed a band that was shifted compared to the Aβ2-40 band from APPwt transfected cells. It was speculated that this shifted band (see section 7.6.1-7.6.3) might be shifted only due to the substitution of a hydrophobic amino acid to a hydrophilic amino acid or also due to a phosphorylation. However, after treatment of the Aβ precipitates with λ-phosphatase, this band still appeared at that position. Yet, these results only indicate that a probable phosphorylation does not induce a shift of the Aβ1-40 or Aβ2-40 band. Still, with this experiment it could not be excluded that A2T-Aβ can be phosphorylated. This, however, might be an interesting target for further studies on that mutation, since a phosphorylation at that position might also contribute to the protective effects described.

For a better understanding of various diseases, different animal/mouse models were generated in the last decades. To gain further understanding of AD, different mouse models were already generated in the 1990´s. These models are immensely important to study the pathophysiology of AD. However, potential weaknesses of these models have to be considered. There are common models to study Aβ plaque pathology that all bear the APP Swedish mutation, such as 5xFAD mice, carrying mutations in the APP and PSEN1 genes (APP K670N/M671L (Swedish), APP I716V (Florida), APP V717I (London), PSEN1 M146L and PSEN1 L286V) (Oakley et al., 2006), J20 mice, carrying mutations only in the APP gene (K670N/M671L (Swedish) and the APP V717F (Indiana)) (Mucke et al., 2000), or the 3xTg mice, carrying mutations in the APP, PSEN1 and the MAPT genes (K670N/M671L (Swedish), MAPT P301L and PSEN1 M146V) (Oddo et al., 2003). These models all manifest an amyloid pathology as well as learning and memory deficits. Thus, they appear to be appropriate models at the first sight. However, the here described results might be challenging the suitability of these models. Surprisingly, in this work it could be observed that Aβ2-x variants were missing in cells overexpressing meprin β and APP bearing the Swedish double mutation K670N/M671L (APPswe) which is located in close vicinity of the β-secretase cleavage site. Here, a significantly reduced meprin β mediated Aβ2-40/42 generation was found. Although BACE-1 is clearly the most prominent enzyme responsible for the generation of Aβ1-40 and Aβ1-42 peptides from the APP wt or APPswe sequences, meprin β may be responsible for generating small amounts of N-terminal truncated Aβ2-40 and Aβ2-42 peptides almost exclusively from the APP wt sequences or APP bearing the wt sequence around the β-cleavage site, respectively. This clearly shows a significant influence of amino acid substitutions around the β-secretase cleavage site

for meprin β mediated Aβ generation. It is suggested that the amino acid substitution close to the meprin β cleavage site provides a mechanistic explanation for the differential generation of truncated Aβ species from APP wt versus APPswe constructs. Notably, the human APPswe is used in almost all AD animal models as it serves as a better substrate for BACE-1, thereby increasing production of total Aβ (Cai et al., 1993; Citron et al., 1992). Therefore, it is likely that the actual effect of meprin β has been overseen in many studies focusing on APP processing. The suitability of models using APPswe might therefore be rethought.

In contrast to supernatants of cells overexpressing APPswe and meprin β, Aβ2-40 could be clearly detected in supernatants of APPlon and meprin β. Additionally, the ratio of A2-40/1-40 is 3.5-fold increased in cells co-expressing APPlon and meprin β compared to cells only overexpressing APPlon. This is very similar to the wild type where a 3.3-fold increase could be observed when co-transfected with meprin β. This suggests that only mutations around the β-cleavage site affect the meprin β mediated Aβ pattern. However, an overall increase of the total Aβ load could be measured. This might be due to the fact that the subcellular distribution of APPlon is changed compared to APP wt. It was shown that the localization of APPlon is rather shifted to acidic endosomal compartments containing active BACE-1 (Muratore). The results of Muratore and colleagues thus confirm the here described data that meprin β cleaves prior the endosomal pathway.

7.4 Aβ MAY INCREASE MEPRIN β GENE EXPRESSION

The results of this work indicate that the Aβ generation by BACE-1 and meprin β is occurring in two independent ways. Which stimuli induce or boost the respective cleavage event needs to be further elucidated in future studies. This might offer new targets in AD therapy.

Dhawan and colleagues have shown that Aβ peptides serve as a specific stimulus for Src kinase-based microglial activation leading to pro-inflammatory changes (Dhawan and Combs, 2012). Src was identified to be an upstream inducer of the AP-1 transcription factor complex (Byun et al., 2006). Interestingly, AP-1 directly binds to the promoter region of meprin β thereby increasing meprin β mRNA expression. Therefore, it can be hypothesized that this event subsequently may also induce meprin β expression, which again would lead to increased Aβ levels. In the same line, it was shown that increased Src activity also positively regulates BACE-1 and enhances Aβ production (Zou et al., 2007). In a preliminary experiment of this work it could be shown

that extracellular Aβ1-42 may indeed have gene regulatory functions in a manner to increase meprin β mRNA levels in N2a cells. This result needs to be confirmed in further experiments and a potential similar effect of other Aβ variants has to be elucidated. If these results can be verified, they might hint to a self-perpetuating process in AD that would represent an important therapeutic target.

Concluding, this work reveals that meprin β functions as an additional protease besides the major secretase BACE-1, to be involved in the generation of Aβ by cleaving the N-terminus of this peptide. The here described increased meprin β levels as well as an increased Aβ2-40/1-40 ratio in AD brains imply that the protease might play an important role in AD pathology. Different experiments of this thesis illustrate that meprin β directly interacts and cleaves APP independently of BACE-1. This cleavage event, however, is dependent on the amino acid composition around the cleavage site, since the recently discovered protective APP A673T mutation protects from meprin β cleavage. Interestingly, it could be also shown that meprin β is incapable of generating Aβ2-40 from the Swedish mutated APP associated with FAD. Moreover, the results indicate that the so far promising GSMs do not affect the Aβ2-40/1-40 ratio. Although, BACE-1 acts as the major β-secretase responsible for Aβ generation, these results show that the role of meprin β should not be ignored as the protease might require a specific therapeutic strategy.

8 REFERENCES

Alzheimer, A., R.A. Stelzmann, H.N. Schnitzlein, and F.R. Murtagh. 1995. An English translation of Alzheimer's 1907 paper, "Uber eine eigenartige Erkankung der Hirnrinde". *Clin Anat*. 8:429-431.

Andersson, E.R., R. Sandberg, and U. Lendahl. 2011. Notch signaling: simplicity in design, versatility in function. *Development*. 138:3593-3612.

Arai, T., H. Akiyama, K. Ikeda, H. Kondo, and H. Mori. 1999. Immunohistochemical localization of amyloid beta-protein with amino-terminal aspartate in the cerebral cortex of patients with Alzheimer's disease. *Brain research*. 823:202-206.

Armstrong, R.A. 2011. Spatial patterns of beta-amyloid (Abeta) deposits in familial and sporadic Alzheimer's disease. *Folia Neuropathol*. 49:153-161.

Arnold, P., F. Schmidt, J. Prox, F. Zunke, C. Pietrzik, R. Lucius, and C. Becker-Pauly. 2015. Calcium negatively regulates meprin beta activity and attenuates substrate cleavage. *FASEB journal : official publication of the Federation of American Societies for Experimental Biology*. 29:000-000.

Arolas, J.L., C. Broder, T. Jefferson, T. Guevara, E.E. Sterchi, W. Bode, W. Stocker, C. Becker-Pauly, and F.X. Gomis-Ruth. 2012. Structural basis for the sheddase function of human meprin beta metalloproteinase at the plasma membrane. *Proceedings of the National Academy of Sciences of the United States of America*.

Arriagada, P.V., K. Marzloff, and B.T. Hyman. 1992. Distribution of Alzheimer-type pathologic changes in nondemented elderly individuals matches the pattern in Alzheimer's disease. *Neurology*. 42:1681-1688.

Banerjee, S., and J.S. Bond. 2008. Prointerleukin-18 is activated by meprin beta in vitro and in vivo in intestinal inflammation. *The Journal of biological chemistry*. 283:31371-31377.

Becker-Pauly, C., O. Barre, O. Schilling, U. Auf dem Keller, A. Ohler, C. Broder, A. Schutte, R. Kappelhoff, W. Stocker, and C.M. Overall. 2011. Proteomic analyses reveal an acidic prime side specificity for the astacin metalloprotease family reflected by physiological substrates. *Molecular & cellular proteomics : MCP*. 10:M111.009233.

Becker-Pauly, C., M. Howel, T. Walker, A. Vlad, K. Aufenvenne, V. Oji, D. Lottaz, E.E. Sterchi, M. Debela, V. Magdolen, H. Traupe, and W. Stocker. 2007. The alpha and beta subunits of the metalloprotease meprin are expressed in separate layers of human epidermis, revealing different functions in keratinocyte proliferation and differentiation. *J Invest Dermatol*. 127:1115-1125.

Becker, A., S. Kohlmann, A. Alexandru, W. Jagla, F. Canneva, C. Bauscher, H. Cynis, R. Sedlmeier, S. Graubner, S. Schilling, H.U. Demuth, and S. von Horsten. 2013. Glutaminyl cyclase-mediated toxicity of pyroglutamate-beta amyloid induces striatal neurodegeneration. *BMC Neurosci*. 14:108.

Beel, A.J., and C.R. Sanders. 2008. Substrate specificity of gamma-secretase and other intramembrane proteases. *Cellular and molecular life sciences : CMLS*. 65:1311-1334.

Benilova, I., R. Gallardo, A.A. Ungureanu, V. Castillo Cano, A. Snellinx, M. Ramakers, C. Bartic, F. Rousseau, J. Schymkowitz, and B. De Strooper. 2014. The Alzheimer Disease Protective Mutation A2T Modulates Kinetic and Thermodynamic Properties of Amyloid-beta (Abeta) Aggregation. *The Journal of biological chemistry*. 289:30977-30989.

Bertenshaw, G.P., M.T. Norcum, and J.S. Bond. 2003. Structure of homo- and hetero-oligomeric meprin metalloproteases. Dimers, tetramers, and high molecular mass multimers. *The Journal of biological chemistry*. 278:2522-2532.

Bertenshaw, G.P., B.E. Turk, S.J. Hubbard, G.L. Matters, J.E. Bylander, J.M. Crisman, L.C. Cantley, and J.S. Bond. 2001. Marked differences between metalloproteases meprin A and B in substrate and peptide bond specificity. *The Journal of biological chemistry*. 276:13248-13255.

Bertenshaw, G.P., J.P. Villa, J.A. Hengst, and J.S. Bond. 2002. Probing the active sites and mechanisms of rat metalloproteases meprin A and B. *Biological chemistry*. 383:1175-1183.

Beynon, R.J., and J.S. Bond. 1983. Deficiency of a kidney metalloproteinase activity in inbred mouse strains. *Science*. 219:1351-1353.

Beynon, R.J., J.D. Shannon, and J.S. Bond. 1981. Purification and characterization of a metallo-endoproteinase from mouse kidney. *The Biochemical journal*. 199:591-598.

Bibl, M., M. Gallus, V. Welge, H. Esselmann, S. Wolf, E. Ruther, and J. Wiltfang. 2012a. Cerebrospinal fluid amyloid-beta 2-42 is decreased in Alzheimer's, but not in frontotemporal dementia. *Journal of neural transmission*. 119:805-813.

Bibl, M., M. Gallus, V. Welge, S. Lehmann, K. Sparbier, H. Esselmann, and J. Wiltfang. 2012b. Characterization of cerebrospinal fluid aminoterminally truncated and oxidized amyloid-beta peptides. *Proteomics Clin Appl*. 6:163-169.

Biederer, T., and T.C. Sudhof. 2000. Mints as adaptors. Direct binding to neurexins and recruitment of munc18. *The Journal of biological chemistry*. 275:39803-39806.

Bien, J., T. Jefferson, M. Causevic, T. Jumpertz, L. Muenter, G. Multhaup, S. Weggen, C. Becker-Pauly, and C.U. Pietrzik. 2012. The metalloprotease meprin beta generates amino terminal truncated Abeta-peptide species. *The Journal of biological chemistry*. 287:33304-33313.

Bonifacino, J.S., and L.M. Traub. 2003. Signals for sorting of transmembrane proteins to endosomes and lysosomes. *Annual review of biochemistry*. 72:395-447.

Bouter, Y., K. Dietrich, J.L. Wittnam, N. Rezaei-Ghaleh, T. Pillot, S. Papot-Couturier, T. Lefebvre, F. Sprenger, O. Wirths, M. Zweckstetter, and T.A. Bayer. 2013. N-truncated amyloid beta (Abeta) 4-42 forms stable aggregates and induces acute and long-lasting behavioral deficits. *Acta neuropathologica*. 126:189-205.

Braak, H., and K. Del Tredici. 2012. Where, when, and in what form does sporadic Alzheimer's disease begin? *Curr Opin Neurol*. 25:708-714.

Broder, C., P. Arnold, S. Vadon-Le Goff, M.A. Konerding, K. Bahr, S. Muller, C.M. Overall, J.S. Bond, T. Koudelka, A. Tholey, D.J. Hulmes, C. Moali, and C. Becker-Pauly. 2013. Metalloproteases meprin alpha and meprin beta are C- and N-procollagen proteinases important for collagen assembly and tensile strength. *Proceedings of the National Academy of Sciences of the United States of America*. 110:14219-14224.

Broder, C., and C. Becker-Pauly. 2013. The metalloproteases meprin alpha and meprin beta: unique enzymes in inflammation, neurodegeneration, cancer and fibrosis. *The Biochemical journal*. 450:253-264.

Brown, M.S., J. Ye, R.B. Rawson, and J.L. Goldstein. 2000. Regulated intramembrane proteolysis: a control mechanism conserved from bacteria to humans. *Cell*. 100:391-398.

Buxbaum, J.D., S.E. Gandy, P. Cicchetti, M.E. Ehrlich, A.J. Czernik, R.P. Fracasso, T.V. Ramabhadran, A.J. Unterbeck, and P. Greengard. 1990. Processing of Alzheimer beta/A4 amyloid precursor protein: modulation by agents that regulate protein phosphorylation. *Proceedings of the National Academy of Sciences of the United States of America*. 87:6003-6006.

Byun, H.J., I.K. Hong, E. Kim, Y.J. Jin, D.I. Jeoung, J.H. Hahn, Y.M. Kim, S.H. Park, and H. Lee. 2006. A splice variant of CD99 increases motility and MMP-9 expression of human breast cancer cells through the AKT-, ERK-, and JNK-dependent AP-1 activation signaling pathways. *The Journal of biological chemistry*. 281:34833-34847.

Cai, H., Y. Wang, D. McCarthy, H. Wen, D.R. Borchelt, D.L. Price, and P.C. Wong. 2001. BACE1 is the major beta-secretase for generation of Abeta peptides by neurons. *Nature neuroscience*. 4:233-234.

Cai, X.D., T.E. Golde, and S.G. Younkin. 1993. Release of excess amyloid beta protein from a mutant amyloid beta protein precursor. *Science*. 259:514-516.

Cao, X., and T.C. Sudhof. 2001. A transcriptionally [correction of transcriptively] active complex of APP with Fe65 and histone acetyltransferase Tip60. *Science*. 293:115-120.

Chavez-Gutierrez, L., L. Bammens, I. Benilova, A. Vandersteen, M. Benurwar, M. Borgers, S. Lismont, L. Zhou, S. Van Cleynenbreugel, H. Esselmann, J. Wiltfang, L. Serneels, E. Karran, H. Gijsen, J. Schymkowitz, F. Rousseau, K. Broersen, and B. De Strooper. 2012. The mechanism of gamma-Secretase dysfunction in familial Alzheimer disease. *The EMBO journal*. 31:2261-2274.

Citron, M., T.S. Diehl, A. Capell, C. Haass, D.B. Teplow, and D.J. Selkoe. 1996. Inhibition of amyloid beta-protein production in neural cells by the serine protease inhibitor AEBSF. *Neuron*. 17:171-179.

Citron, M., T. Oltersdorf, C. Haass, L. McConlogue, A.Y. Hung, P. Seubert, C. Vigo-Pelfrey, I. Lieberburg, and D.J. Selkoe. 1992. Mutation of the beta-amyloid precursor protein in familial Alzheimer's disease increases beta-protein production. *Nature*. 360:672-674.

Craig, S.S., J.F. Reckelhoff, and J.S. Bond. 1987. Distribution of meprin in kidneys from mice with high- and low-meprin activity. *Am J Physiol*. 253:C535-540.

Crisman, J.M., B. Zhang, L.P. Norman, and J.S. Bond. 2004. Deletion of the mouse meprin beta metalloprotease gene diminishes the ability of leukocytes to disseminate through extracellular matrix. *J Immunol*. 172:4510-4519.

Das, U., D.A. Scott, A. Ganguly, E.H. Koo, Y. Tang, and S. Roy. 2013. Activity-induced convergence of APP and BACE-1 in acidic microdomains via an endocytosis-dependent pathway. *Neuron*. 79:447-460.

De Strooper, B. 2014. Lessons from a failed gamma-secretase Alzheimer trial. *Cell*. 159:721-726.

De Strooper, B., W. Annaert, P. Cupers, P. Saftig, K. Craessaerts, J.S. Mumm, E.H. Schroeter, V. Schrijvers, M.S. Wolfe, W.J. Ray, A. Goate, and R. Kopan. 1999. A presenilin-1-dependent gamma-secretase-like protease mediates release of Notch intracellular domain. *Nature*. 398:518-522.

De Strooper, B., P. Saftig, K. Craessaerts, H. Vanderstichele, G. Guhde, W. Annaert, K. Von Figura, and F. Van Leuven. 1998. Deficiency of presenilin-1 inhibits the normal cleavage of amyloid precursor protein. *Nature*. 391:387-390.

Dhawan, G., and C.K. Combs. 2012. Inhibition of Src kinase activity attenuates amyloid associated microgliosis in a murine model of Alzheimer's disease. *J Neuroinflammation*. 9:117.

Dickson, D.W. 1997. The pathogenesis of senile plaques. *Journal of neuropathology and experimental neurology*. 56:321-339.

Dominguez, D., J. Tournoy, D. Hartmann, T. Huth, K. Cryns, S. Deforce, L. Serneels, I.E. Camacho, E. Marjaux, K. Craessaerts, A.J. Roebroek, M. Schwake, R. D'Hooge, P. Bach, U. Kalinke, D. Moechars, C. Alzheimer, K. Reiss, P. Saftig, and B. De Strooper. 2005. Phenotypic and biochemical analyses of BACE1- and BACE2-deficient mice. *The Journal of biological chemistry*. 280:30797-30806.

Eggert, S., K. Paliga, P. Soba, G. Evin, C.L. Masters, A. Weidemann, and K. Beyreuther. 2004. The proteolytic processing of the amyloid precursor protein gene family members APLP-1 and APLP-2 involves alpha-, beta-, gamma-, and epsilon-like cleavages: modulation of APLP-1 processing by n-glycosylation. *The Journal of biological chemistry*. 279:18146-18156.

Esch, F.S., P.S. Keim, E.C. Beattie, R.W. Blacher, A.R. Culwell, T. Oltersdorf, D. McClure, and P.J. Ward. 1990. Cleavage of amyloid beta peptide during constitutive processing of its precursor. *Science*. 248:1122-1124.

Fleck, D., A.N. Garratt, C. Haass, and M. Willem. 2012. BACE1 dependent neuregulin processing: review. *Current Alzheimer research*. 9:178-183.

Fukumoto, H., B.S. Cheung, B.T. Hyman, and M.C. Irizarry. 2002. Beta-secretase protein and activity are increased in the neocortex in Alzheimer disease. *Archives of neurology*. 59:1381-1389.

Gentleman, S.M., D.I. Graham, and G.W. Roberts. 1993. Molecular pathology of head trauma: altered beta APP metabolism and the aetiology of Alzheimer's disease. *Progress in brain research*. 96:237-246.

Glenner, G.G., and C.W. Wong. 1984. Alzheimer's disease: initial report of the purification and characterization of a novel cerebrovascular amyloid protein. *Biochemical and biophysical research communications*. 120:885-890.

Goate, A., M.C. Chartier-Harlin, M. Mullan, J. Brown, F. Crawford, L. Fidani, L. Giuffra, A. Haynes, N. Irving, L. James, and et al. 1991. Segregation of a missense mutation in the amyloid precursor protein gene with familial Alzheimer's disease. *Nature*. 349:704-706.

Goedert, M., C.M. Wischik, R.A. Crowther, J.E. Walker, and A. Klug. 1988. Cloning and sequencing of the cDNA encoding a core protein of the paired helical filament of Alzheimer disease: identification as the microtubule-associated protein tau. *Proceedings of the National Academy of Sciences of the United States of America*. 85:4051-4055.

Golde, T.E., S. Estus, L.H. Younkin, D.J. Selkoe, and S.G. Younkin. 1992. Processing of the amyloid protein precursor to potentially amyloidogenic derivatives. *Science*. 255:728-730.

Graf, E.R., X. Zhang, S.X. Jin, M.W. Linhoff, and A.M. Craig. 2004. Neurexins induce differentiation of GABA and glutamate postsynaptic specializations via neuroligins. *Cell*. 119:1013-1026.

Greenbaum, D., C. Colangelo, K. Williams, and M. Gerstein. 2003. Comparing protein abundance and mRNA expression levels on a genomic scale. *Genome Biol*. 4:117.

Gu, Y., H. Misonou, T. Sato, N. Dohmae, K. Takio, and Y. Ihara. 2001. Distinct intramembrane cleavage of the beta-amyloid precursor protein family resembling gamma-secretase-like cleavage of Notch. *The Journal of biological chemistry*. 276:35235-35238.

Gunn, A.P., C.L. Masters, and R.A. Cherny. 2010. Pyroglutamate-Abeta: role in the natural history of Alzheimer's disease. *The international journal of biochemistry & cell biology*. 42:1915-1918.

Guntert, A., H. Dobeli, and B. Bohrmann. 2006. High sensitivity analysis of amyloid-beta peptide composition in amyloid deposits from human and PS2APP mouse brain. *Neuroscience*. 143:461-475.

Haass, C., A.Y. Hung, M.G. Schlossmacher, D.B. Teplow, and D.J. Selkoe. 1993. beta-Amyloid peptide and a 3-kDa fragment are derived by distinct cellular mechanisms. *The Journal of biological chemistry*. 268:3021-3024.

Haass, C., E.H. Koo, A. Mellon, A.Y. Hung, and D.J. Selkoe. 1992. Targeting of cell-surface beta-amyloid precursor protein to lysosomes: alternative processing into amyloid-bearing fragments. *Nature*. 357:500-503.

Haass, C., and D.J. Selkoe. 2007. Soluble protein oligomers in neurodegeneration: lessons from the Alzheimer's amyloid beta-peptide. *Nature reviews. Molecular cell biology*. 8:101-112.

Hahn, D., A. Pischitzis, S. Roesmann, M.K. Hansen, B. Leuenberger, U. Luginbuehl, and E.E. Sterchi. 2003. Phorbol 12-myristate 13-acetate-induced ectodomain shedding and phosphorylation of the human meprinbeta metalloprotease. *The Journal of biological chemistry*. 278:42829-42839.

Hahn, S., T. Bruning, J. Ness, E. Czirr, S. Baches, H. Gijsen, C. Korth, C.U. Pietrzik, B. Bulic, and S. Weggen. 2011. Presenilin-1 but not amyloid precursor protein mutations present in mouse models of Alzheimer's disease attenuate the response of cultured cells to

gamma-secretase modulators regardless of their potency and structure. *Journal of neurochemistry*. 116:385-395.

Halim, A., G. Brinkmalm, U. Ruetschi, A. Westman-Brinkmalm, E. Portelius, H. Zetterberg, K. Blennow, G. Larson, and J. Nilsson. 2011. Site-specific characterization of threonine, serine, and tyrosine glycosylations of amyloid precursor protein/amyloid beta-peptides in human cerebrospinal fluid. *Proceedings of the National Academy of Sciences of the United States of America*. 108:11848-11853.

Hardy, J., and D.J. Selkoe. 2002. The amyloid hypothesis of Alzheimer's disease: progress and problems on the road to therapeutics. *Science*. 297:353-356.

Harigaya, Y., T.C. Saido, C.B. Eckman, C.M. Prada, M. Shoji, and S.G. Younkin. 2000. Amyloid beta protein starting pyroglutamate at position 3 is a major component of the amyloid deposits in the Alzheimer's disease brain. *Biochemical and biophysical research communications*. 276:422-427.

Hashimoto, Y., T. Chiba, M. Yamada, M. Nawa, K. Kanekura, H. Suzuki, K. Terashita, S. Aiso, I. Nishimoto, and M. Matsuoka. 2005. Transforming growth factor beta2 is a neuronal death-inducing ligand for amyloid-beta precursor protein. *Mol Cell Biol*. 25:9304-9317.

Hashimoto, Y., and M. Matsuoka. 2014. A mutation protective against Alzheimer's disease renders amyloid beta precursor protein incapable of mediating neurotoxicity. *Journal of neurochemistry*. 130:291-300.

Hata, S., M. Taniguchi, Y. Piao, T. Ikeuchi, A.M. Fagan, D.M. Holtzman, R. Bateman, H.R. Sohrabi, R.N. Martins, S. Gandy, K. Urakami, T. Suzuki, and I. Japanese Alzheimer's Disease Neuroimaging. 2012. Multiple gamma-secretase product peptides are coordinately increased in concentration in the cerebrospinal fluid of a subpopulation of sporadic Alzheimer's disease subjects. *Molecular neurodegeneration*. 7:16.

Heber, S., J. Herms, V. Gajic, J. Hainfellner, A. Aguzzi, T. Rulicke, H. von Kretzschmar, C. von Koch, S. Sisodia, P. Tremml, H.P. Lipp, D.P. Wolfer, and U. Muller. 2000. Mice with combined gene knock-outs reveal essential and partially redundant functions of amyloid precursor protein family members. *The Journal of neuroscience : the official journal of the Society for Neuroscience*. 20:7951-7963.

Hedrich, J., D. Lottaz, K. Meyer, I. Yiallouros, W. Jahnen-Dechent, W. Stocker, and C. Becker-Pauly. 2010. Fetuin-A and cystatin C are endogenous inhibitors of human meprin metalloproteases. *Biochemistry*. 49:8599-8607.

Herzog, C., R.S. Haun, V. Kaushal, P.R. Mayeux, S.V. Shah, and G.P. Kaushal. 2009. Meprin A and meprin alpha generate biologically functional IL-1beta from pro-IL-1beta. *Biochemical and biophysical research communications*. 379:904-908.

Herzog, C., G.P. Kaushal, and R.S. Haun. 2005. Generation of biologically active interleukin-1beta by meprin B. *Cytokine*. 31:394-403.

Holsinger, R.M., C.A. McLean, K. Beyreuther, C.L. Masters, and G. Evin. 2002. Increased expression of the amyloid precursor beta-secretase in Alzheimer's disease. *Ann Neurol*. 51:783-786.

Hou, L., I. Kang, R.E. Marchant, and M.G. Zagorski. 2002. Methionine 35 oxidation reduces fibril assembly of the amyloid abeta-(1-42) peptide of Alzheimer's disease. *The Journal of biological chemistry*. 277:40173-40176.

Hu, J., A. Igarashi, M. Kamata, and H. Nakagawa. 2001. Angiotensin-converting enzyme degrades Alzheimer amyloid beta-peptide (A beta); retards A beta aggregation, deposition, fibril formation; and inhibits cytotoxicity. *The Journal of biological chemistry*. 276:47863-47868.

Hu, X., C.W. Hicks, W. He, P. Wong, W.B. Macklin, B.D. Trapp, and R. Yan. 2006. Bace1 modulates myelination in the central and peripheral nervous system. *Nature neuroscience*. 9:1520-1525.

Huang, X.P., W.P. Chang, G. Koelsch, R.T. Turner, 3rd, F. Lupu, and J. Tang. 2004. Internalization of exogenously added memapsin 2 (beta-secretase) ectodomain by cells is mediated by amyloid precursor protein. *The Journal of biological chemistry*. 279:37886-37894.

Hubbs, J.L., N.O. Fuller, W.F. Austin, R. Shen, S.P. Creaser, T.D. McKee, R.M. Loureiro, B. Tate, W. Xia, J. Ives, and B.S. Bronk. 2012. Optimization of a natural product-based class of gamma-secretase modulators. *Journal of medicinal chemistry*. 55:9270-9282.

Huguenin, M., E.J. Muller, S. Trachsel-Rosmann, B. Oneda, D. Ambort, E.E. Sterchi, and D. Lottaz. 2008. The metalloprotease meprinbeta processes E-cadherin and weakens intercellular adhesion. *PloS one*. 3:e2153.

Hussain, I., J. Hawkins, D. Harrison, C. Hille, G. Wayne, L. Cutler, T. Buck, D. Walter, E. Demont, C. Howes, A. Naylor, P. Jeffrey, M.I. Gonzalez, C. Dingwall, A. Michel, S. Redshaw, and J.B. Davis. 2007. Oral administration of a potent and selective non-peptidic BACE-1 inhibitor decreases beta-cleavage of amyloid precursor protein and amyloid-beta production in vivo. *Journal of neurochemistry*. 100:802-809.

Isbert, S., K. Wagner, S. Eggert, A. Schweitzer, G. Multhaup, S. Weggen, S. Kins, and C.U. Pietrzik. 2012. APP dimer formation is initiated in the endoplasmic reticulum and differs between APP isoforms. *Cellular and molecular life sciences : CMLS*. 69:1353-1375.

Iwatsubo, T., A. Odaka, N. Suzuki, H. Mizusawa, N. Nukina, and Y. Ihara. 1994. Visualization of A beta 42(43) and A beta 40 in senile plaques with end-specific A beta monoclonals: evidence that an initially deposited species is A beta 42(43). *Neuron*. 13:45-53.

Jackle, F., F. Schmidt, R. Wichert, P. Arnold, J. Prox, M. Mangold, A. Ohler, C.U. Pietrzik, T. Koudelka, A. Tholey, M. Gutschow, M. Stirnberg, and C. Becker-Pauly. 2015. Metalloprotease meprin beta is activated by transmembrane serine protease matriptase-2 at the cell surface thereby enhancing APP shedding. *The Biochemical journal*. 470:91-103.

Jager, S., S. Leuchtenberger, A. Martin, E. Czirr, J. Wesselowski, M. Dieckmann, E. Waldron, C. Korth, E.H. Koo, M. Heneka, S. Weggen, and C.U. Pietrzik. 2009. alpha-secretase mediated conversion of the amyloid precursor protein derived membrane stub C99 to C83 limits Abeta generation. *Journal of neurochemistry*. 111:1369-1382.

Jawhar, S., O. Wirths, and T.A. Bayer. 2011. Pyroglutamate amyloid-beta (Abeta): a hatchet man in Alzheimer disease. *The Journal of biological chemistry*. 286:38825-38832.

Jefferson, T., U. Auf dem Keller, C. Bellac, V.V. Metz, C. Broder, J. Hedrich, A. Ohler, W. Maier, V. Magdolen, E. Sterchi, J.S. Bond, A. Jayakumar, H. Traupe, A. Chalaris, S. Rose-John, C.U. Pietrzik, R. Postina, C.M. Overall, and C. Becker-Pauly. 2012. The substrate degradome of meprin metalloproteases reveals an unexpected proteolytic link between meprin beta and ADAM10. *Cellular and molecular life sciences : CMLS*.

Jefferson, T., M. Causevic, U. auf dem Keller, O. Schilling, S. Isbert, R. Geyer, W. Maier, S. Tschickardt, T. Jumpertz, S. Weggen, J.S. Bond, C.M. Overall, C.U. Pietrzik, and C. Becker-Pauly. 2011. Metalloprotease meprin beta generates nontoxic N-terminal amyloid precursor protein fragments in vivo. *The Journal of biological chemistry*. 286:27741-27750.

Jonsson, T., J.K. Atwal, S. Steinberg, J. Snaedal, P.V. Jonsson, S. Bjornsson, H. Stefansson, P. Sulem, D. Gudbjartsson, J. Maloney, K. Hoyte, A. Gustafson, Y. Liu, Y. Lu, T. Bhangale, R.R. Graham, J. Huttenlocher, G. Bjornsdottir, O.A. Andreassen, E.G. Jonsson, A. Palotie, T.W. Behrens, O.T. Magnusson, A. Kong, U. Thorsteinsdottir, R.J. Watts, and K. Stefansson. 2012. A mutation in APP protects against Alzheimer's disease and age-related cognitive decline. *Nature*. 488:96-99.

Jorissen, E., J. Prox, C. Bernreuther, S. Weber, R. Schwanbeck, L. Serneels, A. Snellinx, K. Craessaerts, A. Thathiah, I. Tesseur, U. Bartsch, G. Weskamp, C.P. Blobel, M. Glatzel, B. De Strooper, and P. Saftig. 2010. The disintegrin/metalloproteinase ADAM10 is

essential for the establishment of the brain cortex. *The Journal of neuroscience : the official journal of the Society for Neuroscience*. 30:4833-4844.

Kaden, D., L.M. Munter, B. Reif, and G. Multhaup. 2012. The amyloid precursor protein and its homologues: structural and functional aspects of native and pathogenic oligomerization. *Eur J Cell Biol*. 91:234-239.

Kawooya, J.K., T.L. Emmons, P.A. Gonzalez-DeWhitt, M.C. Camp, and S.C. D'Andrea. 2003. Electrophoretic mobility of Alzheimer's amyloid-beta peptides in urea-sodium dodecyl sulfate-polyacrylamide gel electrophoresis. *Analytical biochemistry*. 323:103-113.

Keiffer, T.R., and J.S. Bond. 2014. Meprin metalloproteases inactivate interleukin 6. *The Journal of biological chemistry*. 289:7580-7588.

Kero, M., A. Paetau, T. Polvikoski, M. Tanskanen, R. Sulkava, L. Jansson, L. Myllykangas, and P.J. Tienari. 2013. Amyloid precursor protein (APP) A673T mutation in the elderly Finnish population. *Neurobiology of aging*. 34:1518 e1511-1513.

Kim, D.Y., B.W. Carey, H. Wang, L.A. Ingano, A.M. Binshtok, M.H. Wertz, W.H. Pettingell, P. He, V.M. Lee, C.J. Woolf, and D.M. Kovacs. 2007. BACE1 regulates voltage-gated sodium channels and neuronal activity. *Nat Cell Biol*. 9:755-764.

Kinoshita, A., H. Fukumoto, T. Shah, C.M. Whelan, M.C. Irizarry, and B.T. Hyman. 2003. Demonstration by FRET of BACE interaction with the amyloid precursor protein at the cell surface and in early endosomes. *Journal of cell science*. 116:3339-3346.

Klafki, H.W., J. Wiltfang, and M. Staufenbiel. 1996. Electrophoretic separation of betaA4 peptides (1-40) and (1-42). *Analytical biochemistry*. 237:24-29.

Koh, S.H., M.Y. Noh, and S.H. Kim. 2008. Amyloid-beta-induced neurotoxicity is reduced by inhibition of glycogen synthase kinase-3. *Brain research*. 1188:254-262.

Koike, H., S. Tomioka, H. Sorimachi, T.C. Saido, K. Maruyama, A. Okuyama, A. Fujisawa-Sehara, S. Ohno, K. Suzuki, and S. Ishiura. 1999. Membrane-anchored metalloprotease MDC9 has an alpha-secretase activity responsible for processing the amyloid precursor protein. *The Biochemical journal*. 343 Pt 2:371-375.

Koo, E.H., and S.L. Squazzo. 1994. Evidence that production and release of amyloid beta-protein involves the endocytic pathway. *The Journal of biological chemistry*. 269:17386-17389.

Kopan, R., and M.X. Ilagan. 2009. The canonical Notch signaling pathway: unfolding the activation mechanism. *Cell*. 137:216-233.

Kosik, K.S. 1990. Tau protein and neurodegeneration. *Mol Neurobiol*. 4:171-179.

Kounnas, M.Z., A.M. Danks, S. Cheng, C. Tyree, E. Ackerman, X. Zhang, K. Ahn, P. Nguyen, D. Comer, L. Mao, C. Yu, D. Pleynet, P.J. Digregorio, G. Velicelebi, K.A. Stauderman, W.T. Comer, W.C. Mobley, Y.M. Li, S.S. Sisodia, R.E. Tanzi, and S.L. Wagner. 2010. Modulation of gamma-secretase reduces beta-amyloid deposition in a transgenic mouse model of Alzheimer's disease. *Neuron*. 67:769-780.

Kruse, M.N., C. Becker, D. Lottaz, D. Kohler, I. Yiallouros, H.W. Krell, E.E. Sterchi, and W. Stocker. 2004. Human meprin alpha and beta homo-oligomers: cleavage of basement membrane proteins and sensitivity to metalloprotease inhibitors. *The Biochemical journal*. 378:383-389.

Kuhn, P.H., H. Wang, B. Dislich, A. Colombo, U. Zeitschel, J.W. Ellwart, E. Kremmer, S. Rossner, and S.F. Lichtenthaler. 2010. ADAM10 is the physiologically relevant, constitutive alpha-secretase of the amyloid precursor protein in primary neurons. *The EMBO journal*. 29:3020-3032.

Kumar, S., N. Rezaei-Ghaleh, D. Terwel, D.R. Thal, M. Richard, M. Hoch, J.M. Mc Donald, U. Wullner, K. Glebov, M.T. Heneka, D.M. Walsh, M. Zweckstetter, and J. Walter. 2011. Extracellular phosphorylation of the amyloid beta-peptide promotes formation of toxic aggregates during the pathogenesis of Alzheimer's disease. *The EMBO journal*. 30:2255-2265.

Kumar, S., S. Singh, D. Hinze, M. Josten, H.G. Sahl, M. Siepmann, and J. Walter. 2012. Phosphorylation of amyloid-beta peptide at serine 8 attenuates its clearance via insulin-degrading and angiotensin-converting enzymes. *The Journal of biological chemistry*. 287:8641-8651.

Kummer, M.P., M. Hermes, A. Delekarte, T. Hammerschmidt, S. Kumar, D. Terwel, J. Walter, H.C. Pape, S. Konig, S. Roeber, F. Jessen, T. Klockgether, M. Korte, and M.T. Heneka. 2011. Nitration of tyrosine 10 critically enhances amyloid beta aggregation and plaque formation. *Neuron*. 71:833-844.

Lai, A., S.S. Sisodia, and I.S. Trowbridge. 1995. Characterization of sorting signals in the beta-amyloid precursor protein cytoplasmic domain. *The Journal of biological chemistry*. 270:3565-3573.

Lammich, S., E. Kojro, R. Postina, S. Gilbert, R. Pfeiffer, M. Jasionowski, C. Haass, and F. Fahrenholz. 1999. Constitutive and regulated alpha-secretase cleavage of Alzheimer's amyloid precursor protein by a disintegrin metalloprotease. *Proceedings of the National Academy of Sciences of the United States of America*. 96:3922-3927.

Lammich, S., M. Okochi, M. Takeda, C. Kaether, A. Capell, A.K. Zimmer, D. Edbauer, J. Walter, H. Steiner, and C. Haass. 2002. Presenilin-dependent intramembrane proteolysis of CD44 leads to the liberation of its intracellular domain and the secretion of an Abeta-like peptide. *The Journal of biological chemistry*. 277:44754-44759.

Lee, V.M., B.J. Balin, L. Otvos, Jr., and J.Q. Trojanowski. 1991. A68: a major subunit of paired helical filaments and derivatized forms of normal Tau. *Science*. 251:675-678.

Lewczuk, P., H. Esselmann, M. Bibl, S. Paul, J. Svitek, J. Miertschischk, R. Meyrer, A. Smirnov, J.M. Maler, C. Klein, M. Otto, S. Bleich, W. Sperling, J. Kornhuber, E. Ruther, and J. Wiltfang. 2004a. Electrophoretic separation of amyloid beta peptides in plasma. *Electrophoresis*. 25:3336-3343.

Lewczuk, P., H. Esselmann, M. Otto, J.M. Maler, A.W. Henkel, M.K. Henkel, O. Eikenberg, C. Antz, W.R. Krause, U. Reulbach, J. Kornhuber, and J. Wiltfang. 2004b. Neurochemical diagnosis of Alzheimer's dementia by CSF Abeta42, Abeta42/Abeta40 ratio and total tau. *Neurobiology of aging*. 25:273-281.

Li, Y.J., Y.H. Fan, J. Tang, J.B. Li, and C.H. Yu. 2014. Meprin-beta regulates production of pro-inflammatory factors via a disintegrin and metalloproteinase-10 (ADAM-10) dependent pathway in macrophages. *Int Immunopharmacol*. 18:77-84.

Lorent, K., L. Overbergh, D. Moechars, B. De Strooper, F. Van Leuven, and H. Van den Berghe. 1995. Expression in mouse embryos and in adult mouse brain of three members of the amyloid precursor protein family, of the alpha-2-macroglobulin receptor/low density lipoprotein receptor-related protein and of its ligands apolipoprotein E, lipoprotein lipase, alpha-2-macroglobulin and the 40,000 molecular weight receptor-associated protein. *Neuroscience*. 65:1009-1025.

Lottaz, D., D. Hahn, S. Muller, C. Muller, and E.E. Sterchi. 1999. Secretion of human meprin from intestinal epithelial cells depends on differential expression of the alpha and beta subunits. *Eur J Biochem*. 259:496-504.

Loureiro, R.M., J.A. Dumin, T.D. McKee, W.F. Austin, N.O. Fuller, J.L. Hubbs, R. Shen, J. Jonker, J. Ives, B.S. Bronk, and B. Tate. 2013. Efficacy of SPI-1865, a novel gamma-secretase modulator, in multiple rodent models. *Alzheimers Res Ther*. 5:19.

Luo, Y., B. Bolon, S. Kahn, B.D. Bennett, S. Babu-Khan, P. Denis, W. Fan, H. Kha, J. Zhang, Y. Gong, L. Martin, J.C. Louis, Q. Yan, W.G. Richards, M. Citron, and R. Vassar. 2001. Mice deficient in BACE1, the Alzheimer's beta-secretase, have normal phenotype and abolished beta-amyloid generation. *Nature neuroscience*. 4:231-232.

Maler, J.M., H.W. Klafki, S. Paul, P. Spitzer, T.W. Groemer, A.W. Henkel, H. Esselmann, P. Lewczuk, J. Kornhuber, and J. Wiltfang. 2007. Urea-based two-dimensional electrophoresis of beta-amyloid peptides in human plasma: evidence for novel Abeta species. *Proteomics*. 7:3815-3820.

Maloney, J.A., T. Bainbridge, A. Gustafson, S. Zhang, R. Kyauk, P. Steiner, M. van der Brug, Y. Liu, J.A. Ernst, R.J. Watts, and J.K. Atwal. 2014. Molecular Mechanisms of Alzheimer Disease Protection by the A673T Allele of Amyloid Precursor Protein. *The Journal of biological chemistry*. 289:30990-31000.

Mandler, M., L. Walker, R. Santic, P. Hanson, A.R. Upadhaya, S.J. Colloby, C.M. Morris, D.R. Thal, A.J. Thomas, A. Schneeberger, and J. Attems. 2014. Pyroglutamylated amyloid-beta is associated with hyperphosphorylated tau and severity of Alzheimer's disease. *Acta neuropathologica*. 128:67-79.

Marambaud, P., J. Shioi, G. Serban, A. Georgakopoulos, S. Sarner, V. Nagy, L. Baki, P. Wen, S. Efthimiopoulos, Z. Shao, T. Wisniewski, and N.K. Robakis. 2002. A presenilin-1/gamma-secretase cleavage releases the E-cadherin intracellular domain and regulates disassembly of adherens junctions. *The EMBO journal*. 21:1948-1956.

Marquez-Sterling, N.R., A.C. Lo, S.S. Sisodia, and E.H. Koo. 1997. Trafficking of cell-surface beta-amyloid precursor protein: evidence that a sorting intermediate participates in synaptic vesicle recycling. *The Journal of neuroscience : the official journal of the Society for Neuroscience*. 17:140-151.

Masters, C.L., G. Simms, N.A. Weinman, G. Multhaup, B.L. McDonald, and K. Beyreuther. 1985. Amyloid plaque core protein in Alzheimer disease and Down syndrome. *Proceedings of the National Academy of Sciences of the United States of America*. 82:4245-4249.

Mazanetz, M.P., and P.M. Fischer. 2007. Untangling tau hyperphosphorylation in drug design for neurodegenerative diseases. *Nat Rev Drug Discov*. 6:464-479.

Minogue, A.M., A.K. Stubbs, C.S. Frigerio, B. Boland, J.V. Fadeeva, J. Tang, D.J. Selkoe, and D.M. Walsh. 2009. gamma-secretase processing of APLP1 leads to the production of a p3-like peptide that does not aggregate and is not toxic to neurons. *Brain research*. 1262:89-99.

Moechars, D., I. Dewachter, K. Lorent, D. Reverse, V. Baekelandt, A. Naidu, I. Tesseur, K. Spittaels, C.V. Haute, F. Checler, E. Godaux, B. Cordell, and F. Van Leuven. 1999. Early phenotypic changes in transgenic mice that overexpress different mutants of amyloid precursor protein in brain. *The Journal of biological chemistry*. 274:6483-6492.

Montine, T.J., C.H. Phelps, T.G. Beach, E.H. Bigio, N.J. Cairns, D.W. Dickson, C. Duyckaerts, M.P. Frosch, E. Masliah, S.S. Mirra, P.T. Nelson, J.A. Schneider, D.R. Thal, J.Q. Trojanowski, H.V. Vinters, B.T. Hyman, A. National Institute on, and A. Alzheimer's. 2012. National Institute on Aging-Alzheimer's Association guidelines for the neuropathologic assessment of Alzheimer's disease: a practical approach. *Acta neuropathologica*. 123:1-11.

Mucke, L., E. Masliah, G.Q. Yu, M. Mallory, E.M. Rockenstein, G. Tatsuno, K. Hu, D. Kholodenko, K. Johnson-Wood, and L. McConlogue. 2000. High-level neuronal expression of abeta 1-42 in wild-type human amyloid protein precursor transgenic mice: synaptotoxicity without plaque formation. *The Journal of neuroscience : the official journal of the Society for Neuroscience*. 20:4050-4058.

Mullan, M., F. Crawford, K. Axelman, H. Houlden, L. Lilius, B. Winblad, and L. Lannfelt. 1992. A pathogenic mutation for probable Alzheimer's disease in the APP gene at the N-terminus of beta-amyloid. *Nature genetics*. 1:345-347.

Muratore, C.R., H.C. Rice, P. Srikanth, D.G. Callahan, T. Shin, L.N. Benjamin, D.M. Walsh, D.J. Selkoe, and T.L. Young-Pearse. 2014. The familial Alzheimer's disease APPV717I mutation alters APP processing and Tau expression in iPSC-derived neurons. *Human molecular genetics*.

Murayama, K.S., F. Kametani, T. Tabira, and W. Araki. 2007. A novel monoclonal antibody specific for the amino-truncated beta-amyloid Abeta5-40/42 produced from caspase-cleaved amyloid precursor protein. *Journal of neuroscience methods*. 161:244-249.

Ni, C.Y., M.P. Murphy, T.E. Golde, and G. Carpenter. 2001. gamma -Secretase cleavage and nuclear localization of ErbB-4 receptor tyrosine kinase. *Science*. 294:2179-2181.

Nishitomi, K., G. Sakaguchi, Y. Horikoshi, A.J. Gray, M. Maeda, C. Hirata-Fukae, A.G. Becker, M. Hosono, I. Sakaguchi, S.S. Minami, Y. Nakajima, H.F. Li, C. Takeyama, T. Kihara, A. Ota, P.C. Wong, P.S. Aisen, A. Kato, N. Kinoshita, and Y. Matsuoka. 2006. BACE1 inhibition reduces endogenous Abeta and alters APP processing in wild-type mice. *Journal of neurochemistry*. 99:1555-1563.

Oakley, H., S.L. Cole, S. Logan, E. Maus, P. Shao, J. Craft, A. Guillozet-Bongaarts, M. Ohno, J. Disterhoft, L. Van Eldik, R. Berry, and R. Vassar. 2006. Intraneuronal beta-amyloid aggregates, neurodegeneration, and neuron loss in transgenic mice with five familial Alzheimer's disease mutations: potential factors in amyloid plaque formation. *The Journal of neuroscience : the official journal of the Society for Neuroscience*. 26:10129-10140.

Oberstein, T.J., P. Spitzer, H.W. Klafki, P. Linning, F. Neff, H.J. Knolker, P. Lewczuk, J. Wiltfang, J. Kornhuber, and J.M. Maler. 2015. Astrocytes and microglia but not neurons preferentially generate N-terminally truncated Abeta peptides. *Neurobiology of disease*. 73:24-35.

Oddo, S., A. Caccamo, J.D. Shepherd, M.P. Murphy, T.E. Golde, R. Kayed, R. Metherate, M.P. Mattson, Y. Akbari, and F.M. LaFerla. 2003. Triple-transgenic model of Alzheimer's disease with plaques and tangles: intracellular Abeta and synaptic dysfunction. *Neuron*. 39:409-421.

Ohler, A., M. Debela, S. Wagner, V. Magdolen, and C. Becker-Pauly. 2010. Analyzing the protease web in skin: meprin metalloproteases are activated specifically by KLK4, 5 and 8 vice versa leading to processing of proKLK7 thereby triggering its activation. *Biological chemistry*. 391:455-460.

Ohno, M., E.A. Sametsky, L.H. Younkin, H. Oakley, S.G. Younkin, M. Citron, R. Vassar, and J.F. Disterhoft. 2004. BACE1 deficiency rescues memory deficits and cholinergic dysfunction in a mouse model of Alzheimer's disease. *Neuron*. 41:27-33.

Oltersdorf, T., P.J. Ward, T. Henriksson, E.C. Beattie, R. Neve, I. Lieberburg, and L.C. Fritz. 1990. The Alzheimer amyloid precursor protein. Identification of a stable intermediate in the biosynthetic/degradative pathway. *The Journal of biological chemistry*. 265:4492-4497.

Osenkowski, P., H. Li, W. Ye, D. Li, L. Aeschbach, P.C. Fraering, M.S. Wolfe, D.J. Selkoe, and H. Li. 2009. Cryoelectron microscopy structure of purified gamma-secretase at 12 A resolution. *Journal of molecular biology*. 385:642-652.

Otth, C., Concha, II, T. Arendt, J. Stieler, R. Schliebs, C. Gonzalez-Billault, and R.B. Maccioni. 2002. AbetaPP induces cdk5-dependent tau hyperphosphorylation in transgenic mice Tg2576. *Journal of Alzheimer's disease : JAD*. 4:417-430.

Page, R.M., K. Baumann, M. Tomioka, B.I. Perez-Revuelta, A. Fukumori, H. Jacobsen, A. Flohr, T. Luebbers, L. Ozmen, H. Steiner, and C. Haass. 2008. Generation of Abeta38 and Abeta42 is independently and differentially affected by familial Alzheimer disease-associated presenilin mutations and gamma-secretase modulation. *The Journal of biological chemistry*. 283:677-683.

Palmblad, M., A. Westlind-Danielsson, and J. Bergquist. 2002. Oxidation of methionine 35 attenuates formation of amyloid beta -peptide 1-40 oligomers. *The Journal of biological chemistry*. 277:19506-19510.

Perez, R.G., S. Soriano, J.D. Hayes, B. Ostaszewski, W. Xia, D.J. Selkoe, X. Chen, G.B. Stokin, and E.H. Koo. 1999. Mutagenesis identifies new signals for beta-amyloid precursor protein endocytosis, turnover, and the generation of secreted fragments, including Abeta42. *The Journal of biological chemistry*. 274:18851-18856.

Portelius, E., M. Olsson, G. Brinkmalm, U. Ruetschi, N. Mattsson, U. Andreasson, J. Gobom, A. Brinkmalm, M. Holtta, K. Blennow, and H. Zetterberg. 2013. Mass spectrometric characterization of amyloid-beta species in the 7PA2 cell model of Alzheimer's disease. *Journal of Alzheimer's disease : JAD*. 33:85-93.

Postina, R., A. Schroeder, I. Dewachter, J. Bohl, U. Schmitt, E. Kojro, C. Prinzen, K. Endres, C. Hiemke, M. Blessing, P. Flamez, A. Dequenne, E. Godaux, F. van Leuven, and F. Fahrenholz. 2004. A disintegrin-metalloproteinase prevents amyloid plaque formation and hippocampal defects in an Alzheimer disease mouse model. *The Journal of clinical investigation*. 113:1456-1464.

Price, J.L., P.B. Davis, J.C. Morris, and D.L. White. 1991. The distribution of tangles, plaques and related immunohistochemical markers in healthy aging and Alzheimer's disease. *Neurobiology of aging*. 12:295-312.

Prince, M., R. Bryce, E. Albanese, A. Wimo, W. Ribeiro, and C.P. Ferri. 2013. The global prevalence of dementia: a systematic review and metaanalysis. *Alzheimers Dement*. 9:63-75 e62.

Prince, M.W., A; Guerchet, M; Ali, G; Wu, Y; Prina, M; Alzheimer's Disease International. 2015. World Alzheimer Report 2015 - The Global Impact of Dementia.

Qi-Takahara, Y., M. Morishima-Kawashima, Y. Tanimura, G. Dolios, N. Hirotani, Y. Horikoshi, F. Kametani, M. Maeda, T.C. Saido, R. Wang, and Y. Ihara. 2005. Longer forms of amyloid beta protein: implications for the mechanism of intramembrane cleavage by gamma-secretase. *The Journal of neuroscience : the official journal of the Society for Neuroscience*. 25:436-445.

Radtke, F., I. Ferrero, A. Wilson, R. Lees, M. Aguet, and H.R. MacDonald. 2000. Notch1 deficiency dissociates the intrathymic development of dendritic cells and T cells. *J Exp Med*. 191:1085-1094.

Radtke, F., A. Wilson, G. Stark, M. Bauer, J. van Meerwijk, H.R. MacDonald, and M. Aguet. 1999. Deficient T cell fate specification in mice with an induced inactivation of Notch1. *Immunity*. 10:547-558.

Red Eagle, A.R., R.L. Hanson, W. Jiang, X. Han, G.L. Matters, G. Imperatore, W.C. Knowler, and J.S. Bond. 2005. Meprin beta metalloprotease gene polymorphisms associated with diabetic nephropathy in the Pima Indians. *Hum Genet*. 118:12-22.

Roberds, S.L., J. Anderson, G. Basi, M.J. Bienkowski, D.G. Branstetter, K.S. Chen, S.B. Freedman, N.L. Frigon, D. Games, K. Hu, K. Johnson-Wood, K.E. Kappenman, T.T. Kawabe, I. Kola, R. Kuehn, M. Lee, W. Liu, R. Motter, N.F. Nichols, M. Power, D.W. Robertson, D. Schenk, M. Schoor, G.M. Shopp, M.E. Shuck, S. Sinha, K.A. Svensson, G. Tatsuno, H. Tintrup, J. Wijsman, S. Wright, and L. McConlogue. 2001. BACE knockout mice are healthy despite lacking the primary beta-secretase activity in brain: implications for Alzheimer's disease therapeutics. *Human molecular genetics*. 10:1317-1324.

Rohan de Silva, H.A., A. Jen, C. Wickenden, L.S. Jen, S.L. Wilkinson, and A.J. Patel. 1997. Cell-specific expression of beta-amyloid precursor protein isoform mRNAs and proteins in neurons and astrocytes. *Brain research. Molecular brain research*. 47:147-156.

Roher, A.E., J.D. Lowenson, S. Clarke, C. Wolkow, R. Wang, R.J. Cotter, I.M. Reardon, H.A. Zurcher-Neely, R.L. Heinrikson, M.J. Ball, and et al. 1993. Structural alterations in the peptide backbone of beta-amyloid core protein may account for its deposition and stability in Alzheimer's disease. *The Journal of biological chemistry*. 268:3072-3083.

Rovelet-Lecrux, A., D. Hannequin, G. Raux, N. Le Meur, A. Laquerriere, A. Vital, C. Dumanchin, S. Feuillette, A. Brice, M. Vercelletto, F. Dubas, T. Frebourg, and D. Campion. 2006. APP locus duplication causes autosomal dominant early-onset Alzheimer disease with cerebral amyloid angiopathy. *Nature genetics*. 38:24-26.

Russo, C., E. Violani, S. Salis, V. Venezia, V. Dolcini, G. Damonte, U. Benatti, C. D'Arrigo, E. Patrone, P. Carlo, and G. Schettini. 2002. Pyroglutamate-modified amyloid beta-peptides--AbetaN3(pE)--strongly affect cultured neuron and astrocyte survival. *Journal of neurochemistry*. 82:1480-1489.

Sandbrink, R., U. Monning, C.L. Masters, and K. Beyreuther. 1997. Expression of the APP gene family in brain cells, brain development and aging. *Gerontology*. 43:119-131.

Sastre, M., H. Steiner, K. Fuchs, A. Capell, G. Multhaup, M.M. Condron, D.B. Teplow, and C. Haass. 2001. Presenilin-dependent gamma-secretase processing of beta-amyloid precursor protein at a site corresponding to the S3 cleavage of Notch. *EMBO reports*. 2:835-841.

Schechter, I., and A. Berger. 1967. On the size of the active site in proteases. I. Papain. *Biochemical and biophysical research communications*. 27:157-162.

Scheiffele, P., J. Fan, J. Choih, R. Fetter, and T. Serafini. 2000. Neuroligin expressed in nonneuronal cells triggers presynaptic development in contacting axons. *Cell*. 101:657-669.

Schieb, H., H. Kratzin, O. Jahn, W. Mobius, S. Rabe, M. Staufenbiel, J. Wiltfang, and H.W. Klafki. 2011. Beta-amyloid peptide variants in brains and cerebrospinal fluid from amyloid precursor protein (APP) transgenic mice: comparison with human Alzheimer amyloid. *The Journal of biological chemistry*. 286:33747-33758.

Schilling, O., P.F. Huesgen, O. Barre, U. Auf dem Keller, and C.M. Overall. 2011. Characterization of the prime and non-prime active site specificities of proteases by proteome-derived peptide libraries and tandem mass spectrometry. *Nature protocols*. 6:111-120.

Schilling, S., T. Hoffmann, S. Manhart, M. Hoffmann, and H.U. Demuth. 2004. Glutaminyl cyclases unfold glutamyl cyclase activity under mild acid conditions. *FEBS letters*. 563:191-196.

Schonherr, C., J. Bien, S. Isbert, R. Wichert, J. Prox, H. Altmeppen, S. Kumar, J. Walter, S.F. Lichtenthaler, S. Weggen, M. Glatzel, C. Becker-Pauly, and C.U. Pietrzik. 2016. Generation of aggregation prone N-terminally truncated amyloid beta peptides by meprin beta depends on the sequence specificity at the cleavage site. *Molecular neurodegeneration*. 11:19.

Schutte, A., A. Ermund, C. Becker-Pauly, M.E. Johansson, A.M. Rodriguez-Pineiro, F. Backhed, S. Muller, D. Lottaz, J.S. Bond, and G.C. Hansson. 2014. Microbial-induced meprin beta cleavage in MUC2 mucin and a functional CFTR channel are required to release anchored small intestinal mucus. *Proceedings of the National Academy of Sciences of the United States of America*. 111:12396-12401.

Searfoss, G.H., W.H. Jordan, D.O. Calligaro, E.J. Galbreath, L.M. Schirtzinger, B.R. Berridge, H. Gao, M.A. Higgins, P.C. May, and T.P. Ryan. 2003. Adipsin, a biomarker of gastrointestinal toxicity mediated by a functional gamma-secretase inhibitor. *The Journal of biological chemistry*. 278:46107-46116.

Sevalle, J., A. Amoyel, P. Robert, M.C. Fournie-Zaluski, B. Roques, and F. Checler. 2009. Aminopeptidase A contributes to the N-terminal truncation of amyloid beta-peptide. *Journal of neurochemistry*. 109:248-256.

Shariati, S.A., and B. De Strooper. 2013. Redundancy and divergence in the amyloid precursor protein family. *FEBS letters*. 587:2036-2045.

Sisodia, S.S., E.H. Koo, K. Beyreuther, A. Unterbeck, and D.L. Price. 1990. Evidence that beta-amyloid protein in Alzheimer's disease is not derived by normal processing. *Science*. 248:492-495.

Sisodia, S.S., E.H. Koo, P.N. Hoffman, G. Perry, and D.L. Price. 1993. Identification and transport of full-length amyloid precursor proteins in rat peripheral nervous system. *The Journal of neuroscience : the official journal of the Society for Neuroscience*. 13:3136-3142.

Slack, B.E., L.K. Ma, and C.C. Seah. 2001. Constitutive shedding of the amyloid precursor protein ectodomain is up-regulated by tumour necrosis factor-alpha converting enzyme. *The Biochemical journal*. 357:787-794.

Sleegers, K., N. Brouwers, I. Gijselinck, J. Theuns, D. Goossens, J. Wauters, J. Del-Favero, M. Cruts, C.M. van Duijn, and C. Van Broeckhoven. 2006. APP duplication is sufficient to cause early onset Alzheimer's dementia with cerebral amyloid angiopathy. *Brain : a journal of neurology*. 129:2977-2983.

Soba, P., S. Eggert, K. Wagner, H. Zentgraf, K. Siehl, S. Kreger, A. Lower, A. Langer, G. Merdes, R. Paro, C.L. Masters, U. Muller, S. Kins, and K. Beyreuther. 2005. Homo- and heterodimerization of APP family members promotes intercellular adhesion. *The EMBO journal*. 24:3624-3634.

Sommer, A., F. Kordowski, J. Buch, T. Maretzky, A. Evers, J. Andra, S. Dusterhoft, M. Michalek, I. Lorenzen, P. Somasundaram, A. Tholey, F.D. Sonnichsen, K. Kunzelmann, L. Heinbockel, C. Nehls, T. Gutsmann, J. Grotzinger, S. Bhakdi, and K. Reiss. 2016. Phosphatidylserine exposure is required for ADAM17 sheddase function. *Nat Commun*. 7:11523.

Sterchi, E.E., J.R. Green, and M.J. Lentze. 1982. Non-pancreatic hydrolysis of N-benzoyl-l-tyrosyl-p-aminobenzoic acid (PABA-peptide) in the human small intestine. *Clin Sci (Lond)*. 62:557-560.

Stocker, W., M. Ng, and D.S. Auld. 1990. Fluorescent oligopeptide substrates for kinetic characterization of the specificity of Astacus protease. *Biochemistry*. 29:10418-10425.

Su, A.I., M.P. Cooke, K.A. Ching, Y. Hakak, J.R. Walker, T. Wiltshire, A.P. Orth, R.G. Vega, L.M. Sapinoso, A. Moqrich, A. Patapoutian, G.M. Hampton, P.G. Schultz, and J.B. Hogenesch. 2002. Large-scale analysis of the human and mouse transcriptomes. *Proceedings of the National Academy of Sciences of the United States of America*. 99:4465-4470.

Su, A.I., T. Wiltshire, S. Batalov, H. Lapp, K.A. Ching, D. Block, J. Zhang, R. Soden, M. Hayakawa, G. Kreiman, M.P. Cooke, J.R. Walker, and J.B. Hogenesch. 2004. A gene atlas of the mouse and human protein-encoding transcriptomes. *Proceedings of the National Academy of Sciences of the United States of America*. 101:6062-6067.

Takami, M., Y. Nagashima, Y. Sano, S. Ishihara, M. Morishima-Kawashima, S. Funamoto, and Y. Ihara. 2009. gamma-Secretase: successive tripeptide and tetrapeptide release from the transmembrane domain of beta-carboxyl terminal fragment. *The Journal of neuroscience : the official journal of the Society for Neuroscience*. 29:13042-13052.

Takeda, K., W. Araki, H. Akiyama, and T. Tabira. 2004. Amino-truncated amyloid beta-peptide (Abeta5-40/42) produced from caspase-cleaved amyloid precursor protein is deposited in Alzheimer's disease brain. *FASEB journal : official publication of the Federation of American Societies for Experimental Biology*. 18:1755-1757.

Tanabe, C., N. Hotoda, N. Sasagawa, A. Sehara-Fujisawa, K. Maruyama, and S. Ishiura. 2007. ADAM19 is tightly associated with constitutive Alzheimer's disease APP alpha-secretase in A172 cells. *Biochemical and biophysical research communications*. 352:111-117.

Tanaka, S., S. Nakamura, and K. Ueda. 1990. [Expression of amyloid beta-protein gene in Alzheimer's disease]. *Rinsho Byori*. 38:489-493.

Thal, D.R., A. Glas, W. Schneider, and R. Schober. 1997. Differential pattern of beta-amyloid, amyloid precursor protein and apolipoprotein E expression in cortical senile plaques. *Acta neuropathologica*. 94:255-265.

Thal, D.R., U. Rub, M. Orantes, and H. Braak. 2002. Phases of A beta-deposition in the human brain and its relevance for the development of AD. *Neurology*. 58:1791-1800.

Vassar, R., B.D. Bennett, S. Babu-Khan, S. Kahn, E.A. Mendiaz, P. Denis, D.B. Teplow, S. Ross, P. Amarante, R. Loeloff, Y. Luo, S. Fisher, J. Fuller, S. Edenson, J. Lile, M.A. Jarosinski, A.L. Biere, E. Curran, T. Burgess, J.C. Louis, F. Collins, J. Treanor, G. Rogers, and M. Citron. 1999. Beta-secretase cleavage of Alzheimer's amyloid precursor protein by the transmembrane aspartic protease BACE. *Science*. 286:735-741.

Vassar, R., P.H. Kuhn, C. Haass, M.E. Kennedy, L. Rajendran, P.C. Wong, and S.F. Lichtenthaler. 2014. Function, therapeutic potential and cell biology of BACE proteases: current status and future prospects. *Journal of neurochemistry*. 130:4-28.

Vazeille, E., M.A. Bringer, A. Gardarin, C. Chambon, C. Becker-Pauly, S.L. Pender, C. Jakob, S. Muller, D. Lottaz, and A. Darfeuille-Michaud. 2011. Role of meprins to protect ileal

mucosa of Crohn's disease patients from colonization by adherent-invasive E. coli. *PloS one*. 6:e21199.

von Koch, C.S., H. Zheng, H. Chen, M. Trumbauer, G. Thinakaran, L.H. van der Ploeg, D.L. Price, and S.S. Sisodia. 1997. Generation of APLP2 KO mice and early postnatal lethality in APLP2/APP double KO mice. *Neurobiology of aging*. 18:661-669.

von Rotz, R.C., B.M. Kohli, J. Bosset, M. Meier, T. Suzuki, R.M. Nitsch, and U. Konietzko. 2004. The APP intracellular domain forms nuclear multiprotein complexes and regulates the transcription of its own precursor. *Journal of cell science*. 117:4435-4448.

Wang, D., and D.G. Munoz. 1995. Qualitative and quantitative differences in senile plaque dystrophic neurites of Alzheimer's disease and normal aged brain. *Journal of neuropathology and experimental neurology*. 54:548-556.

Wang, D.S., D.W. Dickson, and J.S. Malter. 2006a. beta-Amyloid degradation and Alzheimer's disease. *J Biomed Biotechnol*. 2006:58406.

Wang, R., J.F. Meschia, R.J. Cotter, and S.S. Sisodia. 1991. Secretion of the beta/A4 amyloid precursor protein. Identification of a cleavage site in cultured mammalian cells. *The Journal of biological chemistry*. 266:16960-16964.

Wang, R., P. Tang, P. Wang, R.E. Boissy, and H. Zheng. 2006b. Regulation of tyrosinase trafficking and processing by presenilins: partial loss of function by familial Alzheimer's disease mutation. *Proceedings of the National Academy of Sciences of the United States of America*. 103:353-358.

Wang, Y., and Y. Ha. 2004. The X-ray structure of an antiparallel dimer of the human amyloid precursor protein E2 domain. *Mol Cell*. 15:343-353.

Weggen, S., J.L. Eriksen, S.A. Sagi, C.U. Pietrzik, V. Ozols, A. Fauq, T.E. Golde, and E.H. Koo. 2003. Evidence that nonsteroidal anti-inflammatory drugs decrease amyloid beta 42 production by direct modulation of gamma-secretase activity. *The Journal of biological chemistry*. 278:31831-31837.

Weidemann, A., S. Eggert, F.B. Reinhard, M. Vogel, K. Paliga, G. Baier, C.L. Masters, K. Beyreuther, and G. Evin. 2002. A novel epsilon-cleavage within the transmembrane domain of the Alzheimer amyloid precursor protein demonstrates homology with Notch processing. *Biochemistry*. 41:2825-2835.

Weidemann, A., G. Konig, D. Bunke, P. Fischer, J.M. Salbaum, C.L. Masters, and K. Beyreuther. 1989. Identification, biogenesis, and localization of precursors of Alzheimer's disease A4 amyloid protein. *Cell*. 57:115-126.

Wenk, G.L. 2003. Neuropathologic changes in Alzheimer's disease. *J Clin Psychiatry*. 64 Suppl 9:7-10.

Willem, M., A.N. Garratt, B. Novak, M. Citron, S. Kaufmann, A. Rittger, B. DeStrooper, P. Saftig, C. Birchmeier, and C. Haass. 2006. Control of peripheral nerve myelination by the beta-secretase BACE1. *Science*. 314:664-666.

Willem, M., S. Lammich, and C. Haass. 2009. Function, regulation and therapeutic properties of beta-secretase (BACE1). *Semin Cell Dev Biol*. 20:175-182.

Wiltfang, J., H. Esselmann, P. Cupers, M. Neumann, H. Kretzschmar, M. Beyermann, D. Schleuder, H. Jahn, E. Ruther, J. Kornhuber, W. Annaert, B. De Strooper, and P. Saftig. 2001. Elevation of beta-amyloid peptide 2-42 in sporadic and familial Alzheimer's disease and its generation in PS1 knockout cells. *The Journal of biological chemistry*. 276:42645-42657.

Wirths, O., T. Bethge, A. Marcello, A. Harmeier, S. Jawhar, P.J. Lucassen, G. Multhaup, D.L. Brody, T. Esparza, M. Ingelsson, H. Kalimo, L. Lannfelt, and T.A. Bayer. 2010. Pyroglutamate Abeta pathology in APP/PS1KI mice, sporadic and familial Alzheimer's disease cases. *Journal of neural transmission*. 117:85-96.

Wittnam, J.L., E. Portelius, H. Zetterberg, M.K. Gustavsson, S. Schilling, B. Koch, H.U. Demuth, K. Blennow, O. Wirths, and T.A. Bayer. 2012. Pyroglutamate amyloid beta (Abeta)

aggravates behavioral deficits in transgenic amyloid mouse model for Alzheimer disease. *The Journal of biological chemistry*. 287:8154-8162.

Wong, G.T., D. Manfra, F.M. Poulet, Q. Zhang, H. Josien, T. Bara, L. Engstrom, M. Pinzon-Ortiz, J.S. Fine, H.J. Lee, L. Zhang, G.A. Higgins, and E.M. Parker. 2004. Chronic treatment with the gamma-secretase inhibitor LY-411,575 inhibits beta-amyloid peptide production and alters lymphopoiesis and intestinal cell differentiation. *The Journal of biological chemistry*. 279:12876-12882.

Wong, H.K., T. Sakurai, F. Oyama, K. Kaneko, K. Wada, H. Miyazaki, M. Kurosawa, B. De Strooper, P. Saftig, and N. Nukina. 2005. beta Subunits of voltage-gated sodium channels are novel substrates of beta-site amyloid precursor protein-cleaving enzyme (BACE1) and gamma-secretase. *The Journal of biological chemistry*. 280:23009-23017.

Wu, L., P. Rosa-Neto, G.Y. Hsiung, A.D. Sadovnick, M. Masellis, S.E. Black, J. Jia, and S. Gauthier. 2012. Early-onset familial Alzheimer's disease (EOFAD). *Can J Neurol Sci*. 39:436-445.

Wunderlich, P., K. Glebov, N. Kemmerling, N.T. Tien, H. Neumann, and J. Walter. 2013. Sequential proteolytic processing of the triggering receptor expressed on myeloid cells-2 (TREM2) protein by ectodomain shedding and gamma-secretase-dependent intramembranous cleavage. *The Journal of biological chemistry*. 288:33027-33036.

Zou, W., H. Kitaura, J. Reeve, F. Long, V.L. Tybulewicz, S.J. Shattil, M.H. Ginsberg, F.P. Ross, and S.L. Teitelbaum. 2007. Syk, c-Src, the alphavbeta3 integrin, and ITAM immunoreceptors, in concert, regulate osteoclastic bone resorption. *J Cell Biol*. 176:877-888.

9 APPENDIX

9.1 SUPPLEMENTARY METHODS

9.1.1 POLYCLONAL ANTISERA AGAINST MEPRIN β

The polyclonal anti-murine meprin β antibody was raised against a peptide corresponding to a sequence of the ectodomain of murine meprin β (NH2-CGMIQSSGDSADWQRVSQ-CONH2). Immunization and purification was performed by Pineda Antibody-Service (Berlin, Germany).

9.2 SUPPLEMENTARY RESULTS

9.2.1 MEPRIN β ANTIBODY SPECIFICITY ANALYSIS

(A) Isolated kidneys of representative wt and *Mep1b*$^{-/-}$ mice were lysed, equal amounts of protein per sample were loaded on SDS-PAGE and meprin β expression was analyzed by immunoblot. (B) Cos7-cells were transfected with human wt-meprin β and immunoblot analysis was performed. The antibody was generated by Professor Becker-Pauly, University of Kiel.

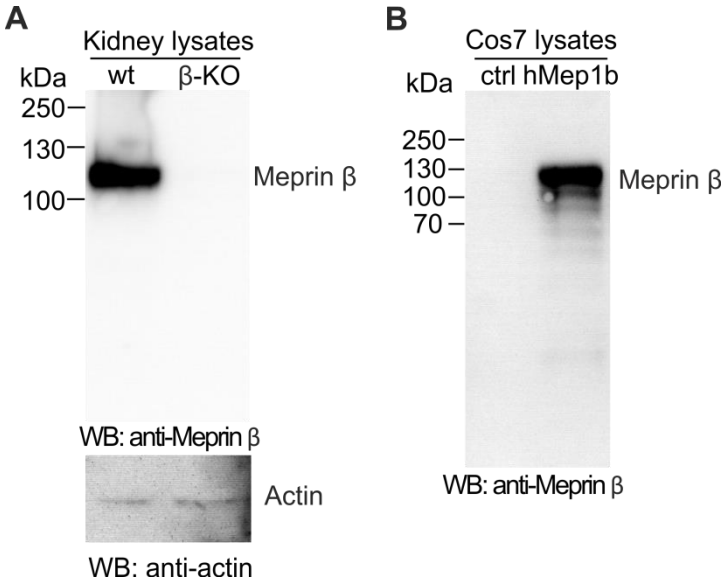

FIGURE 29 Meprin β antibody specificity analysis

(A) Isolated kidneys of representative wt and *Mep1b*$^{-/-}$ mice were lysed, equal amounts of protein per sample were loaded on SDS-PAGE and meprin β expression was analyzed by immunoblot. (B) Cos7-cells were transfected with human wt-meprin β and immunoblot analysis was performed.

9.2.2 INCREASED MEPRIN β EXPRESSION IN BRAINS OF AD PATIENTS

FIGURE 30 Increased meprin β expression in brains of AD patients

Immunostainings of human brain slices of AD patients, non-demented and non-AD patients were performed with polyclonal anti-meprin β antibody.

9.3 DANKSAGUNG

9.4 CURRICULUM VITAE